行政院國家科學委員會補助專題研究計畫 ■成果報告 □期中進度報告

壓電材料迴轉體與楔形板幾何引致電彈奇異性之探討

計畫類別：■個別型計畫　　□整合型計畫

計畫編號：NSC 100－2221－E－009－093－MY2

執行期間：100 年 8 月 1 日至 100 年 10 月 31 日

計畫主持人：黃炯憲

計畫參與人員：胡政甯、詹志偉、劉靖俞、李承哲、郭芳琳 、黃旭進、王裕鈞、楊維莘

成果報告類型(依經費核定清單規定繳交)：□精簡報告　■完整報告

本成果報告包括以下應繳交之附件：

□赴國外出差或研習心得報告一份

□赴大陸地區出差或研習心得報告一份

□出席國際學術會議心得報告及發表之論文各一份

□國際合作研究計畫國外研究報告書一份

執行單位：國立交通大學

中　華　民　國　102 年 11 月 10 日

Table of Contents

Abstract

An eigenfunction expansion approach is combined with a power series solution technique to establish the asymptotic solutions for geometrically induced electroelastic singularities in piezoelectric bodies of revolution and wedges, with arbitrary direction of polarization. The asymptotic solutions are obtained by directly solving the three-dimensional equilibrium and Maxwell's equations in terms of displacement components and electric potential. Since the direction of polarization can be arbitrary in space, the in-plane components of displacement and electric field are generally coupled with the out-of-plane components, and the coupling substantially complicates the solutions. The correctness of the proposed solutions are confirmed by comparing the present results with the published results obtained by assuming axisymmetric deformation or generalized plane deformation. The numerical results related to singularity orders are shown for bodies of revolution and wedges that comprise a single material (PZT-4 or PZT-5H) or bonded piezo/piezo (PZT-4/PZT-5H) or piezo/isotropic elastic (PZT-4/Al or PZT-5H/Al) materials. The numerical results concerning the order of the singularity are expressed in graphic form, and are shown herein for the first time.

Key words: electroelastic singularities, piezoelectric bodies of revolution, piezoelectric wedges, three-dimnsional asymptotic solutions, eigenfunction expansion approach

摘要

本研究透過特徵函數展開法配合級數解建立電磁彈性迴轉體與楔形體之三維電磁彈奇異性漸近解。直接求解於以位移與電勢表示的三維力平衡與馬克斯威爾(Maxwell) 方程組之漸近解。由於考慮材料具任意之極化方向，造成面外與面內之位移與電場彼此耦合，導致求解之困難度。透過與文獻中假設軸對稱變形或廣義平面變形所得結果比較，驗證本研究所得解之正確性。根據漸近解，將探討有關於極化方向、幾何形狀、材料種類與邊界條件對於電磁彈性與壓電迴轉體與楔型體奇異性階數之影響；其中迴轉體與楔形體可為單一壓電材料(PZT-4 與 PZT-6B) 、壓電/各向同向性彈性材料(PZT-4/Si 或 PZT-6B/Si)或雙壓電材料(PZT-4/PZT-6B)。所得數值結果以圖表示，本研究所得均首見於文獻。

關鍵詞：奇異性、壓電迴轉體、壓電楔形體、三維漸近解、特徵函數展開法

I. Introduction

1.1 Literature Review

Piezoelectric material is a widely used, smart or intelligent material, because of the intrinsic effects of coupling between electric fields and mechanical deformation. Piezoelectric materials have been extensively applied in actuators, resonators, oscillators, conductors and sensors. The most interesting feature of piezoelectric materials is that they can serve not only as actuators, providing driving signals, but also as sensors for smart structures. In the practical applications, electroelastic singularities are commonly observed at a sharp corner or because of discontinuity in material properties. Accordingly, either local mechanical failure or dielectric failure can occur at a sharp corner. Understanding of the electroelastic singularity behaviors of piezoelectric wedges is essential to optimize the design of piezoelectric devices and further advance smart material technology. Furthermore, an accurate numerical analysis of problems that involve stress singularities depends on knowledge of such stress singularity behaviors. The two typical geometries that are commonly considered in the literature on geometrically induced stress singularities are wedges and bodies of revolution.

The stress singularities in a wedge have been comprehensively examined. Since Williams (1952a) pioneered the investigation of stress singularities of plates under extension, many studies of stress singularities in wedges of a single material or multiple materials have been carried out, based on the plane strain or stress assumption (e.g. Williams, 1952b; Hein and Erdogan, 1971; England, 1971; Bogy and Wang, 1971; Dempsey and Sinclair, 1981; Ying and Katz, 1987) or three-dimensional elasticity theory (e.g. Hartranft and Sih, 1969; Chaudhuri and Xie, 2000). Geometrically induced stress singularities in plates of a single material and multiple materials have also been extensively studied using classical thin plate theory (e.g. Williams, 1952c; Williams and Owens, 1954), first-order shear deformation plate theory (e.g. Burton and Sinclair, 1986; Huang, 2002a; Huang, 2003; Saidi et al., 2010; McGee and Kim, 2005), and third–order plate theory (Huang, 2002b).

Numerous analyses of stress singularities for elastic bodies of revolution are also available. Making an assumption of axisymmetric deformation, Zak (1964) utilized the Love stress approach (Love, 1927) to investigate geometrically induced stress singularities in bodies of revolution that were made of a single material, while Li *et al.* (1998, 2000) adopted the Love stress approach and Boussinesq's solution (Timoshenko and Goodier, 1970) respectively, to obtain the stress field near the bond edge of a bi-material body of revolution. Ting *et al*. (1985) presented eigenfunctions at a singular point of a body of revolution made of transversely isotropic material. Without assuming axisymmetric deformation, Huang and Leissa (2007) presented three-dimensional sharp corner displacement functions for bodies of revolution, and further studied the geometrically induced stress singularities in bimaterial bodies of revolution (Huang and Leissa, 2008).

A few studies of the geometrically-induced electroelastic singularities at the vertex of a piezoelectric wedge (Fig. 2.1) are based on the assumption that all physical quantities under consideration depend on the planar coordinates. Based on the plane strain assumption (ε_{zz}, ε_{zy}, ε_{zx}, and E_z, which are defined in Chapter 2, equal zero), Xu and Rajapakse (2000) extended Lekhnitskii's complex potential functions for in-plane stresses and electric displacement components to examine the electroelastic singularities at the vertex of a piezoelectric wedge that has a direction of polarization on the *x*-*y* plane (see Fig. 2.1). Based on an assumption of generalized plane deformation, Chue and Chen (2002) presented a decoupled formulation of piezoelectric elasticity and applied it to examine the stress singularities near the apex of a rectilinearly polarized piezoelectric wedge, considering its direction of polarization in the *x*-*y* plane or along the z-axis. Hwu and Ikeda (2008) proposed an extended Stroh formulation in an (*x*, *y*) coordinate system by considering a generalized plane strain and short circuit ($\varepsilon_{zz} = 0$ and $E_z = 0$) and presented numerical results for the electroelastic singularities at the vertices of piezoelectric wedges and multi-material wedges with the directions of polarization in the *x*-*y* plane. Because different plane assumptions were made in these three cited papers, they employed different constitutive laws in their solutions. Notably, Xu and Rajapakse (2000) treated the piezoelectric material as transversely isotropic material as they began to develop solutions while Chue and Chen (2002) and Hwu and Ikeda (2008) treated piezoelectric material as generally anisotropic. The solutions of Xu and Rajapakse (2000) include only in-plane physical quantities, while those of Chue and Chen (2002) and Hwu and Ikeda (2008) included in-plane and out-of-plane physical quantities. Following the assumptions in Chue and Chen (2002), Chen, Chu and Lee (2004) employed the extended Lekhnitskii formulation to determine the eletroelastic singularity behaviors near the apex of a piezoelectric wedge that was polarized in the radial, circular, or axial direction. Chu and Chen (2003) applied the Mellin transform to determine anti-plane stress singularities in a bonded bi-material piezoelectric wedge. Neglecting all out-of-plane physical quantities, Shang and Kitamura (2005) utilized a modified version of the general solution that was developed by Wang and Zheng (1995) and Shang et al. (2005) to investigate the stress singularities at the interface edge of a wedge made of two piezoelectric materials with the direction of polarization parallel to the *x*-axis.

A review of the literature reveals only two investigations that considered eletroelastic singularities in a piezoelectric body of revolution, based on axisymmetric deformation assumptions. To perform stress singularity analysis of axisymmetric piezoelectric bonded structures, Xu and Mutoh (2001) adopted the general solutions for coupled equations for piezoelectric material that was developed by Ding *et al.* (1996), while Li and Sato (2002) extended the method proposed by Ting *et al*. (1985) for an elastic material. These solutions

consist of four and three quasi-harmonic functions, respectively. In these two works, the direction of polarization of the piezoelectric material was assumed to be along the axis of revolution.

1.2 **Purposes of Research**

The main purpose of the present research is to develop an asymptotic solution for the eletroelastic singularities in a piezoelectric body of revolution and wedge without any restrictions on the direction of polarization of the material. When a piezoelectric material is considered to be transversely isotropic, and the axis of material symmetry is not parallel to the axis of revolution, the assumption of axisymmetric deformation is no longer valid. Since the direction of polarization can be arbitrary in space, the in-plane components of displacement and electric field are generally coupled with the out-of-plane components. An eigenfunction expansion approach combined with a power series method is adopted to solve the equilibrium and Maxwell's equations in terms of mechanical displacement components and electric potential. The correctness of the proposed solution is confirmed by comparing the present results with the published results in cases in which the direction of polarization is along some special directions. Analyses are performed on bodies that comprise a single piezoelectric material (PZT-4 or PZT-5H), bonded piezo/piezo (PZT-4/PZT-5H) or piezo/isotropic elastic (PZT-4/Al or PZT-5H/Al) materials. The effects of geometry of body, polarization orientation, material type(s) and boundary conditions on the singularity orders are comprehensively examined. The numerical results concerning the order of the singularity are expressed in graphic form, and are shown herein for the first time.

II **Asymptotic Solutions for a Wedge**

2.1 **Basic Formulation**

Consider a rectilinearly anisotropic piezoelectric wedge that is polarized in the $\hat{z}$ direction, as presented in Fig. 2.1. The constitutive equations of the piezoelectric material are expressed in the material coordinate system ($\hat{x},\hat{y},\hat{z}$) , as

$$\{\hat{\sigma}\}=[\hat{c}]\{\hat{\varepsilon}\}-[\hat{e}]^T\{\hat{E}\}, \tag{2.1a}$$

$$\{\hat{D}\}=[\hat{e}]\{\hat{\varepsilon}\}+[\hat{\eta}]\{\hat{E}\}, \tag{2.1b}$$

where $\{\hat{\sigma}\}=\{\sigma_{\hat{x}\hat{x}} \quad \sigma_{\hat{y}\hat{y}} \quad \sigma_{\hat{z}\hat{z}} \quad \sigma_{\hat{y}\hat{z}} \quad \sigma_{\hat{z}\hat{x}} \quad \sigma_{\hat{x}\hat{y}}\}^T$ is the stress vector; $\{\hat{\varepsilon}\}=\{\varepsilon_{\hat{x}\hat{x}} \quad \varepsilon_{\hat{y}\hat{y}} \quad \varepsilon_{\hat{z}\hat{z}} \quad 2\varepsilon_{\hat{y}\hat{z}} \quad 2\varepsilon_{\hat{z}\hat{x}} \quad 2\varepsilon_{\hat{x}\hat{y}}\}^T$ is the strain vector; $\{\hat{D}\}=\{D_{\hat{x}} \quad D_{\hat{y}} \quad D_{\hat{z}}\}^T$ is the electric displacement vector; $\{\hat{E}\}=\{E_{\hat{x}} \quad E_{\hat{y}} \quad E_{\hat{z}}\}^T$ is the electric field vector, and $[\hat{c}]$, $[\hat{e}]$ and $[\hat{\eta}]$ are the mechanical elastic constant matrix, the piezoelectric constant matrix and the dielectric constant matrix, respectively.

It is easy to solve for the eletroelastic singularities at the vertex of the wedge in the cylindrical coordinate system (r,θ,z) given in Fig. 2.1. In the cylindrical coordinate system, the equilibrium and Maxwell's equations in terms of stress components (σ_{ij}) and electric displacements (D_i) without body force and charges are

$$\frac{\partial\sigma_{rr}}{\partial r}+\frac{1}{r}\frac{\partial\sigma_{r\theta}}{\partial\theta}+\frac{\partial\sigma_{rz}}{\partial z}+\frac{(\sigma_{rr}-\sigma_{\theta\theta})}{r}=0, \tag{2.2a}$$

$$\frac{\partial\sigma_{r\theta}}{\partial r}+\frac{1}{r}\frac{\partial\sigma_{\theta\theta}}{\partial\theta}+\frac{\partial\sigma_{\theta z}}{\partial z}+2\frac{\sigma_{r\theta}}{r}=0, \tag{2.2b}$$

$$\frac{\partial\sigma_{rz}}{\partial r}+\frac{1}{r}\frac{\partial\sigma_{\theta z}}{\partial\theta}+\frac{\partial\sigma_{zz}}{\partial z}+\frac{\sigma_{rz}}{r}=0, \tag{2.2c}$$

$$\frac{1}{r}\frac{\partial(rD_r)}{\partial r}+\frac{1}{r}\frac{\partial D_\theta}{\partial\theta}+\frac{\partial D_z}{\partial z}=0, \tag{2.2d}$$

The constitutive equations of the piezoelectric material in the cylindrical coordinate system are

$$\{\sigma\}=[c]\{\varepsilon\}-[e]\{E\}, \tag{2.3a}$$

$$\{D\}=[e]^T\{\varepsilon\}+[\eta]\{E\}, \tag{2.3b}$$

where $\{\sigma\}=\{\sigma_{rr} \quad \sigma_{\theta\theta} \quad \sigma_{zz} \quad \sigma_{\theta z} \quad \sigma_{zr} \quad \sigma_{r\theta}\}^T$, $\{\varepsilon\}=\{\varepsilon_{rr} \quad \varepsilon_{\theta\theta} \quad \varepsilon_{zz} \quad 2\varepsilon_{\theta z} \quad 2\varepsilon_{zr} \quad 2\varepsilon_{r\theta}\}^T$,

$$\{D\}=\{D_r \quad D_\theta \quad D_z\}^T,\ \{E\}=\{E_r \quad E_\theta \quad E_z\}^T,$$

$$[c]=\begin{bmatrix} c_{11} & c_{12} & c_{13} & c_{14} & c_{15} & c_{16} \\ c_{12} & c_{22} & c_{23} & c_{24} & c_{25} & c_{26} \\ c_{13} & c_{23} & c_{33} & c_{34} & c_{35} & c_{36} \\ c_{14} & c_{24} & c_{34} & c_{44} & c_{45} & c_{46} \\ c_{15} & c_{25} & c_{35} & c_{45} & c_{55} & c_{56} \\ c_{16} & c_{26} & c_{36} & c_{46} & c_{56} & c_{66} \end{bmatrix},\quad [e]=\begin{bmatrix} e_{11} & e_{12} & e_{13} & e_{14} & e_{15} & e_{16} \\ e_{21} & e_{22} & e_{23} & e_{24} & e_{25} & e_{26} \\ e_{31} & e_{32} & e_{33} & e_{34} & e_{35} & e_{36} \end{bmatrix},$$

$$[\eta]=\begin{bmatrix} \eta_{11} & \eta_{12} & \eta_{13} \\ \eta_{12} & \eta_{22} & \eta_{23} \\ \eta_{13} & \eta_{23} & \eta_{33} \end{bmatrix}. \tag{2.4}$$

The components of $[c]$, $[e]$ and $[\eta]$ are related to the components of $[\hat{c}]$, $[\hat{e}]$ and $[\hat{\eta}]$, respectively; and are functions of θ and depend on the direction cosines between ($\hat{x},\hat{y},\hat{z}$) and (*x*, *y*, *z*). These relations are given in Appendix I.

Substituting strain-displacement relations and electric field-potential relations into Eqs. (2.3) and (2.4) enables the stress components and electric displacements to be expressed in terms of mechanical displacement components (u_r, u_θ and u_z) and electric potential (φ), given in Appendix II. Substituting those expressions into Eqs. (2.2) yields the governing equations in terms of mechanical displacement components and electric potential as

$$\left[c_{11}\frac{\partial^2}{\partial r^2}+c_{55}\frac{\partial^2}{\partial z^2}+\left(c_{11}+\frac{\partial c_{16}}{\partial\theta}\right)\frac{\partial}{r\partial r}+\left(c_{15}+\frac{\partial c_{56}}{\partial\theta}\right)\frac{\partial}{r\partial z}+\frac{\partial c_{66}}{\partial\theta}\frac{\partial}{r^2\partial\theta}+2c_{16}\frac{\partial^2}{r\partial r\partial\theta}+2c_{56}\frac{\partial^2}{r\partial\theta\partial z}\right.$$

$$\left.+2c_{15}\frac{\partial^2}{\partial r\partial z}+\left(-c_{22}+\frac{\partial c_{26}}{\partial\theta}+c_{66}\frac{\partial^2}{\partial\theta^2}\right)\frac{1}{r^2}\right]u_r+\left[c_{16}\frac{\partial^2}{\partial r^2}+c_{45}\frac{\partial^2}{\partial z^2}+\left(-c_{26}+\frac{\partial c_{66}}{\partial\theta}\right)\frac{\partial}{r\partial r}\right.$$

$$+\left(c_{14}-c_{24}-c_{56}+\frac{\partial c_{46}}{\partial\theta}\right)\frac{\partial}{r\partial z}+\left(-c_{22}-c_{66}+\frac{\partial c_{26}}{\partial\theta}\right)\frac{\partial}{r^2\partial\theta}+(c_{12}+c_{66})\frac{\partial^2}{r\partial r\partial\theta}+(c_{25}+c_{46})\frac{\partial^2}{r\partial\theta\partial z}$$

$$+(c_{14}+c_{56})\frac{\partial^2}{\partial r\partial z}+\left(c_{26}-\frac{\partial c_{66}}{\partial\theta}+c_{26}\frac{\partial^2}{\partial\theta^2}\right)\frac{1}{r^2}\left]u_\theta+\right[c_{15}\frac{\partial^2}{\partial r^2}+c_{35}\frac{\partial^2}{\partial z^2}+\left(c_{15}-c_{25}+\frac{\partial c_{56}}{\partial\theta}\right)\frac{\partial}{r\partial r}\right.$$

$$+\left(c_{13}-c_{23}+\frac{\partial c_{36}}{\partial\theta}\right)\frac{\partial}{r\partial z}+\left(-c_{24}+\frac{\partial c_{46}}{\partial\theta}\right)\frac{\partial}{r^2\partial\theta}+(c_{14}+c_{56})\frac{\partial^2}{r\partial r\partial\theta}+(c_{36}+c_{45})\frac{\partial^2}{r\partial\theta\partial z}$$

$$\left.+(c_{13}+c_{55})\frac{\partial^2}{\partial r\partial z}+c_{46}\frac{\partial^2}{r^2\partial\theta^2}\right]u_z+\left[e_{11}\frac{\partial^2}{\partial r^2}+e_{35}\frac{\partial^2}{\partial z^2}+\left(e_{11}-e_{12}+\frac{\partial e_{16}}{\partial\theta}\right)\frac{\partial}{r\partial r}\right.$$

$$+\left(e_{31}-e_{32}+\frac{\partial e_{36}}{\partial\theta}\right)\frac{\partial}{r\partial z}+\left(-e_{22}+\frac{\partial e_{26}}{\partial\theta}\right)\frac{\partial}{r^2\partial\theta}+\left(e_{16}+e_{21}\right)\frac{\partial^2}{r\partial r\partial\theta}+\left(e_{25}+e_{36}\right)\frac{\partial^2}{r\partial\theta\partial z}$$

$$+\left(e_{31}+e_{15}\right)\frac{\partial^2}{\partial r\partial z}+e_{26}\frac{\partial^2}{r^2\partial\theta^2}\Bigg]\varphi=0\,, \tag{2.5a}$$

$$\Bigg[c_{16}\frac{\partial^2}{\partial r^2}+c_{45}\frac{\partial^2}{\partial z^2}+\left(2c_{16}+c_{26}+\frac{\partial c_{12}}{\partial\theta}\right)\frac{\partial}{r\partial r}+\left(2c_{56}+c_{24}+\frac{\partial c_{25}}{\partial\theta}\right)\frac{\partial}{r\partial z}+\left(c_{22}+c_{66}+\frac{\partial c_{26}}{\partial\theta}\right)\frac{\partial}{r^2\partial\theta}$$

$$+\left(c_{12}+c_{66}\right)\frac{\partial^2}{r\partial r\partial\theta}+\left(c_{25}+c_{46}\right)\frac{\partial^2}{r\partial\theta\partial z}+\left(c_{56}+c_{14}\right)\frac{\partial^2}{\partial r\partial z}+\left(c_{26}+\frac{\partial c_{22}}{\partial\theta}+c_{26}\frac{\partial^2}{\partial\theta^2}\right)\frac{1}{r^2}\Bigg]u_r$$

$$+\Bigg[c_{66}\frac{\partial^2}{\partial r^2}+c_{44}\frac{\partial^2}{\partial z^2}+\left(c_{66}+\frac{\partial c_{26}}{\partial\theta}\right)\frac{\partial}{r\partial r}+\left(c_{46}+\frac{\partial c_{24}}{\partial\theta}\right)\frac{\partial}{r\partial z}+\left(\frac{\partial c_{22}}{\partial\theta}\right)\frac{\partial}{r^2\partial\theta}+2c_{26}\frac{\partial^2}{r\partial r\partial\theta}$$

$$+2c_{24}\frac{\partial^2}{r\partial\theta\partial z}+2c_{46}\frac{\partial^2}{\partial r\partial z}+\left(-c_{66}-\frac{\partial c_{26}}{\partial\theta}+c_{22}\frac{\partial^2}{\partial\theta^2}\right)\frac{1}{r^2}\Bigg]u_\theta+\Bigg[c_{56}\frac{\partial^2}{\partial r^2}+c_{34}\frac{\partial^2}{\partial z^2}+\left(2c_{56}+\frac{\partial c_{25}}{\partial\theta}\right)$$

$$\times\frac{\partial}{r\partial r}+\left(2c_{36}+\frac{\partial c_{23}}{\partial\theta}\right)\frac{\partial}{r\partial z}+\left(c_{46}+\frac{\partial c_{24}}{\partial\theta}\right)\frac{\partial}{r^2\partial\theta}+\left(c_{25}+c_{46}\right)\frac{\partial^2}{r\partial r\partial\theta}+\left(c_{23}+c_{44}\right)\frac{\partial^2}{r\partial\theta\partial z}$$

$$+\left(c_{36}+c_{45}\right)\frac{\partial^2}{\partial r\partial z}+c_{24}\frac{\partial^2}{r^2\partial\theta^2}\Bigg]u_z+\Bigg[e_{16}\frac{\partial^2}{\partial r^2}+e_{34}\frac{\partial^2}{\partial z^2}+\left(2e_{16}+\frac{\partial e_{12}}{\partial\theta}\right)\frac{\partial}{r\partial r}+\left(2e_{36}+\frac{\partial e_{32}}{\partial\theta}\right)\frac{\partial}{r\partial z}$$

$$+\left(e_{26}+\frac{\partial e_{22}}{\partial\theta}\right)\frac{\partial}{r^2\partial\theta}+\left(e_{12}+e_{26}\right)\frac{\partial^2}{r\partial r\partial\theta}+\left(e_{24}+e_{32}\right)\frac{\partial^2}{r\partial\theta\partial z}+\left(e_{36}+e_{14}\right)\frac{\partial^2}{\partial r\partial z}+e_{22}\frac{\partial^2}{r^2\partial\theta^2}\Bigg]\varphi=0\,,$$

(2.5b)

$$\Bigg[c_{15}\frac{\partial^2}{\partial r^2}+c_{35}\frac{\partial^2}{\partial z^2}+\left(c_{15}+c_{25}+\frac{\partial c_{14}}{\partial\theta}\right)\frac{\partial}{r\partial r}+\left(c_{23}+c_{55}+\frac{\partial c_{45}}{\partial\theta}\right)\frac{\partial}{r\partial z}+\left(c_{24}+\frac{\partial c_{46}}{\partial\theta}\right)\frac{\partial}{r^2\partial\theta}+\left(c_{14}+c_{56}\right)$$

$$\times\frac{\partial^2}{r\partial r\partial\theta}+\left(c_{45}+c_{36}\right)\frac{\partial^2}{r\partial\theta\partial z}+\left(c_{55}+c_{13}\right)\frac{\partial^2}{\partial r\partial z}+\left(\frac{\partial c_{24}}{\partial\theta}+c_{46}\frac{\partial^2}{\partial\theta^2}\right)\frac{1}{r^2}\Bigg]u_r+\Bigg[c_{56}\frac{\partial^2}{\partial r^2}+c_{34}\frac{\partial^2}{\partial z^2}$$

$$+\left(\frac{\partial c_{46}}{\partial\theta}\right)\frac{\partial}{r\partial r}+\left(c_{45}-c_{36}+\frac{\partial c_{44}}{\partial\theta}\right)\frac{\partial}{r\partial z}+\left(-c_{46}+\frac{\partial c_{24}}{\partial\theta}\right)\frac{\partial}{r^2\partial\theta}+\left(c_{25}+c_{46}\right)\frac{\partial^2}{r\partial r\partial\theta}+\left(c_{44}+c_{23}\right)$$

$$\times\frac{\partial^2}{r\partial\theta\partial z}+\left(c_{45}+c_{36}\right)\frac{\partial^2}{\partial r\partial z}+\left(-\frac{\partial c_{46}}{\partial\theta}+c_{24}\frac{\partial^2}{\partial\theta^2}\right)\frac{1}{r^2}\Bigg]u_\theta+\Bigg[c_{55}\frac{\partial^2}{\partial r^2}+c_{33}\frac{\partial^2}{\partial z^2}+\left(c_{55}+\frac{\partial c_{45}}{\partial\theta}\right)\frac{\partial}{r\partial r}$$

$$+\left(c_{35}+\frac{\partial c_{34}}{\partial\theta}\right)\frac{\partial}{r\partial z}+\left(\frac{\partial c_{44}}{\partial\theta}\right)\frac{\partial}{r^2\partial\theta}+2c_{45}\frac{\partial^2}{r\partial r\partial\theta}+2c_{34}\frac{\partial^2}{r\partial\theta\partial z}+2c_{35}\frac{\partial^2}{\partial r\partial z}+c_{44}\frac{\partial^2}{r^2\partial\theta^2}\Bigg]u_z$$

$$+\Bigg[e_{15}\frac{\partial^2}{\partial r^2}+e_{33}\frac{\partial^2}{\partial z^2}+\left(e_{15}+\frac{\partial e_{14}}{\partial\theta}\right)\frac{\partial}{r\partial r}+\left(e_{35}+\frac{\partial e_{34}}{\partial\theta}\right)\frac{\partial}{r\partial z}+\left(\frac{\partial e_{24}}{\partial\theta}\right)\frac{\partial}{r^2\partial\theta}+\left(e_{25}+e_{14}\right)\frac{\partial^2}{r\partial r\partial\theta}$$

$$+\left(e_{34}+e_{23}\right)\frac{\partial^2}{r\partial\theta\partial z}+\left(e_{35}+e_{13}\right)\frac{\partial^2}{\partial r\partial z}+e_{24}\frac{\partial^2}{r^2\partial\theta^2}\Bigg]\varphi=0\,, \tag{2.5c}$$

$$\Bigg[e_{11}\frac{\partial^2}{\partial r^2}+e_{35}\frac{\partial^2}{\partial z^2}+\left(e_{11}+e_{12}+\frac{\partial e_{21}}{\partial\theta}\right)\frac{\partial}{r\partial r}+\left(e_{15}+e_{32}+\frac{\partial e_{25}}{\partial\theta}\right)\frac{\partial}{r\partial z}+\left(e_{22}+\frac{\partial e_{26}}{\partial\theta}\right)\frac{\partial}{r^2\partial\theta}$$

$$+\left(e_{16}+e_{21}\right)\frac{\partial^2}{r\partial r\partial\theta}+\left(e_{25}+e_{36}\right)\frac{\partial^2}{r\partial\theta\partial z}+\left(e_{15}+e_{31}\right)\frac{\partial^2}{\partial r\partial z}+\left(\frac{\partial e_{22}}{\partial\theta}+e_{26}\frac{\partial^2}{\partial\theta^2}\right)\frac{1}{r^2}\Bigg]u_r+\Bigg[e_{16}\frac{\partial^2}{\partial r^2}$$

$$+e_{34}\frac{\partial^2}{\partial z^2}+\left(\frac{\partial e_{26}}{\partial\theta}\right)\frac{\partial}{r\partial r}+\left(e_{14}-e_{36}+\frac{\partial e_{24}}{\partial\theta}\right)\frac{\partial}{r\partial z}+\left(-e_{26}+\frac{\partial e_{22}}{\partial\theta}\right)\frac{\partial}{r^2\partial\theta}+\left(e_{12}+e_{26}\right)\frac{\partial^2}{r\partial r\partial\theta}$$

$$+\left(e_{24}+e_{32}\right)\frac{\partial^2}{r\partial\theta\partial z}+\left(e_{14}+e_{36}\right)\frac{\partial^2}{\partial r\partial z}+\left(-\frac{\partial e_{26}}{\partial\theta}+e_{22}\frac{\partial^2}{\partial\theta^2}\right)\frac{1}{r^2}\Bigg]u_\theta+\Bigg[e_{15}\frac{\partial^2}{\partial r^2}+e_{33}\frac{\partial^2}{\partial z^2}$$

$$+\left(e_{15}+\frac{\partial e_{25}}{\partial\theta}\right)\frac{\partial}{r\partial r}+\left(e_{13}+\frac{\partial e_{23}}{\partial\theta}\right)\frac{\partial}{r\partial z}+\left(\frac{\partial e_{24}}{\partial\theta}\right)\frac{\partial}{r^2\partial\theta}+\left(e_{14}+e_{25}\right)\frac{\partial^2}{r\partial r\partial\theta}+\left(e_{23}+e_{34}\right)\frac{\partial^2}{r\partial\theta\partial z}$$

$$+\left(e_{13}+e_{35}\right)\frac{\partial^2}{r\partial r\partial z}+e_{24}\frac{\partial^2}{r^2\partial\theta^2}\Bigg]u_z-\Bigg[\eta_{11}\frac{\partial^2}{\partial r^2}+\eta_{33}\frac{\partial^2}{\partial z^2}+\left(\eta_{11}+\frac{\partial\eta_{12}}{\partial\theta}\right)\frac{\partial}{r\partial r}+\left(\frac{\partial\eta_{22}}{\partial\theta}\right)\frac{\partial}{r^2\partial\theta}$$

$$+\left(\eta_{13}+\frac{\partial\eta_{23}}{\partial\theta}\right)\frac{\partial}{r\partial z}+2\eta_{12}\frac{\partial^2}{r\partial r\partial\theta}+2\eta_{23}\frac{\partial^2}{r\partial\theta\partial z}+2\eta_{13}\frac{\partial^2}{\partial r\partial z}+\eta_{22}\frac{\partial^2}{r^2\partial\theta^2}\Bigg]\varphi=0\,. \tag{2.5d}$$

2.2. **Construction of Asymptotic Solution**

To determine the asymptotic solution of Eqs. (2.5) as r approaches zero, the mechanical displacement components and electric potential in the double series can be conveniently expanded as follows;

$$u_r\left(r,\theta,z\right)=\sum_{m=0}^{\infty}\sum_{n=0}^{\infty}r^{\lambda_m+n}\hat{U}_n^{(m)}\left(\theta,z\right), \tag{2.6a}$$

$$u_\theta(r,\theta,z)=\sum_{m=0}^{\infty}\sum_{n=0}^{\infty} r^{\lambda_m+n}\hat{V}_n^{(m)}(\theta,z), \tag{2.6b}$$

$$u_z(r,\theta,z)=\sum_{m=0}^{\infty}\sum_{n=0}^{\infty} r^{\lambda_m+n}\hat{W}_n^{(m)}(\theta,z), \tag{2.6c}$$

$$\varphi(r,\theta,z)=\sum_{m=0}^{\infty}\sum_{n=0}^{\infty} r^{\lambda_m+n}\hat{\Phi}_n^{(m)}(\theta,z), \tag{2.6d}$$

where the characteristic values λ_m are assumed to be constants and can be complex numbers. The real part of λ_m has to be positive to satisfy the regularity conditions for mechanical displacement components and electric potential at r=0 (such as finite displacement and electric potential at r=0).

Substituting Eqs. (2.6) into Eqs. (2.5) and carefully arranging the resulting equations yields

$$\sum_{m=0}^{\infty}\sum_{n=0}^{\infty} r^{\lambda_m+n-2}\Bigg[c_{11}(\lambda_m+n)(\lambda_m+n-1)\hat{U}_n^{(m)}+\left(c_{11}+\frac{\partial c_{16}}{\partial\theta}\right)(\lambda_m+n)\hat{U}_n^{(m)}+\frac{\partial c_{66}}{\partial\theta}\frac{\partial\hat{U}_n^{(m)}}{\partial\theta}+2c_{16}(\lambda_m+n)\times$$

$$\frac{\partial\hat{U}_n^{(m)}}{\partial\theta}+\left(-c_{22}+\frac{\partial c_{26}}{\partial\theta}+c_{66}\frac{\partial^2}{\partial\theta^2}\right)\hat{U}_n^{(m)}+c_{16}(\lambda_m+n)(\lambda_m+n-1)\hat{V}_n^{(m)}+\left(-c_{26}+\frac{\partial c_{66}}{\partial\theta}\right)(\lambda_m+n)\hat{V}_n^{(m)}$$

$$+\left(-c_{22}-c_{66}+\frac{\partial c_{26}}{\partial\theta}\right)\frac{\partial\hat{V}_n^{(m)}}{\partial\theta}+(c_{12}+c_{66})(\lambda_m+n)\frac{\partial\hat{V}_n^{(m)}}{\partial\theta}+\left(c_{26}-\frac{\partial c_{66}}{\partial\theta}+c_{26}\frac{\partial^2}{\partial\theta^2}\right)\hat{V}_n^{(m)}+c_{15}(\lambda_m+n)\times$$

$$(\lambda_m+n-1)\hat{W}_n^{(m)}+\left(c_{15}-c_{25}+\frac{\partial c_{56}}{\partial\theta}\right)(\lambda_m+n)\hat{W}_n^{(m)}+\left(-c_{24}+\frac{\partial c_{46}}{\partial\theta}\right)\frac{\partial\hat{W}_n^{(m)}}{\partial\theta}+(c_{14}+c_{56})(\lambda_m+n)\frac{\partial\hat{W}_n^{(m)}}{\partial\theta}$$

$$+c_{46}\frac{\partial^2\hat{W}_n^{(m)}}{\partial\theta^2}+e_{11}(\lambda_m+n)(\lambda_m+n-1)\hat{\Phi}_n^{(m)}+\left(e_{11}-e_{12}+\frac{\partial e_{16}}{\partial\theta}\right)(\lambda_m+n)\hat{\Phi}_n^{(m)}+\left(-e_{22}+\frac{\partial e_{26}}{\partial\theta}\right)\frac{\partial\hat{\Phi}_n^{(m)}}{\partial\theta}$$

$$+(e_{16}+e_{21})(\lambda_m+n)\frac{\partial\hat{\Phi}_n^{(m)}}{\partial\theta}+e_{26}\frac{\partial^2\hat{\Phi}_n^{(m)}}{\partial\theta^2}\Bigg]+r^{\lambda_m+n-1}\Bigg[\left(c_{15}+\frac{\partial c_{56}}{\partial\theta}\right)\frac{\partial\hat{U}_n^{(m)}}{\partial z}+2c_{56}\frac{\partial^2\hat{U}_n^{(m)}}{\partial\theta\partial z}+2c_{15}(\lambda_m+n)\times$$

$$\frac{\partial\hat{U}_n^{(m)}}{\partial z}+\left(c_{14}-c_{24}-c_{56}+\frac{\partial c_{46}}{\partial\theta}\right)\frac{\partial\hat{V}_n^{(m)}}{\partial z}+(c_{25}+c_{46})\frac{\partial^2\hat{V}_n^{(m)}}{\partial\theta\partial z}+(c_{14}+c_{56})(\lambda_m+n)\frac{\partial\hat{V}_n^{(m)}}{\partial z}+(c_{36}+c_{45})\times$$

$$\frac{\partial^2\hat{W}_n^{(m)}}{\partial\theta\partial z}+\left(c_{13}-c_{23}+\frac{\partial c_{36}}{\partial\theta}\right)\frac{\partial\hat{W}_n^{(m)}}{\partial z}+(c_{13}+c_{55})(\lambda_m+n)\frac{\partial\hat{W}_n^{(m)}}{\partial z}+\left(e_{31}-e_{32}+\frac{\partial e_{36}}{\partial\theta}\right)\frac{\partial\hat{\Phi}_n^{(m)}}{\partial z}+(e_{25}+e_{36})\times$$

$$\frac{\partial^2\hat{\Phi}_n^{(m)}}{\partial\theta\partial z}+(e_{31}+e_{15})(\lambda_m+n)\frac{\partial\hat{\Phi}_n^{(m)}}{\partial z}\Bigg]+r^{\lambda_m+n}\left(c_{55}\frac{\partial^2\hat{U}_n^{(m)}}{\partial z^2}+c_{45}\frac{\partial^2\hat{V}_n^{(m)}}{\partial z^2}+c_{35}\frac{\partial^2\hat{W}_n^{(m)}}{\partial z^2}+e_{35}\frac{\partial^2\hat{\Phi}_n^{(m)}}{\partial z^2}\right)=0$$

(2.7a)

$$\sum_{m=0}^{\infty}\sum_{n=0}^{\infty} r^{\lambda_m+n-2}\left[c_{16}\left(\lambda_m+n\right)\left(\lambda_m+n-1\right)\hat{U}_n^{(m)} + \left(2c_{16}+c_{26}+\frac{\partial c_{12}}{\partial\theta}\right)\left(\lambda_m+n\right)\hat{U}_n^{(m)} + \left(c_{22}+c_{66}+\frac{\partial c_{26}}{\partial\theta}\right)\frac{\partial\hat{U}_n^{(m)}}{\partial\theta}\right.$$

$$+\left(c_{12}+c_{66}\right)\left(\lambda_m+n\right)\frac{\partial\hat{U}_n^{(m)}}{\partial\theta} + \left(c_{26}+\frac{\partial c_{22}}{\partial\theta}+c_{26}\frac{\partial^2}{\partial\theta^2}\right)\hat{U}_n^{(m)} + c_{66}\left(\lambda_m+n\right)\left(\lambda_m+n-1\right)\hat{V}_n^{(m)} + \left(\frac{\partial c_{22}}{\partial\theta}\right)\frac{\partial\hat{V}_n^{(m)}}{\partial\theta}$$

$$+\left(c_{66}+\frac{\partial c_{26}}{\partial\theta}\right)\left(\lambda_m+n\right)\hat{V}_n^{(m)} + 2c_{26}\left(\lambda_m+n\right)\frac{\partial\hat{V}_n^{(m)}}{\partial\theta} + \left(-c_{66}-\frac{\partial c_{26}}{\partial\theta}+c_{22}\frac{\partial^2}{\partial\theta^2}\right)\hat{V}_n^{(m)} + c_{56}\left(\lambda_m+n\right)\times$$

$$\left(\lambda_m+n-1\right)\hat{W}_n^{(m)} + \left(2c_{56}+\frac{\partial c_{25}}{\partial\theta}\right)\left(\lambda_m+n\right)\hat{W}_n^{(m)} + \left(c_{46}+\frac{\partial c_{24}}{\partial\theta}\right)\frac{\partial\hat{W}_n^{(m)}}{\partial\theta} + \left(c_{25}+c_{46}\right)\left(\lambda_m+n\right)\frac{\partial\hat{W}_n^{(m)}}{\partial\theta}$$

$$+c_{24}\frac{\partial^2\hat{W}_n^{(m)}}{\partial\theta^2} + e_{16}\left(\lambda_m+n\right)\left(\lambda_m+n-1\right)\hat{\Phi}_n^{(m)} + \left(2e_{16}+\frac{\partial e_{12}}{\partial\theta}\right)\left(\lambda_m+n\right)\hat{\Phi}_n^{(m)} + \left(e_{26}+\frac{\partial e_{22}}{\partial\theta}\right)\frac{\partial\hat{\Phi}_n^{(m)}}{\partial\theta}$$

$$\left.+\left(e_{12}+e_{26}\right)\left(\lambda_m+n\right)\frac{\partial\hat{\Phi}_n^{(m)}}{\partial\theta} + e_{22}\frac{\partial^2\hat{\Phi}_n^{(m)}}{\partial\theta^2}\right] + r^{\lambda_m+n-1}\left[\left(2c_{56}+c_{24}+\frac{\partial c_{25}}{\partial\theta}\right)\frac{\partial\hat{U}_n^{(m)}}{\partial z} + \left(c_{25}+c_{46}\right)\frac{\partial^2\hat{U}_n^{(m)}}{\partial\theta\partial z}\right.$$

$$+\left(c_{56}+c_{14}\right)\left(\lambda_m+n\right)\frac{\partial\hat{U}_n^{(m)}}{\partial z} + \left(c_{46}+\frac{\partial c_{24}}{\partial\theta}\right)\frac{\partial\hat{V}_n^{(m)}}{\partial z} + 2c_{24}\frac{\partial^2\hat{V}_n^{(m)}}{\partial\theta\partial z} + 2c_{46}\left(\lambda_m+n\right)\frac{\partial\hat{V}_n^{(m)}}{\partial z} + \left(2c_{36}+\frac{\partial c_{23}}{\partial\theta}\right)\times$$

$$\frac{\partial\hat{W}_n^{(m)}}{\partial z} + \left(c_{23}+c_{44}\right)\frac{\partial^2\hat{W}_n^{(m)}}{\partial\theta\partial z}\left(c_{36}+c_{45}\right)\left(\lambda_m+n\right)\frac{\partial\hat{W}_n^{(m)}}{\partial z} + \left(2e_{36}+\frac{\partial e_{32}}{\partial\theta}\right)\frac{\partial\hat{\Phi}_n^{(m)}}{\partial z} + \left(e_{24}+e_{32}\right)\frac{\partial^2\hat{\Phi}_n^{(m)}}{\partial\theta\partial z}$$

$$\left.+\left(e_{36}+e_{14}\right)\left(\lambda_m+n\right)\frac{\partial\hat{\Phi}_n^{(m)}}{\partial z}\right] + r^{\lambda_m+n}\left(c_{45}\frac{\partial^2\hat{U}_n^{(m)}}{\partial z^2} + c_{44}\frac{\partial^2\hat{V}_n^{(m)}}{\partial z^2} + c_{34}\frac{\partial^2\hat{W}_n^{(m)}}{\partial z^2} + e_{34}\frac{\partial^2\hat{\Phi}_n^{(m)}}{\partial z^2}\right) = 0 \quad (2.7b)$$

$$\sum_{m=0}^{\infty}\sum_{n=0}^{\infty} r^{\lambda_m+n-2}\left[c_{15}\left(\lambda_m+n\right)\left(\lambda_m+n-1\right)\hat{U}_n^{(m)} + \left(c_{15}+c_{25}+\frac{\partial c_{14}}{\partial\theta}\right)\left(\lambda_m+n\right)\hat{U}_n^{(m)} + \left(c_{24}+\frac{\partial c_{46}}{\partial\theta}\right)\frac{\partial\hat{U}_n^{(m)}}{\partial\theta}\right.$$

$$+\left(c_{14}+c_{56}\right)\left(\lambda_m+n\right)\frac{\partial\hat{U}_n^{(m)}}{\partial\theta} + \left(\frac{\partial c_{24}}{\partial\theta}+c_{46}\frac{\partial^2}{\partial\theta^2}\right)\hat{U}_n^{(m)} + c_{56}\left(\lambda_m+n\right)\left(\lambda_m+n-1\right)\hat{V}_n^{(m)} + \left(\frac{\partial c_{46}}{\partial\theta}\right)\left(\lambda_m+n\right)\times$$

$$\hat{V}_n^{(m)} + \left(-c_{46}+\frac{\partial c_{24}}{\partial\theta}\right)\frac{\partial\hat{V}_n^{(m)}}{\partial\theta} + \left(c_{25}+c_{46}\right)\left(\lambda_m+n\right)\frac{\partial\hat{V}_n^{(m)}}{\partial\theta} + \left(-\frac{\partial c_{46}}{\partial\theta}+c_{24}\frac{\partial^2}{\partial\theta^2}\right)\hat{V}_n^{(m)} + c_{55}\left(\lambda_m+n\right)\times$$

$$\left(\lambda_m+n-1\right)\hat{W}_n^{(m)} + \left(c_{55}+\frac{\partial c_{45}}{\partial\theta}\right)\left(\lambda_m+n\right)\hat{W}_n^{(m)} + \left(\frac{\partial c_{44}}{\partial\theta}\right)\frac{\partial\hat{W}_n^{(m)}}{\partial\theta} + 2c_{45}\left(\lambda_m+n\right)\frac{\partial\hat{W}_n^{(m)}}{\partial\theta} + c_{44}\frac{\partial^2\hat{W}_n^{(m)}}{\partial\theta^2}$$

$$+e_{15}\left(\lambda_m+n\right)\left(\lambda_m+n-1\right)\hat{\Phi}_n^{(m)} + \left(e_{15}+\frac{\partial e_{14}}{\partial\theta}\right)\left(\lambda_m+n\right)\hat{\Phi}_n^{(m)} + \left(\frac{\partial e_{24}}{\partial\theta}\right)\frac{\partial\hat{\Phi}_n^{(m)}}{\partial\theta} + \left(e_{25}+e_{14}\right)\left(\lambda_m+n\right)\frac{\partial\hat{\Phi}_n^{(m)}}{\partial\theta}$$

$$+e_{24}\frac{\partial^2\hat{\Phi}_n^{(m)}}{\partial\theta^2}\Bigg]+r^{\lambda_m+n-1}\Bigg[\left(c_{23}+c_{55}+\frac{\partial c_{45}}{\partial\theta}\right)\frac{\partial\hat{U}_n^{(m)}}{\partial z}+\left(c_{45}+c_{36}\right)\frac{\partial^2\hat{U}_n^{(m)}}{\partial\theta\partial z}+\left(c_{55}+c_{13}\right)\left(\lambda_m+n\right)\frac{\partial\hat{U}_n^{(m)}}{\partial z}$$

$$+\left(c_{45}-c_{36}+\frac{\partial c_{24}}{\partial\theta}\right)\frac{\partial\hat{V}_n^{(m)}}{\partial z}+\left(c_{44}+c_{23}\right)\frac{\partial^2\hat{V}_n^{(m)}}{\partial\theta\partial z}+\left(c_{45}+c_{36}\right)\left(\lambda_m+n\right)\frac{\partial\hat{V}_n^{(m)}}{\partial z}+\left(c_{35}+\frac{\partial c_{34}}{\partial\theta}\right)\frac{\partial\hat{W}_n^{(m)}}{\partial z}$$

$$+2c_{34}\frac{\partial^2\hat{W}_n^{(m)}}{\partial\theta\partial z}+2c_{35}\left(\lambda_m+n\right)\frac{\partial\hat{W}_n^{(m)}}{\partial z}+\left(e_{35}+\frac{\partial e_{34}}{\partial\theta}\right)\frac{\partial\hat{\Phi}_n^{(m)}}{\partial z}+\left(e_{34}+e_{23}\right)\frac{\partial^2\hat{\Phi}_n^{(m)}}{\partial\theta\partial z}+\left(e_{35}+e_{13}\right)\left(\lambda_m+n\right)\times$$

$$\frac{\partial\hat{\Phi}_n^{(m)}}{\partial z}\Bigg]+r^{\lambda_m+n}\left(c_{35}\frac{\partial^2\hat{U}_n^{(m)}}{\partial z^2}+c_{34}\frac{\partial^2\hat{V}_n^{(m)}}{\partial z^2}+c_{33}\frac{\partial^2\hat{W}_n^{(m)}}{\partial z^2}+e_{33}\frac{\partial^2\hat{\Phi}_n^{(m)}}{\partial z^2}\right)=0 \qquad (2.7c)$$

$$\sum_{m=0}^{\infty}\sum_{n=0}^{\infty}r^{\lambda_m+n-2}\Bigg[e_{11}\left(\lambda_m+n\right)\left(\lambda_m+n-1\right)\hat{U}_n^{(m)}+\left(e_{11}+e_{12}+\frac{\partial e_{21}}{\partial\theta}\right)\left(\lambda_m+n\right)\hat{U}_n^{(m)}+\left(e_{22}+\frac{\partial e_{26}}{\partial\theta}\right)\frac{\partial\hat{U}_n^{(m)}}{\partial\theta}$$

$$+\left(e_{16}+e_{21}\right)\left(\lambda_m+n\right)\frac{\partial\hat{U}_n^{(m)}}{\partial\theta}+\left(\frac{\partial e_{22}}{\partial\theta}+e_{26}\frac{\partial^2}{\partial\theta^2}\right)\hat{U}_n^{(m)}+e_{16}\left(\lambda_m+n\right)\left(\lambda_m+n-1\right)\hat{V}_n^{(m)}+\left(\frac{\partial e_{26}}{\partial\theta}\right)\left(\lambda_m+n\right)\times$$

$$\hat{V}_n^{(m)}+\left(-e_{26}+\frac{\partial e_{22}}{\partial\theta}\right)\frac{\partial\hat{V}_n^{(m)}}{\partial\theta}+\left(e_{12}+e_{26}\right)\left(\lambda_m+n\right)\frac{\partial\hat{V}_n^{(m)}}{\partial\theta}+\left(-\frac{\partial e_{26}}{\partial\theta}+e_{22}\frac{\partial^2}{\partial\theta^2}\right)\hat{V}_n^{(m)}+e_{15}\left(\lambda_m+n\right)\times$$

$$\left(\lambda_m+n-1\right)\hat{W}_n^{(m)}+\left(e_{15}+\frac{\partial e_{25}}{\partial\theta}\right)\left(\lambda_m+n\right)\hat{W}_n^{(m)}+\left(\frac{\partial e_{24}}{\partial\theta}\right)\frac{\partial\hat{W}_n^{(m)}}{\partial\theta}+\left(e_{14}+e_{25}\right)\left(\lambda_m+n\right)\frac{\partial\hat{W}_n^{(m)}}{\partial\theta}+e_{24}\frac{\partial^2\hat{W}_n^{(m)}}{\partial\theta^2}$$

$$-\eta_{11}\left(\lambda_m+n\right)\left(\lambda_m+n-1\right)\hat{\Phi}_n^{(m)}-\left(\eta_{11}+\frac{\partial\eta_{12}}{\partial\theta}\right)\left(\lambda_m+n\right)\hat{\Phi}_n^{(m)}-\left(\frac{\partial\eta_{22}}{\partial\theta}\right)\frac{\partial\hat{\Phi}_n^{(m)}}{\partial\theta}-2\eta_{12}\left(\lambda_m+n\right)\frac{\partial\hat{\Phi}_n^{(m)}}{\partial\theta}$$

$$-\eta_{22}\frac{\partial^2\hat{\Phi}_n^{(m)}}{\partial\theta^2}\Bigg]+r^{\lambda_m+n-1}\Bigg[\left(e_{15}+e_{32}+\frac{\partial e_{25}}{\partial\theta}\right)\frac{\partial\hat{U}_n^{(m)}}{\partial z}+\left(e_{25}+e_{36}\right)\frac{\partial^2\hat{U}_n^{(m)}}{\partial\theta\partial z}+\left(e_{15}+e_{31}\right)\left(\lambda_m+n\right)\frac{\partial\hat{U}_n^{(m)}}{\partial z}$$

$$+\left(e_{14}-e_{36}+\frac{\partial e_{24}}{\partial\theta}\right)\frac{\partial\hat{V}_n^{(m)}}{\partial z}+\left(e_{24}+e_{32}\right)\frac{\partial^2\hat{V}_n^{(m)}}{\partial\theta\partial z}+\left(e_{14}+e_{36}\right)\left(\lambda_m+n\right)\frac{\partial\hat{V}_n^{(m)}}{\partial z}+\left(e_{13}+\frac{\partial e_{23}}{\partial\theta}\right)\frac{\partial\hat{W}_n^{(m)}}{\partial z}$$

$$+\left(e_{13}+e_{35}\right)\left(\lambda_m+n\right)\frac{\partial\hat{W}_n^{(m)}}{\partial z}-\left(\eta_{13}+\frac{\partial\eta_{23}}{\partial\theta}\right)\frac{\partial\hat{\Phi}_n^{(m)}}{\partial z}-2\eta_{23}\frac{\partial^2\hat{\Phi}_n^{(m)}}{\partial\theta\partial z}-2\eta_{13}\left(\lambda_m+n\right)\frac{\partial\hat{\Phi}_n^{(m)}}{\partial z}\Bigg]$$

$$+r^{\lambda_m+n}\left(e_{35}\frac{\partial^2\hat{U}_n^{(m)}}{\partial z^2}+e_{34}\frac{\partial^2\hat{V}_n^{(m)}}{\partial z^2}+e_{33}\frac{\partial^2\hat{W}_n^{(m)}}{\partial z^2}-\eta_{33}\frac{\partial^2\hat{\Phi}_n^{(m)}}{\partial z^2}\right)=0 \qquad (2.7d)$$

To investigate the behaviors of the solutions around r=0, only the parts of the solutions with the lowest order of r have to be considered. That is the solution corresponding to n=0 in Eqs. (2.7). Accordingly, the following equations must be solved.

$$\frac{\partial^2 \hat{U}_0^{(m)}}{\partial\theta^2} + p_1(\theta)\frac{\partial \hat{U}_0^{(m)}}{\partial\theta} + p_2(\theta)\hat{U}_0^{(m)} + p_3(\theta)\frac{\partial^2 \hat{V}_0^{(m)}}{\partial\theta^2} + p_4(\theta)\frac{\partial \hat{V}_0^{(m)}}{\partial\theta} + p_5(\theta)\hat{V}_0^{(m)}$$
$$+ p_6(\theta)\frac{\partial^2 \hat{W}_0^{(m)}}{\partial\theta^2} + p_7(\theta)\frac{\partial \hat{W}_0^{(m)}}{\partial\theta} + p_8(\theta)\hat{W}_0^{(m)} + p_9(\theta)\frac{\partial^2 \hat{\Phi}_0^{(m)}}{\partial\theta^2} + p_{10}(\theta)\frac{\partial \hat{\Phi}_0^{(m)}}{\partial\theta} + p_{11}(\theta)\hat{\Phi}_0^{(m)} = 0 \tag{2.8a}$$

$$\frac{\partial^2 \hat{V}_0^{(m)}}{\partial\theta^2} + q_1(\theta)\frac{\partial \hat{V}_0^{(m)}}{\partial\theta} + q_2(\theta)\hat{V}_0^{(m)} + q_3(\theta)\frac{\partial^2 \hat{U}_0^{(m)}}{\partial\theta^2} + q_4(\theta)\frac{\partial \hat{U}_0^{(m)}}{\partial\theta} + q_5(\theta)\hat{U}_0^{(m)}$$
$$+ q_6(\theta)\frac{\partial^2 \hat{W}_0^{(m)}}{\partial\theta^2} + q_7(\theta)\frac{\partial \hat{W}_0^{(m)}}{\partial\theta} + q_8(\theta)\hat{W}_0^{(m)} + q_9(\theta)\frac{\partial^2 \hat{\Phi}_0^{(m)}}{\partial\theta^2} + q_{10}(\theta)\frac{\partial \hat{\Phi}_0^{(m)}}{\partial\theta} + q_{11}(\theta)\hat{\Phi}_0^{(m)} = 0 \tag{2.8b}$$

$$\frac{\partial^2 \hat{W}_0^{(m)}}{\partial\theta^2} + r_1(\theta)\frac{\partial \hat{W}_0^{(m)}}{\partial\theta} + r_2(\theta)\hat{W}_0^{(m)} + r_3(\theta)\frac{\partial^2 \hat{U}_0^{(m)}}{\partial\theta^2} + r_4(\theta)\frac{\partial \hat{U}_0^{(m)}}{\partial\theta} + r_5(\theta)\hat{U}_0^{(m)}$$
$$+ r_6(\theta)\frac{\partial^2 \hat{V}_0^{(m)}}{\partial\theta^2} + r_7(\theta)\frac{\partial \hat{V}_0^{(m)}}{\partial\theta} + r_8(\theta)\hat{V}_0^{(m)} + r_9(\theta)\frac{\partial^2 \hat{\Phi}_0^{(m)}}{\partial\theta^2} + r_{10}(\theta)\frac{\partial \hat{\Phi}_0^{(m)}}{\partial\theta} + r_{11}(\theta)\hat{\Phi}_0^{(m)} = 0 \tag{2.8c}$$

$$\frac{\partial^2 \hat{\Phi}_0^{(m)}}{\partial\theta^2} + s_1(\theta)\frac{\partial \hat{\Phi}_0^{(m)}}{\partial\theta} + s_2(\theta)\hat{\Phi}_0^{(m)} + s_3(\theta)\frac{\partial^2 \hat{U}_0^{(m)}}{\partial\theta^2} + s_4(\theta)\frac{\partial \hat{U}_0^{(m)}}{\partial\theta} + s_5(\theta)\hat{U}_0^{(m)}$$
$$+ s_6(\theta)\frac{\partial^2 \hat{V}_0^{(m)}}{\partial\theta^2} + s_7(\theta)\frac{\partial \hat{V}_0^{(m)}}{\partial\theta} + s_8(\theta)\hat{V}_0^{(m)} + s_9(\theta)\frac{\partial^2 \hat{W}_0^{(m)}}{\partial\theta^2} + s_{10}(\theta)\frac{\partial \hat{W}_0^{(m)}}{\partial\theta} + s_{11}(\theta)\hat{W}_0^{(m)} = 0 \tag{2.8d}$$

Appendix III defines p_i, q_i, r_i, and s_i in Eqs. (2.8).

Equations (2.8) are a set of ordinary differential equations with variable coefficients that depend only on θ. The solutions to Eqs. (2.8) are independent of *z*. The exact closed-form solutions to Eqs. (2.8) are intractable, if they exist. The power series method can be directly adopted to develop a general solution for ordinary differential equations with variable coefficients. Very high-order terms must be considered to obtain an accurate solution and this requirement can cause numerical difficulties. To overcome these difficulties, a domain decomposition technique is used in conjunction with the power series method to establish a general solution of Eqs. (2.8).

The range of θ under consideration is first divided into a number of sub-domains (see Fig. 2.2). A series solution to Eqs. (2.8) is established in each sub-domain. Consequently, a general solution over the whole θ domain is constructed from these series solutions in the sub-domains by imposing the continuity conditions between each pair of adjacent sub-domains. This process is a very convenient means of constructing solutions that can be used to analyze multi-material wedges, which are also considered in this work.

To establish the power series solution for sub-domain i of θ, the variable coefficients in Eqs. (2.8) are expanded in terms of the power series of θ with respect to the middle point of the sub-domain, $\overline{\theta}_i$:

$$p_j(\theta)=\sum_{k=0}^{K}\left(\mu_j\right)_k^{(i)}\left(\theta-\overline{\theta}_i\right)^k,\quad q_j(\theta)=\sum_{k=0}^{K}\left(\varsigma_j\right)_k^{(i)}\left(\theta-\overline{\theta}_i\right)^k,$$
$$r_j(\theta)=\sum_{k=0}^{K}\left(\xi_j\right)_k^{(i)}\left(\theta-\overline{\theta}_i\right)^k,\quad s_j(\theta)=\sum_{k=0}^{K}\left(\vartheta_j\right)_k^{(i)}\left(\theta-\overline{\theta}_i\right)^k. \tag{2.9}$$

Similarly, the solutions of Eqs. (2.8) in sub-domain i are expressed as

$$\hat{U}_{0i}^{(m)}=\sum_{j=0}^{J}\hat{A}_j^{(i)}\left(\theta-\overline{\theta}_i\right)^j,\quad \hat{V}_{0i}^{(m)}=\sum_{j=0}^{J}\hat{B}_j^{(i)}\left(\theta-\overline{\theta}_i\right)^j,\quad \hat{W}_{0i}^{(m)}=\sum_{j=0}^{J}\hat{C}_j^{(i)}\left(\theta-\overline{\theta}_i\right)^j,$$
$$\hat{\Phi}_{0i}^{(m)}=\sum_{j=0}^{J}\hat{D}_j^{(i)}\left(\theta-\overline{\theta}_i\right)^j \tag{2.10}$$

Substituting Eqs. (2.9) and (2.10) into Eqs. (2.8) and carefully rearranging yields the following relations among the coefficients in Eqs. (2.10)

$$\hat{A}_{j+2}^{(i)}+\left(\mu_3\right)_0^{(i)}\hat{B}_{j+2}^{(i)}+\left(\mu_6\right)_0^{(i)}\hat{C}_{j+2}^{(i)}+\left(\mu_9\right)_0^{(i)}\hat{D}_{j+2}^{(i)}=\frac{-1}{(j+2)(j+1)}\left\{\sum_{k=0}^{j-1}\left[(k+2)(k+1)\left(\left(\mu_3\right)_{j-k}^{(i)}\hat{B}_{k+2}^{(i)}\right.\right.\right.$$
$$\left.+\left(\mu_6\right)_{j-k}^{(i)}\hat{C}_{k+2}^{(i)}+\left(\mu_9\right)_{j-k}^{(i)}\hat{D}_{k+2}^{(i)}\right)\Big]+\sum_{k=0}^{j}\Big[(k+1)\left(\mu_1\right)_{j-k}^{(i)}\hat{A}_{k+1}^{(i)}+\left(\mu_2\right)_{j-k}^{(i)}\hat{A}_k^{(i)}+(k+1)\left(\mu_4\right)_{j-k}^{(i)}\hat{B}_{k+1}^{(i)}$$
$$\left.\left.+\left(\mu_5\right)_{j-k}^{(i)}\hat{B}_k^{(i)}+(k+1)\left(\mu_7\right)_{j-k}^{(i)}\hat{C}_{k+1}^{(i)}+\left(\mu_8\right)_{j-k}^{(i)}\hat{C}_k^{(i)}+(k+1)\left(\mu_{10}\right)_{j-k}^{(i)}\hat{D}_{k+1}^{(i)}+\left(\mu_{11}\right)_{j-k}^{(i)}\hat{D}_k^{(i)}\right]\right\} \tag{2.11a}$$

$$\hat{B}_{j+2}^{(i)}+\left(\varsigma_3\right)_0^{(i)}\hat{A}_{j+2}^{(i)}+\left(\varsigma_6\right)_0^{(i)}\hat{C}_{j+2}^{(i)}+\left(\varsigma_9\right)_0^{(i)}\hat{D}_{j+2}^{(i)}=\frac{-1}{(j+2)(j+1)}\left\{\sum_{k=0}^{j-1}\left[(k+2)(k+1)\left(\left(\varsigma_3\right)_{j-k}^{(i)}\hat{A}_{k+2}^{(i)}\right.\right.\right.$$
$$\left.+\left(\varsigma_6\right)_{j-k}^{(i)}\hat{C}_{k+2}^{(i)}+\left(\varsigma_9\right)_{j-k}^{(i)}\hat{D}_{k+2}^{(i)}\right)\Big]+\sum_{k=0}^{j}\Big[(k+1)\left(\varsigma_1\right)_{j-k}^{(i)}\hat{B}_{k+1}^{(i)}+\left(\varsigma_2\right)_{j-k}^{(i)}\hat{B}_k^{(i)}+(k+1)\left(\varsigma_4\right)_{j-k}^{(i)}\hat{A}_{k+1}^{(i)}$$
$$\left.\left.+\left(\varsigma_5\right)_{j-k}^{(i)}\hat{A}_k^{(i)}+(k+1)\left(\varsigma_7\right)_{j-k}^{(i)}\hat{C}_{k+1}^{(i)}+\left(\varsigma_8\right)_{j-k}^{(i)}\hat{C}_k^{(i)}+(k+1)\left(\varsigma_{10}\right)_{j-k}^{(i)}\hat{D}_{k+1}^{(i)}+\left(\varsigma_{11}\right)_{j-k}^{(i)}\hat{D}_k^{(i)}\right]\right\} \tag{2.11b}$$

$$\hat{C}_{j+2}^{(i)}+\left(\xi_3\right)_0^{(i)}\hat{A}_{j+2}^{(i)}+\left(\xi_6\right)_0^{(i)}\hat{B}_{j+2}^{(i)}+\left(\xi_9\right)_0^{(i)}\hat{D}_{j+2}^{(i)}=\frac{-1}{(j+2)(j+1)}\left\{\sum_{k=0}^{j-1}\left[(k+2)(k+1)\left(\left(\xi_3\right)_{j-k}^{(i)}\hat{A}_{k+2}^{(i)}\right.\right.\right.$$
$$\left.+\left(\xi_6\right)_{j-k}^{(i)}\hat{B}_{k+2}^{(i)}+\left(\xi_9\right)_{j-k}^{(i)}\hat{D}_{k+2}^{(i)}\right)\Big]+\sum_{k=0}^{j}\Big[(k+1)\left(\xi_1\right)_{j-k}^{(i)}\hat{C}_{k+1}^{(i)}+\left(\xi_2\right)_{j-k}^{(i)}\hat{C}_k^{(i)}+(k+1)\left(\xi_4\right)_{j-k}^{(i)}\hat{A}_{k+1}^{(i)}$$
$$\left.\left.+\left(\xi_5\right)_{j-k}^{(i)}\hat{A}_k^{(i)}+(k+1)\left(\xi_7\right)_{j-k}^{(i)}\hat{B}_{k+1}^{(i)}+\left(\xi_8\right)_{j-k}^{(i)}\hat{B}_k^{(i)}+(k+1)\left(\xi_{10}\right)_{j-k}^{(i)}\hat{D}_{k+1}^{(i)}+\left(\xi_{11}\right)_{j-k}^{(i)}\hat{D}_k^{(i)}\right]\right\} \tag{2.11c}$$

$$\hat{D}_{j+2}^{(i)}+\left(\vartheta_3\right)_0^{(i)}\hat{A}_{j+2}^{(i)}+\left(\vartheta_6\right)_0^{(i)}\hat{B}_{j+2}^{(i)}+\left(\vartheta_9\right)_0^{(i)}\hat{C}_{j+2}^{(i)}=\frac{-1}{(j+2)(j+1)}\left\{\sum_{k=0}^{j-1}\left[(k+2)(k+1)\left(\left(\vartheta_3\right)_{j-k}^{(i)}\hat{A}_{k+2}^{(i)}\right.\right.\right.$$

$$\left.+\left(\vartheta_6\right)_{j-k}^{(i)}\hat{B}_{k+2}^{(i)}+\left(\vartheta_9\right)_{j-k}^{(i)}\hat{C}_{k+2}^{(i)}\right)\Big]+\sum_{k=0}^{j}\Big[(k+1)\left(\vartheta_1\right)_{j-k}^{(i)}\hat{D}_{k+1}^{(i)}+\left(\vartheta_2\right)_{j-k}^{(i)}\hat{D}_k^{(i)}+(k+1)\left(\vartheta_4\right)_{j-k}^{(i)}\hat{A}_{k+1}^{(i)}$$

$$\left.\left.+\left(\vartheta_5\right)_{j-k}^{(i)}\hat{A}_k^{(i)}+(k+1)\left(\vartheta_7\right)_{j-k}^{(i)}\hat{B}_{k+1}^{(i)}+\left(\vartheta_8\right)_{j-k}^{(i)}\hat{B}_k^{(i)}+(k+1)\left(\vartheta_{10}\right)_{j-k}^{(i)}\hat{C}_{k+1}^{(i)}+\left(\vartheta_{11}\right)_{j-k}^{(i)}\hat{C}_{k+1}^{(i)}\Big]\right\} \quad (2.11d)$$

Close examination of Eqs. (2.11) reveals that if $\hat{A}_0^{(i)}$, $\hat{A}_1^{(i)}$, $\hat{B}_0^{(i)}$, $\hat{B}_1^{(i)}$, $\hat{C}_0^{(i)}$, $\hat{C}_1^{(i)}$, $\hat{D}_0^{(i)}$ and $\hat{D}_1^{(i)}$ are determined, then the other coefficients in Eqs. (2.10) ($\hat{A}_j^{(i)}$, $\hat{B}_j^{(i)}$, $\hat{C}_j^{(i)}$ and $\hat{D}_j^{(i)}$, $j\geq 2$) can be found by solving the linear algebraic equations in Eqs. (2.11). Consequently, the solutions to Eqs. (2.8) in sub-domain *i* of θ can be expressed as

$$\hat{U}_{0i}^{(m)}(\theta,z)=\hat{A}_0^{(i)}\hat{U}_{0i0}^{(m)}(\theta)+\hat{A}_1^{(i)}\hat{U}_{0i1}^{(m)}(\theta)+\hat{B}_0^{(i)}\hat{U}_{0i2}^{(m)}(\theta)+\hat{B}_1^{(i)}\hat{U}_{0i3}^{(m)}(\theta)+\hat{C}_0^{(i)}\hat{U}_{0i4}^{(m)}(\theta)+\hat{C}_1^{(i)}\hat{U}_{0i5}^{(m)}(\theta)$$

$$+\hat{D}_0^{(i)}\hat{U}_{0i6}^{(m)}(\theta)+\hat{D}_1^{(i)}\hat{U}_{0i7}^{(m)}(\theta) \quad (2.12a)$$

$$\hat{V}_{0i}^{(m)}(\theta,z)=\hat{A}_0^{(i)}\hat{V}_{0i0}^{(m)}(\theta)+\hat{A}_1^{(i)}\hat{V}_{0i1}^{(m)}(\theta)+\hat{B}_0^{(i)}\hat{V}_{0i2}^{(m)}(\theta)+\hat{B}_1^{(i)}\hat{V}_{0i3}^{(m)}(\theta)+\hat{C}_0^{(i)}\hat{V}_{0i4}^{(m)}(\theta)+\hat{C}_1^{(i)}\hat{V}_{0i5}^{(m)}(\theta)$$

$$+\hat{D}_0^{(i)}\hat{V}_{0i6}^{(m)}(\theta)+\hat{D}_1^{(i)}\hat{V}_{0i7}^{(m)}(\theta) \quad (2.12b)$$

$$\hat{W}_{0i}^{(m)}(\theta,z)=\hat{A}_0^{(i)}\hat{W}_{0i0}^{(m)}(\theta)+\hat{A}_1^{(i)}\hat{W}_{0i1}^{(m)}(\theta)+\hat{B}_0^{(i)}\hat{W}_{0i2}^{(m)}(\theta)+\hat{B}_1^{(i)}\hat{W}_{0i3}^{(m)}(\theta)+\hat{C}_0^{(i)}\hat{W}_{0i4}^{(m)}(\theta)+\hat{C}_1^{(i)}\hat{W}_{0i5}^{(m)}(\theta)$$

$$+\hat{D}_0^{(i)}\hat{W}_{0i6}^{(m)}(\theta)+\hat{D}_1^{(i)}\hat{W}_{0i7}^{(m)}(\theta) \quad (2.12c)$$

$$\hat{\Phi}_{0i}^{(m)}(\theta,z)=\hat{A}_0^{(i)}\hat{\Phi}_{0i0}^{(m)}(\theta)+\hat{A}_1^{(i)}\hat{\Phi}_{0i1}^{(m)}(\theta)+\hat{B}_0^{(i)}\hat{\Phi}_{0i2}^{(m)}(\theta)+\hat{B}_1^{(i)}\hat{\Phi}_{0i3}^{(m)}(\theta)+\hat{C}_0^{(i)}\hat{\Phi}_{0i4}^{(m)}(\theta)+\hat{C}_1^{(i)}\hat{\Phi}_{0i5}^{(m)}(\theta)$$

$$+\hat{D}_0^{(i)}\hat{\Phi}_{0i6}^{(m)}(\theta)+\hat{D}_1^{(i)}\hat{\Phi}_{0i7}^{(m)}(\theta) \quad (2.12d)$$

The asymptotic solution in sub-domain *i* of θ is

$$u_r^{(i)}(r,\theta,z)=\sum_{m=0}^{\infty}r^{\lambda_m}\hat{U}_{0i}^{(m)}(\theta,z)+O(r^{\lambda_m+1})=\tilde{u}_r^{(i)}(r,\theta,z,\lambda_m)+O(r^{\lambda_m+1}) \quad (2.13a)$$

$$u_\theta^{(i)}(r,\theta,z)=\sum_{m=0}^{\infty}r^{\lambda_m}\hat{V}_{0i}^{(m)}(\theta,z)+O(r^{\lambda_m+1})=\tilde{u}_\theta^{(i)}(r,\theta,z,\lambda_m)+O(r^{\lambda_m+1}) \quad (2.13b)$$

$$u_z^{(i)}(r,\theta,z)=\sum_{m=0}^{\infty} r^{\lambda_m}\hat{W}_{0i}^{(m)}(\theta,z)+O(r^{\lambda_m+1})=\tilde{u}_z^{(i)}(r,\theta,z,\lambda_m)+O(r^{\lambda_m+1}) \tag{2.13c}$$

$$\phi^{(i)}(r,\theta,z)=\sum_{m=0}^{\infty} r^{\lambda_m}\hat{\Phi}_{0i}^{(m)}(\theta,z)+O(r^{\lambda_m+1})=\tilde{\phi}^{(i)}(r,\theta,z,\lambda_m)+O(r^{\lambda_m+1}) \tag{2.13d}$$

When the range of θ is decomposed into *n* sub-domains, a total of 8*n* coefficients must be determined in all of the sub-domain solutions that are constructed using the above procedure. These solutions must satisfy the continuity conditions between pairs of adjacent sub-domains. These include continuities of tractions, mechanical displacements, electric displacements and electric potential. These continuity conditions yield 8(*n*-1) algebraic equations. Homogenous boundary conditions at $\theta=\theta_0$ and $\theta=\theta_n$ must be satisfied, yielding another eight equations. As a result, 8*n* coefficients are to be determined from 8*n* homogenous algebraic equations. A nontrivial solution for the coefficients yields an $8n\times 8n$ matrix with a determinant of zero. The roots of the zero determinant (λ_m), which can be complex numbers, are obtained herein using the numerical approach of Müller (1956).

2.3. **Verification of Solution**

To validate the proposed solution, convergence studies for minimum Re[λ_m] (real part of λ_m) are conducted by increasing the number of sub-domains or increasing the number of polynomial terms in each sub-domain, and the convergent solutions are compared with the published results. The wedges under consideration are made of piezoelectric material PZT-4, which is transversely isotropic. Table 2.1 presents the material properties of PZT-4.

Table 2.2 considers three cases. Four letters specify the boundary conditions of a wedge at $\theta=0$ and $\theta=\gamma$. The first and third letters represent the mechanical boundary conditions at $\theta=0$ and $\theta=\gamma$, respectively; and C and F represent clamped and free boundary conditions, respectively. Similarly, the second and fourth letters concern the electric boundary conditions with C and O's denoting electrically closed and open boundary conditions, respectively. These rules are adopted throughout the paper.

The first case concerns a crack problem with a material having its direction of polarization in the *z* direction (see Fig. 1). The surfaces of the crack are free of surface traction and surface charge. That is $\sigma_{\theta\theta}=\sigma_{\theta r}=\sigma_{\theta z}=D_\theta=0$ at $\theta=0$ and 2π. The results of Sosa and Pak (1990) were obtained by using an eigenfunction approach, which is similar to the present approach. Sosa and Pak (1990) examined a piezoelectric parallelepiped with a cut-through crack and having its direction of polarization in the *z* direction, so that they could find a closed-form solution for λ_m.

The other two cases involve 180^o and 360^o wedges with FOCC boundary conditions and polarization along $\theta=180^o$ and $\theta=270^o$, respectively, in the plane *x*-*y*. Table 2.2 also

presents the results that were published by Hwu and Ikeda (2008). Notably, the solutions of Hwu and Ikeda (2008) are two-dimensional solutions, depending on *x* and *y*, and are based on the assumption of generalized plane strain and a short circuit. They assumed $\varepsilon_{zz}=0$ and $E_z=0$, eliminated the terms that were associated with ε_{zz} and E_z in the constitutive equations, and replaced σ_{zz} and D_z by the other stress and electric displacement components. Thus, they eliminated c_{ij} (i or j=3), e_{k6} and η_{k3} from Eqs. (2.4). Using their assumptions and following the present solution procedure shown in Sections 2.1 and 2.2, one can obtain exactly the same equations as Eqs. (2.8) and the same values of λ_m given in the present work. This fact is indirectly evidenced by two observations. The first is that the terms corresponding to the derivatives with respect to *z* in Eqs. (2.5) are absent from Eqs. (2.8), indicating that the assumption of all physical quantities in Eqs. (2.5) independent of *z* does not affect the establishment of Eqs. (2.8). The other is that the coefficients in Eqs. (2.8), presented in Appendix III, are independence of c_{ij} (i or j=3), e_{k6} and η_{k3}.

The comparison in Table 2.2 of the convergent values obtained herein with those published reveals excellent agreement. The present convergent solutions can be obtained by increasing the number of sub-domains or increasing the order of the polynomials. Using a large number of sub-domains in combination with a small number of polynomial terms can yield convergent results without any numerical difficulty.

It is also interesting to demonstrate the accuracy of the values of λ_m other than minimum Re[λ_m] obtained by the present approach. Herein, λ_m are in order of Re[λ_i] ≤ Re[λ_{i+1}] (i=0, 1, 2,…). Table 3 compares λ_0, λ_1 and λ_2 determined by the present approach with the results published by Hwu and Ikeda (2008) and Sze and Wang (2001) for PZT-4 wedges with different γ, boundary conditions and directions of polarization. Notably, the results of Sze and Wang (2001) were obtained by a finite element approach with three-dimensional formulations and assuming all the physical quantities under consideration independent on *z*. The material properties of PZT-4, which were used in Sze and Wang (2001) and are different from those given in Table 2.3, were applied for the wedges with FOFO boundary conditions in Table 2.3. The different material properties from those in Table 1 and used in Sze and Wang (2001) are $\hat{c}_{33}$=113 GPa, $\hat{e}_{15}$=13.44 C/m^2, $\hat{e}_{31}$= -6.98 C/m^2, $\hat{e}_{33}$ =13.84 C/m^2, $\hat{\eta}_{11}$=60.0×10^{-10} F/m, and $\hat{\eta}_{33}$= 54.7×10^{-10} F/m. The present results were obtained by dividing the whole domain of θ into four sub-domains and using 12 polynomial terms in the solutions for each sub-domain. Table 2.3 discloses excellent agreement between the present and the published results.

2.4. **Numerical Results and Discussion**

After the correctness of the proposed solutions was verified by performing the

convergence studies and comparisons with the published results, the proposed solution was further applied to investigate the electroelastic singularities in a piezoelectric wedge with varying directions of polarization. The wedges under consideration are made of a single piezoelectric material, a piezoelectric material and an isotropic elastic material, or two piezoelectric materials. Two parameters α and β are introduced to specify the direction of polarization, where α is the angle between the *x*-axis and the projection of the polarization axis onto the *x*-*y* plane, and β is the angle between the *z* axis and the polarization axis. The order of electroelastic singularity at the apex of a wedge is determined by the real part of (λ_m-1), and the root of primary interest is the one with the smallest positive real part between zero and one. The following presents the values of minimum Re[λ_m] for wedges with various combinations of boundary conditions along $\theta = 0$ and $\theta = \gamma$.

2.4.1 *Wedges made of a single piezoelectric material*

Figures 2.3 illustrates the effects of the direction of polarization on the minimum values of Re[λ_m] for a 270^o wedge made of PZT-5H, whose material properties are given in Table 2.1. Four combinations of boundary conditions were considered - FOFO, FCFC, COCO and CCCC. As stated in Section 4, FOFO means free mechanical boundary conditions and open electric boundary conditions at both of $\theta = 0^o$ and $\theta = 270^o$. In Fig. 3a, $\alpha = 0^o$ means that the direction of polarization is in the *x*-*z* plane, while $\beta = 90^o$ in Fig. 3b indicates that the direction of polarization is in the *x*-*y* plane. Figure 2.3a only considers $0^o \le \beta \le 90^o$ because $\beta + 90^0$ and $90^0 - \beta$ yield the same λ_m. Similarly, Fig. 3b only presents the results for $0^o \le \alpha \le 180^o$ because $\alpha + 180^o$ and $180^o - \alpha$ have the same λ_m. Figures 2.3a and 2.3b demonstrate that the FF mechanical boundary conditions cause more severe electroelastic singularities than do the CC mechanical boundary conditions. Electric boundary conditions do not affect minimum Re[λ_m] in the FCFC and FOFO cases. The variation in minimum Re[λ_m] owing to changes in the direction of polarization is less than 5%.

Figures 2.4 plots the variation of minimum Re[λ_m] of PZT-5H wedges with wedge angle γ and under FOFO and COCO boundary conditions. Three different directions of polarization in the *x*-*y* plane were considered - $\alpha = 0^o$, 60^o, and 120^o. The λ_m values that correspond to minimum Re[λ_m] are all real. As expected, minimum Re[λ_m] decreases as γ increases; and the FOFO boundary conditions yield a smaller minimum Re[λ_m] than do the COCO boundary conditions. When $\gamma = 360^o$ (representing a crack), both sets of boundary conditions result in $\lambda_m = 0.5$, and the orientation of the polarization in the *x*-*y* plane does not

influence the singularity order.

2.4.2 *Bi-material wedges made of piezoelectric and elastic materials*

The integration of piezoelectric films on silicon (Si) substrates is favored in the design and formation of micro electromechanical systems. This section study the electroelastic singularities at the interface in wedges that are made of PZT-5H and Si, whose material properties are found in Table 2.1. Two typical wedge configurations – those of 180^o and 270^o wedges – were considered first. In a 180^o wedge, Si and PZT-5H occupy $0^o \le \theta \le 90^o$ and $90^o \le \theta \le 180^o$, respectively, while in a 270^o wedge, Si and PZT-5H occupy $0^o \le \theta \le 180^o$ and $180^o \le \theta \le 270^o$, respectively. Figures 2.5 an 2.6 plot the values of minimum Re[λ_m] of these two wedges versus their directions of polarization, respectively. Again, four sets of boundary conditions were considered. These are F-FO, F-FC, C-CO, and C-CC, where "-" denotes the absence of any electric boundary conditions at $\theta = 0^o$, according to the rule for defining boundary conditions described in Section 2.3.

In Figs. 2.5a and 2.5b, the directions of polarization of PZT-5H are in the *x-z* plane and *x-y* plane, respectively, while Fig. 2.5c displays the results for the wedges with the F-FO boundary conditions and having the directions of polarization on the surfaces with $\beta = 30^o$, 60^o and 90^o. It is interesting to observe that the direction of polarization can be especially arranged to eliminate electroelastic singularities at the interface of the wedge. For example, Fig. 2.5a reveals no electroelastic singularities when $80^o \le \beta \le 90^o$ and $38^o \le \beta \le 90^o$ for boundary conditions F-FO and C-CO, respectively; Fig. 2.5b shows no electroelastic singularities when $90^o < \alpha \le 180^o$ under boundary conditions F-FO and F-FC, and Fig. 5c shows no electroelastic singularities when $18^o < \alpha < 88^o$ and $23^o < \alpha < 72^o$ under the conditions $\beta = 60^o$ and 30^o, respectively. Notably, boundary conditions C-CC yield more severe singularities at the interface than do the other three sets of boundary conditions.

According to Fig. 2.6, in investigating the singularities in 270^o wedges, changes in the direction of polarization may yield considerable changes in minimum Re[λ_m]. In Fig. 6a, the order of the singularity falls by approximately 10% under boundary conditions F-FO as β changes from 0^o to 90^o, and in Fig. 2.6b, it increases by about 25% under boundary conditions F-FC as α changes from 45^o to 135^o.

Figures 2.7a and 2.7b plot the variation of minimum Re[λ_m] with the angle of PZT-5H, γ_1, under boundary conditions F-FO and C-CO, respectively. In the wedges in Figs. 2.7, Si occupies $0^o \le \theta \le 180^o$, and the wedge angle γ equals $\gamma_1 + 180^o$. The directions of polarization are in the *x-y* plane and $\alpha = 0^o$, 60^o and 120^o. As expected, the strength of the singularity generally increases with the increase of γ_1, and the order of the singularity equals 0.5 when $\gamma_1 = 180^o$ (representing a crack). The relatively abrupt changes of the

minimum Re[λ_m] around $\gamma_1 = 160^o$ in Fig. 2.7a are caused by the changes of λ_m from real numbers to complex numbers.

2.4.3 *Bi-material wedges made of piezoelectric materials*

Bi-material wedges that comprise piezoelectric materials are commonly encountered in smart structures. This section investigates electroelastic singularities at the interface of bi-material wedges comprised of PZT-5H and PZT-4, whose material properties are provided in Table 1. The configurations of wedges considered in this section are the same as those in the preceding section, except in that the elastic material in the previous section is replaced by the piezoelectric material PZT-4.

Figures 2.8 illustrate the effects of the orientations of polarization on the electroelastic singularities in wedges with a wedge angle 180^o. When the direction of polarization lies in the *x-y* plane (see Fig. 8b), $2^o < \alpha < 88^o$ and $6^o < \alpha < 84^o$ yield no singularities under boundary conditions COCO and CCCC, respectively. When the direction of polarization is on the surface with $\beta = 30^o$ (see Fig. 2.8c), no singularities are found for $108^o < \alpha < 168^o$ under the FOFO boundary conditions. Changes in the direction of polarization alter the order of the singularity by less than 4%.

Free-free mechanical boundary conditions cause more severe electroelastic singularities in 270^o wedges (Figs. 2.9) than do clamped-clamped boundary conditions. The orientation of polarization may change the order of the singularity by approximately 9%. For wedges with other angles, that percentage exceeds 10% (Figs. 2.10).

III **Asymptotic Solutions for a Body of Revolution**

3.1 **Basic Formulation**

Consider a body of revolution made of a piezoelectric material polarized along the direction $\bar{Z}$, which makes an angle γ with the axis of revolution *Z* (Fig. 3.1). Although Fig. 1 displays a bi-material body of revolution, a body of a single material will be first considered in the following development of basic equations and solutions. The solutions are then easily extended to a bimaterial body. Define two Cartesian coordinate systems (*X*, *Y*, *Z*) and ($\bar{X},\bar{Y},\bar{Z}$), where *Y* and $\bar{Y}$ axes are coincidental. A cylindrical coordinate system (r,θ, *Z*) (Fig. 3.1) can be conveniently used to solve problems of bodies of revolution. Without body force and charges, the equilibrium and Maxwell's equations in terms of displacement components and electric potential are given in Eqs. (2.5). Notably, the material coordinate system ($\hat{x},\hat{y},\hat{z}$) and geometry coordinate system (*x*, *y*, *z*) in chapter 2 are replaced by ($\bar{X},\bar{Y},\bar{Z}$) and (*X*, *Y*, *Z*) herein, respectively.

Figure 3.2 shows a half plane with any constant θ in Fig. 3.1. To find an asymptotic solution around the sharp corner in Fig. 3.2, (*r*, *Z*) coordinates are transformed to (ρ, φ) coordinates as shown in Fig. 3.2. Transforming Eqs. (2.5) from (*r*, *Z*) to (ρ, φ) using the relations,

$$\rho=\sqrt{(r-R)^2+z^2}\ ,\quad \phi=\tan^{-1}\left(\frac{-z}{r-R}\right),\quad r-R=\rho\cos\phi\text{, and }\quad z=-\rho\sin\phi\,, \tag{3.1}$$

yields the following complicated partial differential equations with variable coefficients;

$$\left\{\left(c_{11}L_1+c_{55}L_3+2c_{15}L_5\right)+\frac{1}{\rho\cos\phi+R}\left[\left(c_{11}+\frac{\partial c_{16}}{\partial\theta}+2c_{16}\frac{\partial}{\partial\theta}\right)L_2+\left(c_{15}+\frac{\partial c_{56}}{\partial\theta}+2c_{56}\frac{\partial}{\partial\theta}\right)L_4\right]\right.$$

$$\left.+\frac{1}{(\rho\cos\phi+R)^2}\left[-c_{22}+\frac{\partial c_{26}}{\partial\theta}+c_{66}\frac{\partial^2}{\partial\theta^2}+\frac{\partial c_{66}}{\partial\theta}\frac{\partial}{\partial\theta}\right]\right\}u_r+\left\{\left(c_{16}L_1+c_{45}L_3+(c_{14}+c_{56})L_5\right)\right.$$

$$+\frac{1}{\rho\cos\phi+R}\left[\left(-c_{26}+\frac{\partial c_{66}}{\partial\theta}+(c_{12}+c_{66})\frac{\partial}{\partial\theta}\right)L_2+\left(c_{14}-c_{24}-c_{56}+\frac{\partial c_{46}}{\partial\theta}+(c_{25}+c_{46})\frac{\partial}{\partial\theta}\right)L_4\right]$$

$$\left.+\frac{1}{(\rho\cos\phi+R)^2}\left[c_{26}-\frac{\partial c_{66}}{\partial\theta}+\left(-c_{22}-c_{66}+\frac{\partial c_{26}}{\partial\theta}\right)\frac{\partial}{\partial\theta}+c_{26}\frac{\partial^2}{\partial\theta^2}\right]\right\}u_\theta+\left\{\left(c_{15}L_1+c_{35}L_3\right.\right.$$

$$\left.\left.+(c_{13}+c_{55})L_5\right)+\frac{1}{\rho\cos\phi+R}\left[\left(c_{15}-c_{25}+\frac{\partial c_{56}}{\partial\theta}+(c_{14}+c_{56})\frac{\partial}{\partial\theta}\right)L_2+\left(c_{13}-c_{23}+\frac{\partial c_{36}}{\partial\theta}\right.\right.\right.$$

$$\left.\left.\left.+(c_{36}+c_{45})\frac{\partial}{\partial\theta}\right)L_4\right]+\frac{1}{(\rho\cos\phi+R)^2}\left[\left(-c_{24}+\frac{\partial c_{46}}{\partial\theta}\right)\frac{\partial}{\partial\theta}+c_{46}\frac{\partial^2}{\partial\theta^2}\right]\right\}u_z+\left\{\left(e_{11}L_1+e_{35}L_3\right.\right.$$

$$+\left(e_{31}+e_{15}\right)L_5\Bigg) + \frac{1}{\rho\cos\phi+R}\Bigg[\Bigg(e_{11}-e_{12}+\frac{\partial e_{16}}{\partial\theta}+\left(e_{16}+e_{21}\right)\frac{\partial}{\partial\theta}\Bigg)L_2+\Bigg(e_{31}-e_{32}+\frac{\partial e_{36}}{\partial\theta}$$

$$+\left(e_{25}+e_{36}\right)\frac{\partial}{\partial\theta}\Bigg)L_4\Bigg]+\frac{1}{\left(\rho\cos\phi+R\right)^2}\Bigg[\Bigg(-e_{22}+\frac{\partial e_{26}}{\partial\theta}\Bigg)\frac{\partial}{\partial\theta}+e_{26}\frac{\partial^2}{\partial\theta^2}\Bigg]\Bigg\}\varphi=0\,, \qquad (3.2a)$$

$$\Bigg\{\Bigg(c_{16}L_1+c_{45}L_3+\left(c_{56}+c_{14}\right)L_5\Bigg)+\frac{1}{\rho\cos\phi+R}\Bigg[\Bigg(2c_{16}+c_{26}+\frac{\partial c_{12}}{\partial\theta}+\left(c_{21}+c_{66}\right)\frac{\partial}{\partial\theta}\Bigg)L_2$$

$$+\Bigg(2c_{56}+c_{24}+\frac{\partial c_{25}}{\partial\theta}+\left(c_{25}+c_{46}\right)\frac{\partial}{\partial\theta}\Bigg)L_4\Bigg]+\frac{1}{\left(\rho\cos\phi+R\right)^2}\Bigg(c_{26}+\frac{\partial c_{22}}{\partial\theta}+\Bigg(c_{22}+c_{66}+\frac{\partial c_{26}}{\partial\theta}\Bigg)\frac{\partial}{\partial\theta}$$

$$+c_{26}\frac{\partial^2}{\partial\theta^2}\Bigg)\Bigg\}u_r+\Bigg\{\Bigg(c_{66}L_1+c_{44}L_3+2c_{46}L_5\Bigg)+\frac{1}{\rho\cos\phi+R}\Bigg[\Bigg(c_{66}+\frac{\partial c_{26}}{\partial\theta}+2c_{26}\frac{\partial}{\partial\theta}\Bigg)L_2$$

$$+\Bigg(c_{46}+\frac{\partial c_{24}}{\partial\theta}+2c_{24}\frac{\partial}{\partial\theta}\Bigg)L_4\Bigg]+\frac{1}{\left(\rho\cos\phi+R\right)^2}\Bigg(-c_{66}-\frac{\partial c_{26}}{\partial\theta}+\Bigg(\frac{\partial c_{22}}{\partial\theta}\Bigg)\frac{\partial}{\partial\theta}+c_{22}\frac{\partial^2}{\partial\theta^2}\Bigg)\Bigg\}u_\theta$$

$$+\Bigg\{\Bigg(c_{56}L_1+c_{34}L_3+\left(c_{36}+c_{45}\right)L_5\Bigg)+\frac{1}{\rho\cos\phi+R}\Bigg[\Bigg(2c_{56}+\frac{\partial c_{25}}{\partial\theta}+\left(c_{25}+c_{46}\right)\frac{\partial}{\partial\theta}\Bigg)L_2$$

$$+\Bigg(2c_{36}+\frac{\partial c_{23}}{\partial\theta}+\left(c_{23}+c_{44}\right)\frac{\partial}{\partial\theta}\Bigg)L_4\Bigg]+\frac{1}{\left(\rho\cos\phi+R\right)^2}\Bigg[\Bigg(c_{46}+\frac{\partial c_{24}}{\partial\theta}\Bigg)\frac{\partial}{\partial\theta}+c_{24}\frac{\partial^2}{\partial\theta^2}\Bigg]\Bigg\}u_z$$

$$+\Bigg\{\Bigg(e_{16}L_1+e_{34}L_3+\left(e_{36}+e_{14}\right)L_5\Bigg)+\frac{1}{\rho\cos\phi+R}\Bigg[\Bigg(2e_{16}+\frac{\partial e_{12}}{\partial\theta}+\left(e_{12}+e_{26}\right)\frac{\partial}{\partial\theta}\Bigg)L_2+\left(2e_{36}\right.$$

$$+\frac{\partial e_{32}}{\partial\theta}+\left(e_{24}+e_{32}\right)\frac{\partial}{\partial\theta}\Bigg)L_4\Bigg]+\frac{1}{\left(\rho\cos\phi+R\right)^2}\Bigg[\Bigg(e_{26}+\frac{\partial e_{22}}{\partial\theta}\Bigg)\frac{\partial}{\partial\theta}+e_{22}\frac{\partial^2}{\partial\theta^2}\Bigg]\Bigg\}\varphi=0\,, \qquad (3.2b)$$

$$\Bigg\{\Bigg(c_{15}L_1+c_{35}L_3+\left(c_{55}+c_{13}\right)L_5\Bigg)+\frac{1}{\rho\cos\phi+R}\Bigg[\Bigg(c_{15}+c_{25}+\frac{\partial c_{14}}{\partial\theta}+\left(c_{14}+c_{56}\right)\frac{\partial}{\partial\theta}\Bigg)L_2+\Bigg(c_{23}+c_{55}$$

$$+\frac{\partial c_{45}}{\partial\theta}+\left(c_{45}+c_{36}\right)\frac{\partial}{\partial\theta}\Bigg)L_4\Bigg]+\frac{1}{\left(\rho\cos\phi+R\right)^2}\Bigg(\frac{\partial c_{24}}{\partial\theta}+\Bigg(c_{24}+\frac{\partial c_{46}}{\partial\theta}\Bigg)\frac{\partial}{\partial\theta}+c_{46}\frac{\partial^2}{\partial\theta^2}\Bigg)\Bigg\}u_r$$

$$+\left\{\left(c_{56}L_1+c_{34}L_3+\left(c_{45}+c_{36}\right)L_5\right)+\frac{1}{\rho\cos\phi+R}\left[\left(\frac{\partial c_{46}}{\partial\theta}+\left(c_{25}+c_{46}\right)\frac{\partial}{\partial\theta}\right)L_2+\left(c_{45}-c_{36}+\frac{\partial c_{44}}{\partial\theta}\right.\right.\right.$$

$$\left.\left.\left.+\left(c_{44}+c_{23}\right)\frac{\partial}{\partial\theta}\right)L_4\right]+\frac{1}{\left(\rho\cos\phi+R\right)^2}\left[-\frac{\partial c_{46}}{\partial\theta}+\left(-c_{46}+\frac{\partial c_{24}}{\partial\theta}\right)\frac{\partial}{\partial\theta}+c_{24}\frac{\partial^2}{\partial\theta^2}\right]\right\}u_\theta+\left\{\left(c_{55}L_1\right.\right.$$

$$\left.\left.+c_{33}L_3+2c_{35}L_5\right)+\frac{1}{\rho\cos\phi+R}\left[\left(c_{55}+\frac{\partial c_{45}}{\partial\theta}+2c_{45}\frac{\partial}{\partial\theta}\right)L_2+\left(c_{35}+\frac{\partial c_{34}}{\partial\theta}+2c_{34}\frac{\partial}{\partial\theta}\right)L_4\right]\right.$$

$$\left.+\frac{1}{\left(\rho\cos\phi+R\right)^2}\left(\left(\frac{\partial c_{44}}{\partial\theta}\right)\frac{\partial}{\partial\theta}+c_{44}\frac{\partial^2}{\partial\theta^2}\right)\right\}u_z+\left\{\left(e_{15}L_1+e_{33}L_3+\left(e_{35}+e_{13}\right)L_5\right)\right.$$

$$+\frac{1}{\rho\cos\phi+R}\left[\left(e_{15}+\frac{\partial e_{14}}{\partial\theta}+\left(e_{25}+e_{14}\right)\frac{\partial}{\partial\theta}\right)L_2+\left(e_{35}+\frac{\partial e_{34}}{\partial\theta}+\left(e_{34}+e_{23}\right)\frac{\partial}{\partial\theta}\right)L_4\right]$$

$$\left.+\frac{1}{\left(\rho\cos\phi+R\right)^2}\left[\left(\frac{\partial e_{24}}{\partial\theta}\right)\frac{\partial}{\partial\theta}+e_{24}\frac{\partial^2}{\partial\theta^2}\right]\right\}\varphi=0\,, \qquad (3.2c)$$

$$\left\{\left(e_{11}L_1+e_{35}L_3+\left(e_{15}+e_{31}\right)L_5\right)+\frac{1}{\rho\cos\phi+R}\left[\left(e_{11}+e_{12}+\frac{\partial e_{21}}{\partial\theta}+\left(e_{16}+e_{21}\right)\frac{\partial}{\partial\theta}\right)L_2+\left(e_{15}+e_{32}\right.\right.\right.$$

$$\left.\left.\left.+\frac{\partial e_{25}}{\partial\theta}+\left(e_{25}+e_{36}\right)\frac{\partial}{\partial\theta}\right)L_4\right]+\frac{1}{\left(\rho\cos\phi+R\right)^2}\left(\frac{\partial e_{22}}{\partial\theta}+\left(e_{22}+\frac{\partial e_{26}}{\partial\theta}\right)\frac{\partial}{\partial\theta}+e_{26}\frac{\partial^2}{\partial\theta^2}\right)\right\}u_r$$

$$+\left\{\left(e_{16}L_1+e_{34}L_3+\left(e_{14}+e_{36}\right)L_5\right)+\frac{1}{\rho\cos\phi+R}\left[\left(\frac{\partial e_{26}}{\partial\theta}+\left(e_{12}+e_{26}\right)\frac{\partial}{\partial\theta}\right)L_2+\left(e_{14}-e_{36}+\frac{\partial e_{24}}{\partial\theta}\right.\right.\right.$$

$$\left.\left.\left.+\left(e_{24}+e_{32}\right)\frac{\partial}{\partial\theta}\right)L_4\right]+\frac{1}{\left(\rho\cos\phi+R\right)^2}\left[-\frac{\partial e_{26}}{\partial\theta}+\left(-e_{26}+\frac{\partial e_{22}}{\partial\theta}\right)\frac{\partial}{\partial\theta}+e_{22}\frac{\partial^2}{\partial\theta^2}\right]\right\}u_\theta$$

$$+\left\{\left(e_{15}L_1+e_{33}L_3+\left(e_{13}+e_{35}\right)L_5\right)+\frac{1}{\rho\cos\phi+R}\left[\left(e_{15}+\frac{\partial e_{25}}{\partial\theta}+\left(e_{14}+e_{25}\right)\frac{\partial}{\partial\theta}\right)L_2\right.\right.$$

$$\left.\left.+\left(e_{13}+\frac{\partial e_{23}}{\partial\theta}+\left(e_{23}+e_{34}\right)\frac{\partial}{\partial\theta}\right)L_4\right]+\frac{1}{\left(\rho\cos\phi+R\right)^2}\left[\left(\frac{\partial e_{24}}{\partial\theta}\right)\frac{\partial}{\partial\theta}+e_{24}\frac{\partial^2}{\partial\theta^2}\right]\right\}u_z-\left\{\left(\eta_{11}L_1\right.\right.$$

$$\left.\left.+\eta_{33}L_3+2\eta_{13}L_5\right)+\frac{1}{\rho\cos\phi+R}\left[\left(\eta_{11}+\frac{\partial\eta_{12}}{\partial\theta}+2\eta_{12}\frac{\partial}{\partial\theta}\right)L_2+\left(\eta_{13}+\frac{\partial\eta_{23}}{\partial\theta}+2\eta_{23}\frac{\partial}{\partial\theta}\right)L_4\right]\right.$$

$$+\frac{1}{\left(\rho\cos\phi+R\right)^2}\left[\left(\frac{\partial\eta_{22}}{\partial\theta}\right)\frac{\partial}{\partial\theta}+\eta_{22}\frac{\partial^2}{\partial\theta^2}\right]\Bigg\}\varphi=0\,, \tag{3.2d}$$

where

$$L_1=\cos^2\phi\frac{\partial^2}{\partial\rho^2}+\frac{\sin^2\phi}{\rho}\frac{\partial}{\partial\rho}-\frac{2\sin\phi\cos\phi}{\rho}\frac{\partial^2}{\partial\rho\partial\phi}+\frac{2\sin\phi\cos\phi}{\rho^2}\frac{\partial}{\partial\phi}+\frac{\sin^2\phi}{\rho^2}\frac{\partial^2}{\partial\phi^2}\quad,$$

$$L_2=\cos\phi\frac{\partial}{\partial\rho}-\frac{\sin\phi}{\rho}\frac{\partial}{\partial\phi}\quad,$$

$$L_3=\sin^2\phi\frac{\partial^2}{\partial\rho^2}+\frac{\cos^2\phi}{\rho}\frac{\partial}{\partial\rho}+\frac{2\sin\phi\cos\phi}{\rho}\frac{\partial^2}{\partial\rho\partial\phi}-\frac{2\sin\phi\cos\phi}{\rho^2}\frac{\partial}{\partial\phi}+\frac{\cos^2\phi}{\rho^2}\frac{\partial^2}{\partial\phi^2}\quad,$$

$$L_4=\frac{\partial}{\partial\rho}\frac{\partial\rho}{\partial z}+\frac{\partial}{\partial\phi}\frac{\partial\phi}{\partial z}=-\sin\phi\frac{\partial}{\partial\rho}-\frac{\cos\phi}{\rho}\frac{\partial}{\partial\phi}\quad,$$

$$L_5=-\sin\varphi\cos\varphi\frac{\partial^2}{\partial\rho^2}+\frac{\sin\varphi\cos\varphi}{\rho}\frac{\partial}{\partial\rho}-\frac{\cos2\varphi}{\rho}\frac{\partial^2}{\partial\rho\partial\varphi}+\frac{\cos2\varphi}{\rho^2}\frac{\partial}{\partial\varphi}+\frac{\sin\varphi\cos\varphi}{\rho^2}\frac{\partial^2}{\partial\varphi^2}\quad,$$

3.2 **Construction of Asymptotic Solution**

To find solutions to Eqs. (3.2) for bodies of revolution, the methodology of Hartranft and Sih (1969) for elastic wedges can be applied. The solutions are expressed as

$$u_r(r,\theta,z)=\sum_{m=0}^{\infty}\sum_{n=0}^{\infty}\rho^{\lambda_m+n}\hat{U}_n^{(m)}(\theta,\varphi),\quad u_\theta(r,\theta,z)=\sum_{m=0}^{\infty}\sum_{n=0}^{\infty}\rho^{\lambda_m+n}\hat{V}_n^{(m)}(\theta,\varphi),$$

$$u_z(r,\theta,z)=\sum_{m=0}^{\infty}\sum_{n=0}^{\infty}\rho^{\lambda_m+n}\hat{W}_n^{(m)}(\theta,\varphi),\quad \phi(r,\theta,z)=\sum_{m=0}^{\infty}\sum_{n=0}^{\infty}\rho^{\lambda_m+n}\hat{\Phi}_n^{(m)}(\theta,\varphi) \tag{3.3}$$

where λ_m is a parameter to be determined, which can be a complex number, and the real part of λ_m must be positive to ensure finite displacement and electric potential at $\rho=0$. To determine the eletroelastic singularity behaviors as ρ approaches zero, substituting Eqs. (3.3) into Eqs. (3.2) with careful arrangement and considering only the equations for the least power order of ρ yield

$$\frac{\partial^2\hat{U}_0^{(m)}}{\partial\varphi^2}+\frac{1}{\Delta_1}(\lambda_m-1)\left[(c_{55}-c_{11})\sin2\varphi-2c_{15}\cos2\varphi\right]\frac{\partial\hat{U}_0^{(m)}}{\partial\varphi}+\frac{1}{\Delta_1}\Bigg[\lambda_m\left((\lambda_m-1)c_{55}+c_{11}\right)\sin^2\varphi$$
$$+\lambda_m\left((\lambda_m-1)c_{11}+c_{55}\right)\cos^2\varphi+\lambda_m(2-\lambda_m)c_{15}\sin2\varphi\Bigg]\hat{U}_0^{(m)}+\frac{1}{\Delta_1}\Bigg\{\Bigg[c_{16}\sin^2\varphi+c_{45}\cos^2\varphi$$
$$+\frac{(c_{14}+c_{56})}{2}\sin2\varphi\Bigg]\frac{\partial^2\hat{V}_0^{(m)}}{\partial\varphi^2}+(\lambda_m-1)\left[(c_{45}-c_{16})\sin2\varphi-(c_{14}+c_{56})\cos2\varphi\right]\frac{\partial\hat{V}_0^{(m)}}{\partial\varphi}$$
$$+\Bigg[\lambda_m(\lambda_m-1)\left(c_{16}\cos^2\varphi+c_{45}\sin^2\varphi-\frac{(c_{14}+c_{56})}{2}\sin2\varphi\right)+\lambda_m\left(c_{16}\sin^2\varphi+c_{45}\cos^2\varphi\right.$$

$$+\frac{(c_{14}+c_{56})}{2}\sin 2\varphi\Big)\Big]\Big\}\hat{V}_0^{(m)}+\frac{1}{\Delta_1}\Big\{\Big[c_{15}\sin^2\varphi+c_{35}\cos^2\varphi+\frac{(c_{13}+c_{55})}{2}\sin 2\varphi\Big]\frac{\partial^2\hat{W}_0^{(m)}}{\partial\varphi^2}$$

$$+(\lambda_m-1)\big[(c_{35}-c_{15})\sin 2\varphi-(c_{13}+c_{55})\cos 2\varphi\big]\frac{\partial\hat{W}_0^{(m)}}{\partial\varphi}+\Big[\lambda_m(\lambda_m-1)\Big(c_{15}\cos^2\varphi+c_{35}\sin^2\varphi$$

$$-\frac{(c_{13}+c_{55})}{2}\sin 2\varphi\Big)+\lambda_m\Big(c_{15}\sin^2\varphi+c_{35}\cos^2\varphi+\frac{(c_{13}+c_{55})}{2}\sin 2\varphi\Big)\Big]\Big\}\hat{W}_0^{(m)}$$

$$+\frac{1}{\Delta_1}\Big[e_{11}\sin^2\varphi+e_{35}\cos^2\varphi+\frac{(e_{15}+e_{31})}{2}\sin 2\varphi\Big]\frac{\partial^2\hat{\Phi}_0^{(m)}}{\partial\varphi^2}+(\lambda_m-1)\big[(e_{35}-e_{15})\sin 2\varphi$$

$$-(e_{15}+e_{31})\cos 2\varphi\big]\frac{\partial\hat{\Phi}_0^{(m)}}{\partial\varphi}+\Big[\lambda_m(\lambda_m-1)\Big(e_{11}\cos^2\varphi+e_{35}\sin^2\varphi-\frac{(e_{15}+e_{31})}{2}\sin 2\varphi\Big)$$

$$+\lambda_m\Big(e_{11}\sin^2\varphi+e_{35}\cos^2\varphi+\frac{(e_{15}+e_{31})}{2}\sin 2\varphi\Big)\Big]\Big\}\hat{\Phi}_0^{(m)}=0\,, \qquad (3.4a)$$

$$\frac{\partial^2\hat{V}_0^{(m)}}{\partial\varphi^2}+\frac{1}{\Delta_2}(\lambda_m-1)\big[(c_{44}-c_{66})\sin 2\varphi-2c_{46}\cos 2\varphi\big]\frac{\partial\hat{V}_0^{(m)}}{\partial\varphi}+\frac{1}{\Delta_2}\Big[\lambda_m\big((\lambda_m-1)c_{44}+c_{66}\big)\sin^2\varphi$$

$$+\lambda_m\big((\lambda_m-1)c_{66}+c_{44}\big)\cos^2\varphi+\lambda_m(2-\lambda_m)c_{46}\sin 2\varphi\Big]\hat{V}_0^{(m)}+\frac{1}{\Delta_2}\Big\{\Big[c_{16}\sin^2\varphi+c_{45}\cos^2\varphi$$

$$+\frac{(c_{56}+c_{14})}{2}\sin 2\varphi\Big]\frac{\partial^2\hat{U}_0^{(m)}}{\partial\varphi^2}+(\lambda_m-1)\big[(c_{45}-c_{16})\sin 2\varphi-(c_{56}+c_{14})\cos 2\varphi\big]\frac{\partial\hat{U}_0^{(m)}}{\partial\varphi}$$

$$+\Big[\lambda_m(\lambda_m-1)\Big(c_{16}\cos^2\varphi+c_{45}\sin^2\varphi-\frac{(c_{56}+c_{14})}{2}\sin 2\varphi\Big)+\lambda_m\Big(c_{16}\sin^2\varphi+c_{45}\cos^2\varphi$$

$$+\frac{(c_{56}+c_{14})}{2}\sin 2\varphi\Big)\Big]\Big\}\hat{U}_0^{(m)}+\frac{1}{\Delta_3}\Big\{\Big[c_{56}\sin^2\varphi+c_{34}\cos^2\varphi+\frac{(c_{36}+c_{45})}{2}\sin 2\varphi\Big]\frac{\partial^2\hat{W}_0^{(m)}}{\partial\varphi^2}$$

$$+(\lambda_m-1)\big[(c_{34}-c_{56})\sin 2\varphi-(c_{36}+c_{45})\cos 2\varphi\big]\frac{\partial\hat{W}_0^{(m)}}{\partial\varphi}+\Big[\lambda_m(\lambda_m-1)\Big(c_{56}\cos^2\varphi+c_{34}\sin^2\varphi$$

$$-\frac{(c_{36}+c_{45})}{2}\sin 2\varphi\Big)+\lambda_m\Big(c_{56}\sin^2\varphi+c_{34}\cos^2\varphi+\frac{(c_{36}+c_{45})}{2}\sin 2\varphi\Big)\Big]\Big\}\hat{W}_0^{(m)}$$

$$+\frac{1}{\Delta_2}\Big\{\Big[e_{16}\sin^2\varphi+e_{34}\cos^2\varphi+\frac{(e_{36}+e_{14})}{2}\sin 2\varphi\Big]\frac{\partial^2\hat{\Phi}_0^{(m)}}{\partial\varphi^2}+(\lambda_m-1)\big[(e_{34}-e_{16})\sin 2\varphi$$

$$-(e_{36}+e_{14})\cos 2\varphi\big]\frac{\partial\hat{\Phi}_0^{(m)}}{\partial\varphi}+\Big[\lambda_m(\lambda_m-1)\Big(e_{16}\cos^2\varphi+e_{34}\sin^2\varphi-\frac{(e_{36}+e_{14})}{2}\sin 2\varphi\Big)$$

$$+\lambda_m\Big(e_{16}\sin^2\varphi+e_{34}\cos^2\varphi+\frac{(e_{36}+e_{14})}{2}\sin 2\varphi\Big)\Big]\Big\}\hat{\Phi}_0^{(m)}=0\,, \qquad (3.4b)$$

$$\frac{\partial^2\hat{W}_0^{(m)}}{\partial\varphi^2}+\frac{1}{\Delta_3}(\lambda_m-1)\big[(c_{33}-c_{55})\sin 2\varphi-2c_{35}\cos 2\varphi\big]\frac{\partial\hat{W}_0^{(m)}}{\partial\varphi}+\frac{1}{\Delta_3}\Big[\lambda_m\big((\lambda_m-1)c_{33}+c_{55}\big)\sin^2\varphi$$

$$+\lambda_m\left((\lambda_m-1)c_{55}+c_{33}\right)\cos^2\varphi+\lambda_m(2-\lambda_m)c_{35}\sin 2\varphi\Big]\hat{W}_0^{(m)}+\frac{1}{\Delta_3}\Bigg\{\Bigg[c_{15}\sin^2\varphi+c_{35}\cos^2\varphi$$

$$+\frac{(c_{31}+c_{55})}{2}\sin 2\varphi\Bigg]\frac{\partial^2\hat{U}_0^{(m)}}{\partial\varphi^2}+(\lambda_m-1)\left[(c_{35}-c_{15})\sin 2\varphi-(c_{13}+c_{55})\cos 2\varphi\right]\frac{\partial\hat{U}_0^{(m)}}{\partial\varphi}$$

$$+\Bigg[\lambda_m(\lambda_m-1)\Bigg(c_{15}\cos^2\varphi+c_{35}\sin^2\varphi-\frac{(c_{13}+c_{55})}{2}\sin 2\varphi\Bigg)+\lambda_m\Bigg(c_{15}\sin^2\varphi+c_{35}\cos^2\varphi$$

$$+\frac{(c_{13}+c_{55})}{2}\sin 2\varphi\Bigg)\Bigg]\Bigg\}\hat{U}_0^{(m)}+\frac{1}{\Delta_3}\Bigg\{\Bigg[c_{56}\sin^2\varphi+c_{34}\cos^2\varphi+\frac{(c_{36}+c_{45})}{2}\sin 2\varphi\Bigg]\frac{\partial^2\hat{V}_0^{(m)}}{\partial\varphi^2}$$

$$+(\lambda_m-1)\left[(c_{34}-c_{56})\sin 2\varphi-(c_{36}+c_{45})\cos 2\varphi\right]\frac{\partial\hat{V}_0^{(m)}}{\partial\varphi}+\Bigg[\lambda_m(\lambda_m-1)\Bigg(c_{56}\cos^2\varphi+c_{34}\sin^2\varphi$$

$$-\frac{(c_{36}+c_{45})}{2}\sin 2\varphi\Bigg)+\lambda_m\Bigg(c_{56}\sin^2\varphi+c_{34}\cos^2\varphi+\frac{(c_{36}+c_{45})}{2}\sin 2\varphi\Bigg)\Bigg]\Bigg\}\hat{V}_0^{(m)}$$

$$+\frac{1}{\Delta_3}\Bigg\{\Bigg[e_{15}\sin^2\varphi+e_{33}\cos^2\varphi+\frac{(e_{13}+e_{35})}{2}\sin 2\varphi\Bigg]\frac{\partial^2\hat{\Phi}_0^{(m)}}{\partial\varphi^2}+(\lambda_m-1)\left[(e_{33}-e_{15})\sin 2\varphi\right.$$

$$\left.-(e_{13}+e_{35})\cos 2\varphi\right]\frac{\partial\hat{\Phi}_0^{(m)}}{\partial\varphi}+\Bigg[\lambda_m(\lambda_m-1)\Bigg(e_{15}\cos^2\varphi+e_{33}\sin^2\varphi-\frac{(e_{13}+e_{35})}{2}\sin 2\varphi\Bigg)$$

$$+\lambda_m\Bigg(e_{15}\sin^2\varphi+e_{33}\cos^2\varphi+\frac{(e_{13}+e_{35})}{2}\sin 2\varphi\Bigg)\Bigg]\Bigg\}\hat{\Phi}_0^{(m)}=0\,, \qquad (3.4c)$$

$$\frac{\partial^2\hat{\Phi}_0^{(m)}}{\partial\varphi^2}+\frac{1}{\Delta_4}(\lambda_m-1)\left[(\eta_{33}-\eta_{11})\sin 2\varphi-2\eta_{13}\cos 2\varphi\right]\frac{\partial\hat{\Phi}_0^{(m)}}{\partial\varphi}+\frac{1}{\Delta_4}\Bigg[\lambda_m\left((\lambda_m-1)\eta_{33}+\eta_{11}\right)\sin^2\varphi$$

$$+\lambda_m\left((\lambda_m-1)\eta_{11}+\eta_{33}\right)\cos^2\varphi+\lambda_m(2-\lambda_m)\eta_{13}\sin 2\varphi\Big]\hat{\Phi}_0^{(m)}-\frac{1}{\Delta_4}\Bigg\{\Bigg[e_{11}\sin^2\varphi+e_{35}\cos^2\varphi$$

$$+\frac{(e_{15}+e_{31})}{2}\sin 2\varphi\Bigg]\frac{\partial^2\hat{U}_0^{(m)}}{\partial\varphi^2}+(\lambda_m-1)\left[(e_{35}-e_{11})\sin 2\varphi-(e_{15}+e_{31})\cos 2\varphi\right]\frac{\partial\hat{U}_0^{(m)}}{\partial\varphi}$$

$$+\Bigg[\lambda_m(\lambda_m-1)\Bigg(e_{11}\cos^2\varphi+e_{35}\sin^2\varphi-\frac{(e_{15}+e_{31})}{2}\sin 2\varphi\Bigg)+\lambda_m\Bigg(e_{11}\sin^2\varphi+e_{35}\cos^2\varphi$$

$$+\frac{(e_{15}+e_{31})}{2}\sin 2\varphi\Bigg)\Bigg]\Bigg\}\hat{U}_0^{(m)}-\frac{1}{\Delta_4}\Bigg\{\Bigg[e_{16}\sin^2\varphi+e_{34}\cos^2\varphi+\frac{(e_{14}+e_{36})}{2}\sin 2\varphi\Bigg]\frac{\partial^2\hat{V}_0^{(m)}}{\partial\varphi^2}$$

$$+(\lambda_m-1)\left[(e_{34}-e_{16})\sin 2\varphi-(e_{14}+e_{36})\cos 2\varphi\right]\frac{\partial\hat{V}_0^{(m)}}{\partial\varphi}+\Bigg[\lambda_m(\lambda_m-1)\Bigg(e_{16}\cos^2\varphi+e_{34}\sin^2\varphi$$

$$-\frac{(e_{14}+e_{36})}{2}\sin 2\varphi\Bigg)+\lambda_m\Bigg(e_{16}\sin^2\varphi+e_{34}\cos^2\varphi+\frac{(e_{14}+e_{36})}{2}\sin 2\varphi\Bigg)\Bigg]\Bigg\}\hat{V}_0^{(m)}$$

$$-\frac{1}{\Delta_4}\Bigg\{\Bigg[e_{15}\sin^2\varphi+e_{33}\cos^2\varphi+\frac{(e_{13}+e_{35})}{2}\sin 2\varphi\Bigg]\frac{\partial^2\hat{W}_0^{(m)}}{\partial\varphi^2}+(\lambda_m-1)\left[(e_{33}-e_{15})\sin 2\varphi\right.$$

$$\left.-(e_{13}+e_{35})\cos 2\varphi\right]\frac{\partial\hat{W}_0^{(m)}}{\partial\varphi}+\Bigg[\lambda_m(\lambda_m-1)\Bigg(e_{15}\cos^2\varphi+e_{33}\sin^2\varphi-\frac{(e_{13}+e_{35})}{2}\sin 2\varphi\Bigg)$$

$$+\lambda_m\left(e_{15}\sin^2\varphi+e_{33}\cos^2\varphi+\frac{(e_{13}+e_{35})}{2}\sin 2\varphi\right)\Bigg]\Bigg\}\hat{W}_0^{(m)}=0, \tag{3.4d}$$

where

$\Delta_1=c_{11}\sin^2\varphi+c_{55}\cos^2\varphi+c_{15}\sin 2\varphi$, $\Delta_2=c_{66}\sin^2\varphi+c_{44}\cos^2\varphi+c_{46}\sin 2\varphi$,

$\Delta_3=c_{55}\sin^2\varphi+c_{33}\cos^2\varphi+c_{35}\sin 2\varphi$, $\Delta_4=\eta_{11}\sin^2\varphi+\eta_{33}\cos^2\varphi+\eta_{13}\sin 2\varphi$.

Equations (3.4) are a set of ordinary differential equations with variable coefficients that are functions of φ, θ and γ. Finding a closed-form solution for these equations is generally impossible.

The power series method is utilized to find a general solution for Eqs. (3.4). Very high-order terms are typically required to obtain an accurate solution and can cause numerical difficulties. To overcome these difficulties, the range of φ under consideration is divided into a number of sub-domains (see Fig. 3.3). A series solution for Eqs. (3.4) is established in each sub-domain. Then, a general solution for the whole domain of φ is constructed from these series solutions in the sub-domains by satisfying the continuity conditions between each pair of adjacent sub-domains. This means of constructing solutions is very convenient for analyzing the bi-material body that is considered in this work.

With fixed θ and γ, the following functions that specify the variable coefficients in Eqs. (3.4) are expressed as Taylor expansions over sub-domain *i*;

$$\frac{\sin 2\varphi}{\Delta_1}=\sum_{k=0}^{K}a_k^{(i)}(\varphi-\overline{\varphi}_i)^k,\quad \frac{\cos^2\varphi}{\Delta_1}=\sum_{k=0}^{K}b_k^{(i)}(\varphi-\overline{\varphi}_i)^k,\quad \frac{\sin^2\varphi}{\Delta_1}=\sum_{k=0}^{K}c_k^{(i)}(\varphi-\overline{\varphi}_i)^k,$$

$$\frac{\cos 2\varphi}{\Delta_1}=\sum_{k=0}^{K}d_k^{(i)}(\varphi-\overline{\varphi}_i)^k,\ \frac{\sin 2\varphi}{\Delta_2}=\sum_{k=0}^{K}e_k^{(i)}(\varphi-\overline{\varphi}_i)^k,\quad \frac{\cos^2\varphi}{\Delta_2}=\sum_{k=0}^{K}f_k^{(i)}(\varphi-\overline{\varphi}_i)^k,$$

$$\frac{\sin^2\varphi}{\Delta_2}=\sum_{k=0}^{K}g_k^{(i)}(\varphi-\overline{\varphi}_i)^k,\quad \frac{\cos 2\varphi}{\Delta_2}=\sum_{k=0}^{K}h_k^{(i)}(\varphi-\overline{\varphi}_i)^k,\ \frac{\sin 2\varphi}{\Delta_3}=\sum_{k=0}^{K}l_k^{(i)}(\varphi-\overline{\varphi}_i)^k,$$

$$\frac{\cos^2\varphi}{\Delta_3}=\sum_{k=0}^{K}m_k^{(i)}(\varphi-\overline{\varphi}_i)^k,\quad \frac{\sin^2\varphi}{\Delta_3}=\sum_{k=0}^{K}n_k^{(i)}(\varphi-\overline{\varphi}_i)^k,\quad \frac{\cos 2\varphi}{\Delta_3}=\sum_{k=0}^{K}o_k^{(i)}(\varphi-\overline{\varphi}_i)^k,$$

$$\frac{\sin 2\varphi}{\Delta_4}=\sum_{k=0}^{K}p_k^{(i)}(\varphi-\overline{\varphi}_i)^k,\quad \frac{\cos^2\varphi}{\Delta_4}=\sum_{k=0}^{K}q_k^{(i)}(\varphi-\overline{\varphi}_i)^k,\quad \frac{\sin^2\varphi}{\Delta_4}=\sum_{k=0}^{K}r_k^{(i)}(\varphi-\overline{\varphi}_i)^k,$$

$$\frac{\cos 2\varphi}{\Delta_4}=\sum_{k=0}^{K}s_k^{(i)}(\varphi-\overline{\varphi}_i)^k, \tag{3.5}$$

where $\overline{\varphi}_i$ is a reference point in sub-domain *i*. Here, $\overline{\varphi}_i$ is chosen as the middle point along the φ in the sub-domain *i*. Consequently, the general solutions of Eqs. (3.4) in sub-domain *i* are expressed in the following form:

$$\hat{U}_{0i}^{(m)}=\sum_{j=0}^{J}\hat{A}_j^{(i)}(\varphi-\overline{\varphi}_i)^j,\quad \hat{V}_{0i}^{(m)}=\sum_{j=0}^{J}\hat{B}_j^{(i)}(\varphi-\overline{\varphi}_i)^j,\quad \hat{W}_{0i}^{(m)}=\sum_{j=0}^{J}\hat{C}_j^{(i)}(\varphi-\overline{\varphi}_i)^j,$$

$$\hat{\Phi}_{0i}^{(m)} = \sum_{j=0}^{J} \hat{D}_j^{(i)} \left(\varphi - \overline{\varphi}_i\right)^j \tag{3.6}$$

Substituting Eqs. (3.5) and (3.6) into Eqs. (3.4) with careful arrangement yields the recursive equations for the coefficients in Eqs. (3.6),

$$\begin{aligned}
&\hat{A}_{j+2}^{(i)} + \left(c_{16}c_0^{(i)} + c_{45}b_0^{(i)} + \frac{\left(c_{14}+c_{56}\right)}{2} a_0^{(i)} \right) \hat{B}_{j+2}^{(i)} + \left(c_{15}c_0^{(i)} + c_{35}b_0^{(i)} + \frac{\left(c_{13}+c_{55}\right)}{2} a_0^{(i)} \right) \hat{C}_{j+2}^{(i)} \\
&+ \left(e_{11}c_0^{(i)} + e_{35}b_0^{(i)} + \frac{\left(e_{15}+e_{31}\right)}{2} a_0^{(i)} \right) \hat{D}_{j+2}^{(i)} = \frac{-1}{\left(j+2\right)\left(j+1\right)} \left\{ \sum_{k=0}^{j-1} \left[\left(c_{16}c_{j-k}^{(i)} + c_{45}b_{j-k}^{(i)} + \frac{\left(c_{14}+c_{56}\right)}{2} a_{j-k}^{(i)} \right) \right. \right. \\
&\times \left(k+2\right)\left(k+1\right) \hat{B}_{k+2}^{(i)} + \left(c_{15}c_{j-k}^{(i)} + c_{35}b_{j-k}^{(i)} + \frac{\left(c_{13}+c_{55}\right)}{2} a_{j-k}^{(i)} \right) \left(k+2\right)\left(k+1\right) \hat{C}_{k+2}^{(i)} \\
&+ \left(e_{11}c_{j-k}^{(i)} + e_{35}b_{j-k}^{(i)} + \frac{\left(e_{15}+e_{31}\right)}{2} a_{j-k}^{(i)} \right) \left(k+2\right)\left(k+1\right) \hat{D}_{k+2}^{(i)} + \sum_{k=0}^{j} \left[\left(\lambda_m - 1\right) \left[\left(c_{55} - c_{11}\right) a_{j-k}^{(i)} - 2c_{15}d_{j-k}^{(i)} \right] \right. \\
&\times \left(k+1\right) \hat{A}_{k+1}^{(i)} + \left[\lambda_m \left(\left(\lambda_m - 1\right) c_{55} + c_{11} \right) c_{j-k}^{(i)} + \lambda_m \left(\left(\lambda_m - 1\right) c_{11} + c_{55} \right) b_{j-k}^{(i)} + \lambda \left(2 - \lambda\right) c_{15} a_{j-k}^{(i)} \right] \hat{A}_k^{(i)} \\
&+ \left(\lambda_m - 1\right) \left[\left(c_{45} - c_{16}\right) a_{j-k}^{(i)} - \left(c_{14} + c_{56}\right) d_{j-k}^{(i)} \right] \left(k+1\right) \hat{B}_{k+1}^{(i)} + \left[\lambda_m \left(\lambda_m - 1\right) \right. \\
&\times \left. \left(c_{16}b_{j-k}^{(i)} + c_{45}c_{j-k}^{(i)} - \frac{\left(c_{14}+c_{56}\right)}{2} a_{j-k}^{(i)} \right) + \lambda_m \left(c_{16}c_{j-k}^{(i)} + c_{45}b_{j-k}^{(i)} + \frac{\left(c_{14}+c_{56}\right)}{2} a_{j-k}^{(i)} \right) \right] \hat{B}_k^{(i)} \\
&+ \left(\lambda_m - 1\right) \left[\left(c_{35} - c_{15}\right) a_{j-k}^{(i)} - \left(c_{13} + c_{55}\right) d_{j-k}^{(i)} \right] \left(k+1\right) \hat{C}_{k+1}^{(i)} + \left[\lambda_m \left(\lambda_m - 1\right) \right. \\
&\times \left. \left(c_{15}b_{j-k}^{(i)} + c_{35}c_{j-k}^{(i)} - \frac{\left(c_{13}+c_{55}\right)}{2} a_{j-k}^{(i)} \right) + \lambda_m \left(c_{15}c_{j-k}^{(i)} + c_{35}b_{j-k}^{(i)} + \frac{\left(c_{13}+c_{55}\right)}{2} a_{j-k}^{(i)} \right) \right] \hat{C}_k^{(i)} \\
&+ \left(\lambda_m - 1\right) \left[\left(e_{35} - e_{11}\right) a_{j-k}^{(i)} - \left(e_{15} + e_{31}\right) d_{j-k}^{(i)} \right] \left(k+1\right) \hat{D}_{k+1}^{(i)} + \left[\lambda_m \left(\lambda_m - 1\right) \right. \\
&\times \left. \left. \left. \left(e_{11}b_{j-k}^{(i)} + e_{35}c_{j-k}^{(i)} - \frac{\left(e_{15}+e_{31}\right)}{2} a_{j-k}^{(i)} \right) + \lambda_m \left(e_{11}c_{j-k}^{(i)} + e_{35}b_{j-k}^{(i)} + \frac{\left(e_{15}+e_{31}\right)}{2} a_{j-k}^{(i)} \right) \right] \hat{D}_k^{(i)} \right] \right\}, \quad (3.7a)
\end{aligned}$$

$$\begin{aligned}
&\hat{B}_{j+2}^{(i)} + \left(c_{16}g_0^{(i)} + c_{45}f_0^{(i)} + \frac{\left(c_{56}+c_{14}\right)}{2} e_0^{(i)} \right) \hat{A}_{j+2}^{(i)} + \left(c_{56}g_0^{(i)} + c_{34}f_0^{(i)} + \frac{\left(c_{36}+c_{45}\right)}{2} e_0^{(i)} \right) \hat{C}_{j+2}^{(i)} \\
&+ \left(e_{16}g_0^{(i)} + e_{34}f_0^{(i)} + \frac{\left(e_{36}+e_{14}\right)}{2} e_0^{(i)} \right) \hat{D}_{j+2}^{(i)} = \frac{-1}{\left(j+2\right)\left(j+1\right)} \left\{ \sum_{k=0}^{j-1} \left[\left(c_{16}g_{j-k}^{(i)} + c_{45}f_{j-k}^{(i)} + \frac{\left(c_{56}+c_{14}\right)}{2} e_{j-k}^{(i)} \right) \right. \right. \\
&\times \left(k+2\right)\left(k+1\right) \hat{A}_{k+2}^{(i)} + \left(c_{56}g_{j-k}^{(i)} + c_{34}f_{j-k}^{(i)} + \frac{\left(c_{36}+c_{45}\right)}{2} e_{j-k}^{(i)} \right) \left(k+2\right)\left(k+1\right) \hat{C}_{k+2}^{(i)} \\
&+ \left(e_{16}g_{j-k}^{(i)} + e_{34}f_{j-k}^{(i)} + \frac{\left(e_{36}+e_{14}\right)}{2} e_{j-k}^{(i)} \right) \left(k+2\right)\left(k+1\right) \hat{D}_{k+2}^{(i)} + \sum_{k=0}^{j} \left[\left(\lambda_m - 1\right) \left[\left(c_{44} - c_{66}\right) e_{j-k}^{(i)} - 2c_{46}h_{j-k}^{(i)} \right] \right. \\
&\times \left(k+1\right) \hat{B}_{k+1}^{(i)} + \left[\lambda_m \left(\left(\lambda_m - 1\right) c_{44} + c_{66} \right) g_{j-k}^{(i)} + \lambda_m \left(\left(\lambda_m - 1\right) c_{66} + c_{44} \right) f_{j-k}^{(i)} + \lambda_m \left(2 - \lambda_m\right) c_{46} e_{j-k}^{(i)} \right] \hat{B}_k^{(i)}
\end{aligned}$$

$$+(\lambda_m-1)\left[(c_{45}-c_{16})e_{j-k}^{(i)}-(c_{56}+c_{14})h_{j-k}^{(i)}\right](k+1)\hat{A}_{k+1}^{(i)}+\Bigg[\lambda_m(\lambda_m-1)$$
$$\times\left(c_{16}f_{j-k}^{(i)}+c_{45}g_{j-k}^{(i)}-\frac{(c_{56}+c_{14})}{2}e_{j-k}^{(i)}\right)+\lambda_m\left(c_{16}g_{j-k}^{(i)}+c_{45}f_{j-k}^{(i)}+\frac{(c_{56}+c_{14})}{2}e_{j-k}^{(i)}\right)\Bigg]\hat{A}_k^{(i)}$$
$$+(\lambda_m-1)\left[(c_{34}-c_{56})e_{j-k}^{(i)}-(c_{36}+c_{45})h_{j-k}^{(i)}\right](k+1)\hat{C}_{k+1}^{(i)}+\Bigg[\lambda_m(\lambda_m-1)$$
$$\times\left(c_{56}f_{j-k}^{(i)}+c_{34}g_{j-k}^{(i)}-\frac{(c_{36}+c_{45})}{2}e_{j-k}^{(i)}\right)+\lambda_m\left(c_{56}g_{j-k}^{(i)}+c_{34}f_{j-k}^{(i)}+\frac{(c_{36}+c_{45})}{2}e_{j-k}^{(i)}\right)\Bigg]\hat{C}_k^{(i)}$$
$$+(\lambda_m-1)\left[(e_{34}-e_{16})e_{j-k}^{(i)}-(e_{36}+e_{14})h_{j-k}^{(i)}\right](k+1)\hat{D}_{k+1}^{(i)}+\Bigg[\lambda_m(\lambda_m-1)$$
$$\times\left(e_{16}f_{j-k}^{(i)}+e_{34}g_{j-k}^{(i)}-\frac{(e_{36}+e_{14})}{2}e_{j-k}^{(i)}\right)+\lambda_m\left(e_{16}g_{j-k}^{(i)}+e_{34}f_{j-k}^{(i)}+\frac{(e_{36}+e_{14})}{2}e_{j-k}^{(i)}\right)\Bigg]\hat{D}_k^{(i)}\Bigg]\Bigg\},\quad(3.7b)$$

$$\hat{C}_{j+2}^{(i)}+\left(c_{15}n_0^{(i)}+c_{35}m_0^{(i)}+\frac{(c_{13}+c_{55})}{2}l_0^{(i)}\right)\hat{A}_{j+2}^{(i)}+\left(c_{56}n_0^{(i)}+c_{34}m_0^{(i)}+\frac{(c_{36}+c_{45})}{2}l_0^{(i)}\right)\hat{B}_{j+2}^{(i)}$$
$$+\left(e_{15}n_0^{(i)}+e_{33}m_0^{(i)}+\frac{(e_{13}+e_{35})}{2}l_0^{(i)}\right)\hat{D}_{j+2}^{(i)}=\frac{-1}{(j+2)(j+1)}\Bigg\{\sum_{k=0}^{j-1}\Bigg[\left(c_{15}n_{j-k}^{(i)}+c_{35}m_{j-k}^{(i)}+\frac{(c_{13}+c_{55})}{2}l_{j-k}^{(i)}\right)$$
$$\times(k+2)(k+1)\hat{A}_{k+2}^{(i)}+\left(c_{56}n_{j-k}^{(i)}+2+c_{34}m_{j-k}^{(i)}+\frac{(c_{36}+c_{45})}{2}l_{j-k}^{(i)}\right)(k+2)(k+1)\hat{B}_{k+2}^{(i)}$$
$$+\left(e_{15}n_{j-k}^{(i)}+e_{33}m_{j-k}^{(i)}+\frac{(e_{13}+e_{35})}{2}l_{j-k}^{(i)}\right)(k+2)(k+1)\hat{D}_{k+2}^{(i)}+\sum_{k=0}^{j}\Bigg[(\lambda_m-1)\left[(c_{33}-c_{55})l_{j-k}^{(i)}-2c_{35}o_{j-k}^{(i)}\right]$$
$$\times(k+1)\hat{C}_{k+1}^{(i)}+\Bigg[\lambda_m\left((\lambda_m-1)c_{33}+c_{55}\right)n_{j-k}^{(i)}+\lambda_m\left((\lambda_m-1)c_{55}+c_{33}\right)m_{j-k}^{(i)}+\lambda_m(2-\lambda)c_{35}l_{j-k}^{(i)}\Bigg]\hat{C}_k^{(i)}$$
$$+(\lambda_m-1)\left[(c_{35}-c_{15})l_{j-k}^{(i)}-(c_{13}+c_{55})o_{j-k}^{(i)}\right](k+1)\hat{A}_{k+1}^{(i)}+\Bigg[\lambda_m(\lambda_m-1)$$
$$\times\left(c_{15}m_{j-k}^{(i)}+c_{35}n_{j-k}^{(i)}-\frac{(c_{13}+c_{55})}{2}l_{j-k}^{(i)}\right)+\lambda_m\left(c_{15}n_{j-k}^{(i)}+c_{35}m_{j-k}^{(i)}+\frac{(c_{13}+c_{55})}{2}l_{j-k}^{(i)}\right)\Bigg]\hat{A}_k^{(i)}$$
$$+(\lambda_m-1)\left[(c_{34}-c_{56})l_{j-k}^{(i)}-(c_{36}+c_{45})o_{j-k}^{(i)}\right](k+1)\hat{B}_{k+1}^{(i)}+\Bigg[\lambda_m(\lambda_m-1)$$
$$\times\left(c_{56}m_{j-k}^{(i)}+c_{34}n_{j-k}^{(i)}-\frac{(c_{36}+c_{45})}{2}l_{j-k}^{(i)}\right)+\lambda_m\left(c_{56}n_{j-k}^{(i)}+c_{34}m_{j-k}^{(i)}+\frac{(c_{36}+c_{45})}{2}l_{j-k}^{(i)}\right)\Bigg]\hat{B}_k^{(i)}$$
$$+(\lambda_m-1)\left[(e_{33}-e_{15})l_{j-k}^{(i)}-(e_{13}+e_{35})o_{j-k}^{(i)}\right](k+1)\hat{D}_{k+1}^{(i)}+\Bigg[\lambda_m(\lambda_m-1)$$
$$\times\left(e_{15}m_{j-k}^{(i)}+e_{33}n_{j-k}^{(i)}-\frac{(e_{13}+e_{35})}{2}l_{j-k}^{(i)}\right)+\lambda_m\left(e_{15}n_{j-k}^{(i)}+e_{33}m_{j-k}^{(i)}+\frac{(e_{13}+e_{35})}{2}l_{j-k}^{(i)}\right)\Bigg]\hat{D}_k^{(i)}\Bigg]\Bigg\},\quad(3.7c)$$

$$\hat{D}_{j+2}^{(i)}-\left(e_{11}r_0^{(i)}+e_{35}q_0^{(i)}+\frac{(e_{15}+e_{31})}{2}p_0^{(i)}\right)\hat{A}_{j+2}^{(i)}-\left(e_{16}r_0^{(i)}+e_{34}q_0^{(i)}+\frac{(e_{14}+e_{36})}{2}p_0^{(i)}\right)\hat{B}_{j+2}^{(i)}$$

$$-\left(e_{15}r_0^{(i)}+e_{33}q_0^{(i)}+\frac{(e_{13}+e_{35})}{2}p_0^{(i)}\right)\hat{C}_{j+2}^{(i)}=\frac{-1}{(j+2)(j+1)}\left\{\sum_{k=0}^{j-1}\left[-\left(e_{11}r_{j-k}^{(i)}+e_{35}q_{j-k}^{(i)}+\frac{(e_{15}+e_{31})}{2}p_{j-k}^{(i)}\right)\right.\right.$$
$$\times(k+2)(k+1)\hat{A}_{k+2}^{(i)}-\left(e_{16}r_{j-k}^{(i)}+e_{34}q_{j-k}^{(i)}+\frac{(e_{14}+e_{36})}{2}p_{j-k}^{(i)}\right)(k+2)(k+1)\hat{B}_{k+2}^{(i)}-\left(e_{15}r_{j-k}^{(i)}+e_{33}q_{j-k}^{(i)}\right.$$
$$\left.+\frac{(e_{13}+e_{35})}{2}p_{j-k}^{(i)}\right)(k+2)(k+1)\hat{C}_{k+2}^{(i)}+\sum_{k=0}^{j}\left[(\lambda_m-1)\left[(\eta_{33}-\eta_{11})p_{j-k}^{(i)}-2\eta_{13}s_{j-k}^{(i)}\right]\right.$$
$$\times(k+1)\hat{D}_{k+1}^{(i)}+\left[\lambda_m((\lambda_m-1)\eta_{33}+\eta_{11})r_{j-k}^{(i)}+\lambda_m((\lambda_m-1)\eta_{11}+\eta_{33})q_{j-k}^{(i)}+\lambda_m(2-\lambda)\eta_{13}p_{j-k}^{(i)}\right]\hat{D}_k^{(i)}$$
$$-(\lambda_m-1)\left[(e_{35}-e_{11})p_{j-k}^{(i)}-(e_{15}+e_{31})s_{j-k}^{(i)}\right](k+1)\hat{A}_{k+1}^{(i)}-\left[\lambda_m(\lambda_m-1)\right.$$
$$\left.\times\left(e_{11}q_{j-k}^{(i)}+e_{35}r_{j-k}^{(i)}-\frac{(e_{15}+e_{31})}{2}p_{j-k}^{(i)}\right)+\lambda_m\left(e_{11}r_{j-k}^{(i)}+e_{35}q_{j-k}^{(i)}+\frac{(e_{15}+e_{31})}{2}p_{j-k}^{(i)}\right)\right]\hat{A}_k^{(i)}$$
$$-(\lambda_m-1)\left[(e_{34}-e_{16})p_{j-k}^{(i)}-(e_{14}+e_{36})s_{j-k}^{(i)}\right](k+1)\hat{B}_{k+1}^{(i)}-\left[\lambda_m(\lambda_m-1)\right.$$
$$\left.\times\left(e_{16}q_{j-k}^{(i)}+e_{34}r_{j-k}^{(i)}-\frac{(e_{14}+e_{36})}{2}p_{j-k}^{(i)}\right)+\lambda_m\left(e_{16}r_{j-k}^{(i)}+e_{34}q_{j-k}^{(i)}+\frac{(e_{14}+e_{36})}{2}p_{j-k}^{(i)}\right)\right]\hat{B}_k^{(i)}$$
$$-(\lambda_m-1)\left[(e_{33}-e_{15})p_{j-k}^{(i)}-(e_{13}+e_{35})s_{j-k}^{(i)}\right](k+1)\hat{C}_{k+1}^{(i)}-\left[\lambda_m(\lambda_m-1)\right.$$
$$\left.\left.\left.\times\left(e_{15}q_{j-k}^{(i)}+e_{33}r_{j-k}^{(i)}-\frac{(e_{13}+e_{35})}{2}p_{j-k}^{(i)}\right)+\lambda_m\left(e_{15}r_{j-k}^{(i)}+e_{33}q_{j-k}^{(i)}+\frac{(e_{13}+e_{35})}{2}p_{j-k}^{(i)}\right)\right]\hat{C}_k^{(i)}\right]\right\}. \quad (3.7d)$$

If $\hat{A}_0^{(i)}$, $\hat{A}_1^{(i)}$, $\hat{B}_0^{(i)}$, $\hat{B}_1^{(i)}$, $\hat{C}_0^{(i)}$, $\hat{C}_1^{(i)}$, $\hat{D}_0^{(i)}$ and $\hat{D}_1^{(i)}$ are known, then $\hat{A}_{j+2}^{(i)}$, $\hat{B}_{j+2}^{(i)}$, $\hat{C}_{j+2}^{(i)}$ and $\hat{D}_{j+2}^{(i)}$ can be determined using Eqs. (3.7). Hence, the solutions of Eqs. (3.4) in subdomain *i* can be simply represented as,

$$\hat{U}_{0i}^{(m)}(\theta,\varphi)=\hat{A}_0^{(i)}\hat{U}_{0i0}^{(m)}+\hat{A}_1^{(i)}\hat{U}_{0i1}^{(m)}+\hat{B}_0^{(i)}\hat{U}_{0i2}^{(m)}+\hat{B}_1^{(i)}\hat{U}_{0i3}^{(m)}+\hat{C}_0^{(i)}\hat{U}_{0i4}^{(m)}+\hat{C}_1^{(i)}\hat{U}_{0i5}^{(m)}+\hat{D}_0^{(i)}\hat{U}_{0i6}^{(m)}+\hat{D}_1^{(i)}\hat{U}_{0i7}^{(m)},$$

$$\hat{V}_{0i}^{(m)}(\theta,\varphi)=\hat{A}_0^{(i)}\hat{V}_{0i0}^{(m)}+\hat{A}_1^{(i)}\hat{V}_{0i1}^{(m)}+\hat{B}_0^{(i)}\hat{V}_{0i2}^{(m)}+\hat{B}_1^{(i)}\hat{V}_{0i3}^{(m)}+\hat{C}_0^{(i)}\hat{V}_{0i4}^{(m)}+\hat{C}_1^{(i)}\hat{V}_{0i5}^{(m)}+\hat{D}_0^{(i)}\hat{V}_{0i6}^{(m)}+\hat{D}_1^{(i)}\hat{V}_{0i7}^{(m)},$$

$$\hat{W}_{0i}^{(m)}(\theta,\varphi)=\hat{A}_0^{(i)}\hat{W}_{0i0}^{(m)}+\hat{A}_1^{(i)}\hat{W}_{0i1}^{(m)}+\hat{B}_0^{(i)}\hat{W}_{0i2}^{(m)}+\hat{B}_1^{(i)}\hat{W}_{0i3}^{(m)}+\hat{C}_0^{(i)}\hat{W}_{0i4}^{(m)}+\hat{C}_1^{(i)}\hat{W}_{0i5}^{(m)}+\hat{D}_1^{(i)}\hat{W}_{0i6}^{(m)}+\hat{D}_1^{(i)}\hat{W}_{0i7}^{(m)},$$

$$\hat{\Phi}_{0i}^{(m)}(\theta,\varphi)=\hat{A}_0^{(i)}\hat{\Phi}_{0i0}^{(m)}+\hat{A}_1^{(i)}\hat{\Phi}_{0i1}^{(m)}+\hat{B}_0^{(i)}\hat{\Phi}_{0i2}^{(m)}+\hat{B}_1^{(i)}\hat{\Phi}_{0i3}^{(m)}+\hat{C}_0^{(i)}\hat{\Phi}_{0i4}^{(m)}+\hat{C}_1^{(i)}\hat{\Phi}_{0i5}^{(m)}+\hat{D}_0^{(i)}\hat{\Phi}_{0i6}^{(m)}+\hat{D}_1^{(i)}\hat{\Phi}_{0i7}^{(m)}. \quad (3.8)$$

To obtain the solutions of Eqs. (3.4) for the whole domain of φ, the following continuity conditions at the interface $(\varphi=\varphi_i)$ between sub-domains *i* and *i*+1 have to be satisfied;

$$\sigma_{rr}^{(i)}(\rho,\theta,\varphi_i)\sin\varphi_i+\sigma_{rz}^{(i)}(\rho,\theta,\varphi_i)\cos\varphi_i=\sigma_{rr}^{(i+1)}(\rho,\theta,\varphi_i)\sin\varphi_i+\sigma_{rz}^{(i+1)}(\rho,\theta,\varphi_i)\cos\varphi_i, \quad (3.9a)$$

$$\sigma_{rz}^{(i)}(\rho,\theta,\varphi_i)\sin\varphi_i+\sigma_{zz}^{(i)}(\rho,\theta,\varphi_i)\cos\varphi_i=\sigma_{rz}^{(i+1)}(\rho,\theta,\varphi_i)\sin\varphi_i+\sigma_{zz}^{(i+1)}(\rho,\theta,\varphi_i)\cos\varphi_i, \quad (3.9b)$$

$$\sigma_{\theta r}^{(i)}(\rho,\theta,\varphi_i)\sin\varphi_i+\sigma_{\theta z}^{(i)}(\rho,\theta,\varphi_i)\cos\varphi_i=\sigma_{\theta r}^{(i+1)}(\rho,\theta,\varphi_i)\sin\varphi_i+\sigma_{\theta z}^{(i+1)}(\rho,\theta,\varphi_i)\cos\varphi_i, \quad (3.9c)$$

$$D_r^{(i)}(\rho,\theta,\varphi_i)\sin\varphi_i+D_z^{(i)}(\rho,\theta,\varphi_i)\cos\varphi_i=D_r^{(i+1)}(\rho,\theta,\varphi_i)\sin\varphi_i+D_z^{(i+1)}(\rho,\theta,\varphi_i)\cos\varphi_i, \quad (3.9d)$$

$$u_r^{(i)}(\rho,\theta,\varphi_i)=u_r^{(i+1)}(\rho,\theta,\varphi_i), \quad (3.9e)$$

$$u_\theta^{(i)}(\rho,\theta,\varphi_i)=u_\theta^{(i+1)}(\rho,\theta,\varphi_i), \quad (3.9f)$$

$$u_z^{(i)}(\rho,\theta,\varphi_i)=u_z^{(i+1)}(\rho,\theta,\varphi_i), \quad (3.9g)$$

$$\phi^{(i)}(\rho,\theta,\varphi_i)=\phi^{(i+1)}(\rho,\theta,\varphi_i). \quad (3.9h)$$

If the domain of φ under consideration is divided into *n* sub-domains (Fig. 3.3), the 8*n* coefficients in Eqs. (3.8) for *i*=1, 2,…, *n*, must be determined. The interface continuity conditions yield 8(*n*-1) equations (Eqs. (3.9) with *i*=1, 2,…, (*n*-1)). The homogenous boundary conditions at $\varphi=\varphi_0$ and $\varphi=\varphi_n$ yield another eight equations. In total, 8*n* homogeneous algebraic equations for these 8*n* coefficients can thus be constructed. A nontrivial solution yields an $8n\times 8n$ determinant of zero. The roots of the zero determinant (λ_m) can be complex numbers, and were obtained herein using the subroutine, "DZANLY", in IMSL (International Mathematical and Statistical Library). The subroutine is based on the numerical approach of Müller (1956).

Two types of mechanical boundary condition were considered herein - free and clamped. For free traction at $\varphi=\varphi_0$ or $\varphi=\varphi_n$,

$\sigma_{rr}\sin\varphi+\sigma_{rz}\cos\varphi=0,\ \sigma_{rz}\sin\varphi+\sigma_{zz}\cos\varphi=0,\ \sigma_{\theta r}\sin\varphi+\sigma_{\theta z}\cos\varphi=0$

while the clamped boundary conditions require $u_r=u_z=u_\theta=0$. Two types of electric boundary conditions can also be specified at $\varphi=\varphi_0$ or $\varphi=\varphi_n$. They are electrically open and closed boundary conditions. Electrically open and closed conditions are $D_r\sin\varphi+D_z\cos\varphi=0$ and $\phi=0$, respectively.

3.3. **Convergence and Comparison**

The convergence and comparison of the minimum Re[λ_m] (real part of λ_m) of bi-material bodies of revolution are summarized here to confirm the correctness of the proposed solutions. Two geometric shapes with a horizontal interface, called geometry I and geometry II, displayed in Fig. 3.4, are considered. Geometry I has $\varphi_0=90^\circ$ and $\varphi_n=270^\circ$ while geometry II has $\varphi_0=0^\circ$ and $\varphi_n=270^\circ$, as shown in Fig. 3.3. Table 2.1 gives the material constants, and the direction of polarization of the material is assumed to be along the axis of revolution ($\gamma=0^\circ$). Notably, material PZT-6B(Im.) in Table 2.1 is an imaginary material with the same elastic properties as PZT-6B, and is adopted here to obtain results that can be compared with those of Xu and Mutoh (2001). The boundary conditions at $\varphi=\varphi_0$ and $\varphi=\varphi_n$ are traction-free and electrically open.

Table 3.1 lists the minimum values of Re[λ_m] that were obtained by dividing the domain

of φ into various numbers of sub-domains of equal size, using different numbers of terms in the series solution for each sub-domain. Notably, the λ_m, which correspond to minimum of Re[λ_m], are all real in the cases considered in Table 3.1. The convergent solutions can be obtained by fixing the number of sub-domains and increasing the number of terms in series solutions or by fixing the number of terms in series solutions and increasing the number of sub-domains. The results published in Xu and Mutoh (2001) and Li *et al*. (2002), which were obtained based on the assumption of axisymmetric deformation, are also given in Table 3.1. The excellent agreement between the convergent results herein and the published data validates the proposed solutions.

3.4. **Numerical Results and Discussion**

The electroelastic singularity is governed by the real part of (λ_m-1), and the root of primary interest is the one with the smallest positive real part between zero and one. In this section, the values of minimum Re[λ_m] are shown for single material and bi-material bodies of revolution. The piezoelectric materials, PZT-4 and PZT-5H, and an elastic material, Al (aluminium), are considered. The material properties of PZT-4 and PZT-5H are given in Table 1, while the elastic constants for Al are E (Young's modulus) = 68.9 GPa and ν (Poisson's ratio) = 0.25. The results were obtained using eight equal sub-domains for φ and 15-term series solutions for each sub-domain. The boundary conditions under consideration are specified by four letters. The first pair of letters refers to the boundary conditions at $\varphi = \varphi_0$, while the second pair specifies the boundary conditions at $\varphi = \varphi_n$. The first letter in each pair concerns the mechanical boundary conditions, with C and F's denoting clamped and free boundary conditions, respectively, while the second letter concerns the electric boundary conditions with C and O's representing electrically closed and open boundary conditions, respectively. Accordingly, in the following, COFO boundary conditions mean that the mechanical boundary conditions are clamped and free at $\varphi = \varphi_0$ and $\varphi = \varphi_n$, respectively, and the electric boundary conditions are open at $\varphi = \varphi_0$ and $\varphi = \varphi_n$.

3.4.1 Bodies of revolution made of a single piezoelectric material

Consider a PZT-4 or PZT-5H body of revolution with a direction of polarization that may not be along the Z-axis (axis of revolution). The geometry of the body considered in this section is similar to geometry II in Fig. 3.4. Figures 3.5 plots the variations of minimum Re[λ_m] with θ for PZT-4 bodies with $\gamma = 0^\circ$, 45° and 90°, while Fig. 3.6 plots corresponding curves for PZT-5H bodies. Notably, the results at $\theta = 2\pi - \theta_0$ are identical to those at $\theta = \theta_0$ in all the cases that are considered in this work. Consequently, the range of θ considered is between 0° and 180°. The λ_m that corresponds to minimum Re[λ_m] are all real in the cases examined in Figs. 3.5 and 3.6.

As expected, minimum Re[λ_m] does not change with θ when the direction of polarization is along the Z-axis ($\gamma = 0^\circ$). When the direction of polarization is not along the Z-axis, minimum Re[λ_m] varies significantly with θ. For example, when $\gamma = 45^\circ$, the maximum relative difference may reach 7.8% for a PZT-4 body with COCO boundary conditions, while the maximum difference is about 5.2 % for a PZT-5H body. When γ changes from 0° to 45° or 90°, the minimum Re[λ_m] may increase or decrease,

depending on the values of θ and the boundary conditions. PZT-4 bodies exhibit more severe electroelastic singularities than PZT-5H bodies under clamped-clamped mechanical boundary conditions; the opposite is true under free-free mechanical boundary conditions.

Figures 3.7 and 3.8 display the variations in minimum Re[λ_m] at $\theta = 60^\circ$ with β for PZT-4 and PZT-5H bodies, respectively. Two values of γ, 0° and 45°, were considered. Generally, minimum Re[λ_m] declines as β increases, such that a larger β induces more severe electroelastic singularities at the sharp corner of a body of revolution. Electroelastic singularities under free-free boundary conditions are more severe than those obtained under clamped-clamped boundary conditions. When $\gamma = 0^\circ$, the electric boundary conditions do not significantly affect the singularities. However, when $\gamma = 45^\circ$, open-open electric boundary conditions results in a smaller minimum Re[λ_m] than closed-closed electric boundary conditions for clamped-clamped bodies of revolution, while the opposite trend is true for bodies of revolution with free-free mechanical boundary conditions. As γ changes from 0° to 45°, the λ_m, which corresponds to minimum Re[λ_m], may change from real to complex or from complex to real. For instance, under CCCC boundary conditions, λ_m are complex for $\gamma = 45^\circ$ when β is between 48° and 73° for PZT-4 bodies and between 52° and 70° for PZT-5H bodies, while they are all real for $\gamma = 0^\circ$. A comparison of Figs. 3.7 and 3.8 reveals that PZT-4 bodies have stronger singularities than PZT-5H bodies under clamped-clamped boundary conditions, but not at all values of β under free-free boundary conditions

3.4.2 Bi-material bodies of revolution made of piezoelectric and elastic materials

This section investigates bi-material bodies of revolution with a geometry that is similar to geometry II in Fig. 3.4, in which material 1 is an isotropic elastic material, Al, and material 2 is PZT-4 or PZT-5H. The arrangements considered in Figs. 3.9 to 3.12 are the same as those in Figs. 3.5 to 3.7, respectively, except that bi-material bodies of revolution are considered in Figs. 3.9 to 3.12. Notably, the continuity conditions on the interface between the piezoelectric material and the elastic material are given by Eqs. (3.9a) to (3.9c), (3.9e) to (3.9g) and $\phi^{(i+1)}(\rho, \theta, \varphi_i) = 0$. No electric boundary condition applies at $\varphi = \varphi_0$, and the second letter of the four letters that denote the boundary conditions is replaced by "-".

Figures 3.9 and 3.10 discover that when $\gamma \neq 0^\circ$, the minimum Re[λ_m] does significantly vary with θ. When $\gamma = 45^\circ$, the maximum relative difference may reach 25% for a PZT-4/Al body under C-CC boundary conditions, while the maximum difference is approximately 16 % for a PZT-5H/Al body. Unlike in Figs. 3.5 and 3.6, the minimum Re[λ_m] for the C-CC boundary conditions can be smaller than those for C-CO boundary conditions, depending on γ and θ. When $\gamma = 45^\circ$, the λ_m, which correspond to minimum Re[λ_m] under C-CC boundary conditions, are no longer all real; they are complex for $63^\circ \le \theta \le 110^\circ$ in Fig. 3.9(b) and $68^\circ \le \theta \le 101^\circ$ in Fig. 3.10(b). Figure 3.9(b) demonstrates that the minimum Re[λ_m] under C-CC boundary conditions are lower than those under free-free boundary conditions when $\theta \le 14^\circ$.

Figures 3.11 and 3.12 plot the variations of minimum Re[λ_m] at $\theta = 60^\circ$ with β for PZT-4/Al and PZT-5H/Al bodies, respectively. The relatively abrupt changes in the curves (i.e., at $\beta \approx 159^\circ$ under F-FC boundary conditions and $\beta \approx 99^\circ$ under C-CO boundary

conditions in Fig. 3.11(a)) are caused by the roots's changing from real to complex numbers or from complex to real numbers. Generally, the strength of the electroelastic singularity increases with β. Free-free boundary conditions produce singularities that are more severe than clamped-clamped boundary conditions do, except for $\beta \geq 160^\circ$. Interestingly, the minimum Re[λ_m] for the bodies with $\gamma = 0^\circ$ are more considerably affected by electric boundary conditions than those for the bodies with $\gamma = 45^\circ$. Changing γ from 0° to 45° can alter the minimum Re[λ_m] with the maximum relative difference of 9.6% occurring at $\beta = 99^\circ$ under C-CO boundary conditions in Fig. 3.11. Unlike the minimum Re[λ_m] $\geq$ 0.5 for bodies of revolution made of two isotropic elastic materials under free-free boundary conditions given in Huang and Leissa [26], the minimum Re[λ_m] can be smaller than 0.5 for β larger than around 150° under F-FO boundary conditions.

3.4.3 Bi-material bodies of revolution made of piezoelectric materials

The results for bi-material bodies of revolution consisting of PZT-4 and PZT-5H with a horizontal interface are given in Figs. 3.13 and 3.14. Figure 3.13 concerns bodies of revolution with geometry I and geometry II displayed in Fig. 3.4, where materials 1 and 2 are PZT-5H and PZT-4, respectively. Figure 3.14 considers bodies of revolution with geometry II and having various β.

As expected, Fig. 3.13 demonstrates that bodies of revolution with geometry II ($\alpha = 270^\circ$) have more severe singularities at the interface corner than do bodies of revolution with geometry I ($\alpha = 180^\circ$). When $\gamma = 0^\circ$, the roots corresponding to minimum Re[λ_m] are all real. As γ changes from 0° to 45° or 90°, the roots may change from real to complex, depending on θ and the boundary conditions. For instance, for $\gamma = 45^\circ$ and under COCO boundary conditions, when $\theta < 51^\circ$ and $\theta < 36^\circ$ for geometries I and II, respectively, the roots corresponding to minimum Re[λ_m] are complex. The variations of minimum Re[λ_m] with θ in Fig. 3.13(b) indicate that the maximum difference can reach 11% for geometry I under FOFO boundary conditions, and 7.2% for geometry II under FOFO boundary conditions. When $\gamma = 90^\circ$, the maximum difference between values of minimum Re[λ_m] for various θ reaches 4.5% for geometry I under COCO boundary conditions, and 4.3% for geometry II under FOFO boundary conditions.

Figure 3.14 plots the variations of minimum Re[λ_m] at $\theta = 60^\circ$ with β for bodies of revolution with geometry II. Two values of γ, 0° and 45°, were considered. Again, the relatively abrupt changes in the curves are caused by a change in the roots from real to complex or from complex to real. Generally, free-free boundary conditions give more severe singularities at the interface corner than do clamped-clamped boundary conditions. Changing γ from 0° to 45° changes the minimum Re[λ_m] by up to 5.0%, as for the body of revolution with $\beta = 105^\circ$ under COCO boundary conditions.

IV **Concluding Remarks**

This study found asymptotic solutions to piezoelectric wedges and bodies of revolution to investigate geometrically-induced electroelastic singularities in these bodies based on three-dimensional piezoelaticity theory in a cylindrical coordinate system. The piezoelectric material is first assumed to be anisotropic and its direction of polarization to be arbitrary. The solutions were obtained using an eigenfunction expansion approach in conjunction with a power series technique to solve the equilibrium and Maxwell's equations, which are four coupled partial differential equations in terms of the displacement components and electric potential. The present solutions are easily reduced to the solution for anisotropic elastic wedges by eliminating the piezoelastic and dielectric constants. The proposed solutions are verified by performing convergence studies and comparing the results with the published results.

The proposed solution were employed to examine electroelastic singularities in wedges and bodies of revolution that comprise a single piezoelectric material, bounded piezo/isotropic elastic materials, or piezo/piezo materials. The minimum Re[λ_m], which is directly related to the order of the singularity, is displayed for different corner angles, combinations of boundary conditions, and directions of polarization. As expected, the strength of the singularity generally increases with the increase of corner angle. The geometrically induced electroelastic singularity order can depend significantly on the polarized direction. Interestingly, the direction of polarization can be set to eliminate the singularities at the interface of 180^o wedges made of PZT-5H/Si or PZT-5H/PZT-4 with free-free mechanical boundary conditions. This phenomenon is particularly important because such wedges are frequently encountered in many smart structures.

Appendix I

$$[c]=[\mathbf{T}]_{\sigma}[\mathbf{K}][\hat{c}][\mathbf{K}]^{\mathrm{T}}[\mathbf{T}]_{\varepsilon}^{-1},\quad [e]=[\mathbf{T}]_{\mathrm{D}}[\mathbf{L}][\hat{e}][\mathbf{K}]^{\mathrm{T}}[\mathbf{T}]_{\varepsilon}^{-1},[\eta]=[\mathbf{T}]_{\mathrm{D}}[\mathbf{L}][\hat{\eta}][\mathbf{L}]^{\mathrm{T}}[\mathbf{T}]_{\mathrm{E}}^{-1}$$

where

$$[\mathbf{T}]_{\sigma}=\begin{bmatrix}\cos^2\theta & \sin^2\theta & 0 & 0 & 0 & 2\cos\theta\sin\theta\\ \sin^2\theta & \cos^2\theta & 0 & 0 & 0 & -2\cos\theta\sin\theta\\ 0 & 0 & 1 & 0 & 0 & 0\\ 0 & 0 & 0 & \cos\theta & -\sin\theta & 0\\ 0 & 0 & 0 & \sin\theta & \cos\theta & 0\\ -\cos\theta\sin\theta & \cos\theta\sin\theta & 0 & 0 & 0 & \cos^2\theta-\sin^2\theta\end{bmatrix},$$

$$[\mathbf{T}]_{\varepsilon}=\begin{bmatrix}\cos^2\theta & \sin^2\theta & 0 & 0 & 0 & \cos\theta\sin\theta\\ \sin^2\theta & \cos^2\theta & 0 & 0 & 0 & -\cos\theta\sin\theta\\ 0 & 0 & 1 & 0 & 0 & 0\\ 0 & 0 & 0 & \cos\theta & -\sin\theta & 0\\ 0 & 0 & 0 & \sin\theta & \cos\theta & 0\\ -2\cos\theta\sin\theta & 2\cos\theta\sin\theta & 0 & 0 & 0 & \cos^2\theta-\sin^2\theta\end{bmatrix},$$

$$[\mathbf{T}]_{E}=[\mathbf{T}]_{D}=\begin{bmatrix}\cos\theta & \sin\theta & 0\\ -\sin\theta & \cos\theta & 0\\ 0 & 0 & 1\end{bmatrix},$$

$$[\mathbf{L}]=\begin{bmatrix}\cos(x,\hat{x}) & \cos(x,\hat{y}) & \cos(x,\hat{z})\\ \cos(y,\hat{x}) & \cos(y,\hat{y}) & \cos(y,\hat{z})\\ \cos(z,\hat{x}) & \cos(z,\hat{y}) & \cos(z,\hat{z})\end{bmatrix}=\begin{bmatrix}l_{11} & l_{12} & l_{13}\\ l_{21} & l_{22} & l_{23}\\ l_{31} & l_{32} & l_{33}\end{bmatrix},$$

$$[\mathbf{K}]=\begin{bmatrix}\mathbf{K}_1 & \mathbf{2K}_2\\ \mathbf{K}_3 & \mathbf{K}_4\end{bmatrix},$$

$$\mathbf{K}_1=\begin{bmatrix}l_{11}^2 & l_{12}^2 & l_{13}^2\\ l_{21}^2 & l_{22}^2 & l_{23}^2\\ l_{31}^2 & l_{32}^2 & l_{33}^2\end{bmatrix},\ \mathbf{K}_2=\begin{bmatrix}l_{12}l_{13} & l_{13}l_{11} & l_{11}l_{12}\\ l_{22}l_{23} & l_{23}l_{21} & l_{21}l_{22}\\ l_{32}l_{33} & l_{33}l_{31} & l_{31}l_{32}\end{bmatrix},\ \mathbf{K}_3=\begin{bmatrix}l_{21}l_{31} & l_{22}l_{32} & l_{23}l_{33}\\ l_{31}l_{11} & l_{32}l_{12} & l_{33}l_{13}\\ l_{11}l_{21} & l_{12}l_{22} & l_{13}l_{23}\end{bmatrix},$$

$$\mathbf{K}_4=\begin{bmatrix}l_{22}l_{33}+l_{23}l_{32} & l_{23}l_{31}+l_{21}l_{33} & l_{21}l_{32}+l_{22}l_{31}\\ l_{32}l_{13}+l_{33}l_{12} & l_{33}l_{11}+l_{31}l_{13} & l_{31}l_{12}+l_{32}l_{11}\\ l_{12}l_{23}+l_{13}l_{22} & l_{13}l_{21}+l_{11}l_{23} & l_{11}l_{22}+l_{12}l_{21}\end{bmatrix}$$

Appendix II

$$\sigma_{rr} = c_{11}\frac{\partial u_r}{\partial r} + c_{12}\left(\frac{1}{r}\frac{\partial u_\theta}{\partial \theta} + \frac{u_r}{r}\right) + c_{13}\frac{\partial u_z}{\partial z} + c_{14}\left(\frac{\partial u_\theta}{\partial z} + \frac{1}{r}\frac{\partial u_z}{\partial \theta}\right) + c_{15}\left(\frac{\partial u_z}{\partial r} + \frac{\partial u_r}{\partial z}\right)$$
$$+ c_{16}\left(\frac{1}{r}\frac{\partial u_r}{\partial \theta} + \frac{\partial u_\theta}{\partial r} - \frac{u_\theta}{r}\right) + e_{11}\frac{\partial \phi}{\partial r} + e_{21}\frac{1}{r}\frac{\partial \phi}{\partial \theta} + e_{31}\frac{\partial \phi}{\partial z}$$

$$\sigma_{zz} = c_{13}\frac{\partial u_r}{\partial r} + c_{23}\left(\frac{1}{r}\frac{\partial u_\theta}{\partial \theta} + \frac{u_r}{r}\right) + c_{33}\frac{\partial u_z}{\partial z} + c_{34}\left(\frac{\partial u_\theta}{\partial z} + \frac{1}{r}\frac{\partial u_z}{\partial \theta}\right) + c_{35}\left(\frac{\partial u_z}{\partial r} + \frac{\partial u_r}{\partial z}\right)$$
$$+ c_{36}\left(\frac{1}{r}\frac{\partial u_r}{\partial \theta} + \frac{\partial u_\theta}{\partial r} - \frac{u_\theta}{r}\right) + e_{13}\frac{\partial \phi}{\partial r} + e_{23}\frac{1}{r}\frac{\partial \phi}{\partial \theta} + e_{33}\frac{\partial \phi}{\partial z}$$

$$\sigma_{z\theta} = c_{14}\frac{\partial u_r}{\partial r} + c_{24}\left(\frac{1}{r}\frac{\partial u_\theta}{\partial \theta} + \frac{u_r}{r}\right) + c_{34}\frac{\partial u_z}{\partial z} + c_{44}\left(\frac{\partial u_\theta}{\partial z} + \frac{1}{r}\frac{\partial u_z}{\partial \theta}\right) + c_{45}\left(\frac{\partial u_z}{\partial r} + \frac{\partial u_r}{\partial z}\right)$$
$$+ c_{46}\left(\frac{1}{r}\frac{\partial u_r}{\partial \theta} + \frac{\partial u_\theta}{\partial r} - \frac{u_\theta}{r}\right) + e_{14}\frac{\partial \phi}{\partial r} + e_{24}\frac{1}{r}\frac{\partial \phi}{\partial \theta} + e_{34}\frac{\partial \phi}{\partial z}$$

$$\sigma_{\theta\theta} = c_{12}\frac{\partial u_r}{\partial r} + c_{22}\left(\frac{1}{r}\frac{\partial u_\theta}{\partial \theta} + \frac{u_r}{r}\right) + c_{23}\frac{\partial u_z}{\partial z} + c_{24}\left(\frac{\partial u_\theta}{\partial z} + \frac{1}{r}\frac{\partial u_z}{\partial \theta}\right) + c_{25}\left(\frac{\partial u_z}{\partial r} + \frac{\partial u_r}{\partial z}\right)$$
$$+ c_{26}\left(\frac{1}{r}\frac{\partial u_r}{\partial \theta} + \frac{\partial u_\theta}{\partial r} - \frac{u_\theta}{r}\right) + e_{12}\frac{\partial \phi}{\partial r} + e_{22}\frac{1}{r}\frac{\partial \phi}{\partial \theta} + e_{32}\frac{\partial \phi}{\partial z}$$

$$\sigma_{zr} = c_{15}\frac{\partial u_r}{\partial r} + c_{25}\left(\frac{1}{r}\frac{\partial u_\theta}{\partial \theta} + \frac{u_r}{r}\right) + c_{35}\frac{\partial u_z}{\partial z} + c_{45}\left(\frac{\partial u_\theta}{\partial z} + \frac{1}{r}\frac{\partial u_z}{\partial \theta}\right) + c_{55}\left(\frac{\partial u_z}{\partial r} + \frac{\partial u_r}{\partial z}\right)$$
$$+ c_{56}\left(\frac{1}{r}\frac{\partial u_r}{\partial \theta} + \frac{\partial u_\theta}{\partial r} - \frac{u_\theta}{r}\right) + e_{15}\frac{\partial \phi}{\partial r} + e_{25}\frac{1}{r}\frac{\partial \phi}{\partial \theta} + e_{35}\frac{\partial \phi}{\partial z}$$

$$\sigma_{r\theta} = c_{16}\frac{\partial u_r}{\partial r} + c_{26}\left(\frac{1}{r}\frac{\partial u_\theta}{\partial \theta} + \frac{u_r}{r}\right) + c_{36}\frac{\partial u_z}{\partial z} + c_{46}\left(\frac{\partial u_\theta}{\partial z} + \frac{1}{r}\frac{\partial u_z}{\partial \theta}\right) + c_{56}\left(\frac{\partial u_z}{\partial r} + \frac{\partial u_r}{\partial z}\right)$$
$$+ c_{66}\left(\frac{1}{r}\frac{\partial u_r}{\partial \theta} + \frac{\partial u_\theta}{\partial r} - \frac{u_\theta}{r}\right) + e_{16}\frac{\partial \phi}{\partial r} + e_{26}\frac{1}{r}\frac{\partial \phi}{\partial \theta} + e_{36}\frac{\partial \phi}{\partial z}$$

$$D_r = e_{11}\frac{\partial u_r}{\partial r} + e_{12}\left(\frac{1}{r}\frac{\partial u_\theta}{\partial \theta} + \frac{u_r}{r}\right) + e_{13}\frac{\partial u_z}{\partial z} + e_{14}\left(\frac{\partial u_\theta}{\partial z} + \frac{1}{r}\frac{\partial u_z}{\partial \theta}\right) + e_{15}\left(\frac{\partial u_z}{\partial r} + \frac{\partial u_r}{\partial z}\right)$$
$$+ e_{16}\left(\frac{1}{r}\frac{\partial u_r}{\partial \theta} + \frac{\partial u_\theta}{\partial r} - \frac{u_\theta}{r}\right) - \eta_{11}\frac{\partial \phi}{\partial r} - \eta_{12}\frac{1}{r}\frac{\partial \phi}{\partial \theta} - \eta_{13}\frac{\partial \phi}{\partial z}$$

$$D_\theta = e_{21}\frac{\partial u_r}{\partial r} + e_{22}\left(\frac{1}{r}\frac{\partial u_\theta}{\partial \theta} + \frac{u_r}{r}\right) + e_{23}\frac{\partial u_z}{\partial z} + e_{24}\left(\frac{\partial u_\theta}{\partial z} + \frac{1}{r}\frac{\partial u_z}{\partial \theta}\right) + e_{25}\left(\frac{\partial u_z}{\partial r} + \frac{\partial u_r}{\partial z}\right)$$
$$+ e_{26}\left(\frac{1}{r}\frac{\partial u_r}{\partial \theta} + \frac{\partial u_\theta}{\partial r} - \frac{u_\theta}{r}\right) - \eta_{12}\frac{\partial \phi}{\partial r} - \eta_{22}\frac{1}{r}\frac{\partial \phi}{\partial \theta} - \eta_{23}\frac{\partial \phi}{\partial z}$$

$$D_z = e_{31}\frac{\partial u_r}{\partial r} + e_{32}\left(\frac{1}{r}\frac{\partial u_\theta}{\partial \theta} + \frac{u_r}{r}\right) + e_{33}\frac{\partial u_z}{\partial z} + e_{34}\left(\frac{\partial u_\theta}{\partial z} + \frac{1}{r}\frac{\partial u_z}{\partial \theta}\right) + e_{35}\left(\frac{\partial u_z}{\partial r} + \frac{\partial u_r}{\partial z}\right)$$
$$+ e_{36}\left(\frac{1}{r}\frac{\partial u_r}{\partial \theta} + \frac{\partial u_\theta}{\partial r} - \frac{u_\theta}{r}\right) - \eta_{13}\frac{\partial \phi}{\partial r} - \eta_{23}\frac{1}{r}\frac{\partial \phi}{\partial \theta} - \eta_{33}\frac{\partial \phi}{\partial z}$$

where the electric potential, ϕ, is related to the electric field by,

$E_r = \frac{\partial \phi}{\partial r}$, $E_\theta = \frac{1}{r}\frac{\partial \phi}{\partial \theta}$ and $E_z = \frac{\partial \phi}{\partial z}$.

Appendix III

$$p_1(\theta)=\frac{1}{c_{66}}\left(2\lambda_m c_{16}+\frac{\partial c_{66}}{\partial\theta}\right),\quad p_2(\theta)=\frac{1}{c_{66}}\left(\lambda_m^2 c_{11}+\lambda_m\frac{\partial c_{16}}{\partial\theta}-c_{22}+\frac{\partial c_{26}}{\partial\theta}\right),\quad p_3(\theta)=\frac{c_{26}}{c_{66}},$$

$$p_4(\theta)=\frac{1}{c_{66}}\left[(\lambda_m-1)c_{66}+\lambda_m c_{12}-c_{22}+\frac{\partial c_{26}}{\partial\theta}\right],\ p_5(\theta)=\frac{1}{c_{66}}(\lambda_m-1)\left(\lambda_m c_{16}-c_{26}+\frac{\partial c_{66}}{\partial\theta}\right),$$

$$p_6(\theta)=\frac{c_{46}}{c_{66}},$$

$$p_7(\theta)=\frac{1}{c_{66}}\left[\lambda_m(c_{14}+c_{56})-c_{24}+\frac{\partial c_{46}}{\partial\theta}\right],\quad p_8(\theta)=\frac{1}{c_{66}}\lambda_m\left(\lambda_m c_{15}-c_{25}+\frac{\partial c_{56}}{\partial\theta}\right),\quad p_9(\theta)=\frac{e_{26}}{c_{66}},$$

$$p_{10}(\theta)=\frac{1}{c_{66}}\left[\lambda_m(e_{16}+e_{21})-e_{22}+\frac{\partial e_{26}}{\partial\theta}\right],\quad p_{11}(\theta)=\frac{1}{c_{66}}\lambda_m\left(\lambda_m e_{11}-e_{12}+\frac{\partial e_{16}}{\partial\theta}\right)$$

$$q_1(\theta)=\frac{1}{c_{22}}\left(2\lambda_m c_{26}+\frac{\partial c_{22}}{\partial\theta}\right),\quad q_2(\theta)=\frac{1}{c_{22}}(\lambda_m-1)\left[(\lambda_m+1)c_{66}+\frac{\partial c_{26}}{\partial\theta}\right],\quad q_3(\theta)=\frac{c_{26}}{c_{22}},$$

$$q_4(\theta)=\frac{1}{c_{22}}\left[\lambda_m(c_{12}+c_{66})+c_{66}+c_{22}+\frac{\partial c_{26}}{\partial\theta}\right],$$

$$q_5(\theta)=\frac{1}{c_{22}}\left[(\lambda_m+1)(\lambda_m c_{16}+c_{26})+\lambda_m\frac{\partial c_{12}}{\partial\theta}+\frac{\partial c_{22}}{\partial\theta}\right],\quad q_6(\theta)=\frac{c_{24}}{c_{22}},$$

$$q_7(\theta)=\frac{1}{c_{22}}\left[\lambda_m(c_{25}+c_{46})+c_{46}+\frac{\partial c_{24}}{\partial\theta}\right],\quad q_8(\theta)=\lambda_m\left[(\lambda_m+1)c_{56}+\frac{\partial c_{25}}{\partial\theta}\right],$$

$$q_9(\theta)=\frac{e_{22}}{c_{22}},\quad q_{10}(\theta)=\frac{1}{c_{22}}\left[\lambda_m(e_{12}+e_{26})+e_{26}+\frac{\partial e_{22}}{\partial\theta}\right],\quad q_{11}(\theta)=\frac{1}{c_{22}}\lambda_m\left[(\lambda_m+1)e_{16}+\frac{\partial e_{12}}{\partial\theta}\right]$$

$$r_1(\theta)=\frac{1}{c_{44}}\left(2\lambda_m c_{45}+\frac{\partial c_{44}}{\partial\theta}\right),\quad r_2(\theta)=\frac{1}{c_{44}}\lambda_m\left(\lambda_m c_{55}+\frac{\partial c_{45}}{\partial\theta}\right),\quad r_3(\theta)=\frac{c_{46}}{c_{44}},$$

$$r_4(\theta)=\frac{1}{c_{44}}\left[\lambda_m(c_{14}+c_{56})+c_{24}+\frac{\partial c_{46}}{\partial\theta}\right],\quad r_5(\theta)=\frac{1}{c_{44}}\left[\lambda_m\left(\lambda_m c_{15}+c_{25}+\frac{\partial c_{14}}{\partial\theta}\right)+\frac{\partial c_{24}}{\partial\theta}\right],$$

$$r_6(\theta)=\frac{c_{24}}{c_{44}}$$

$$r_7(\theta)=\frac{1}{c_{44}}\left[\lambda_m(c_{25}+c_{46})-c_{46}+\frac{\partial c_{24}}{\partial\theta}\right],\quad r_8(\theta)=\frac{1}{c_{44}}(\lambda_m-1)\left(\lambda_m c_{56}+\frac{\partial c_{46}}{\partial\theta}\right),\quad r_9(\theta)=\frac{e_{24}}{c_{44}},$$

$$r_{10}(\theta)=\frac{1}{c_{44}}\left[\lambda_m(e_{14}+e_{25})+\frac{\partial e_{24}}{\partial\theta}\right],\quad r_{11}(\theta)=\frac{1}{c_{44}}\lambda_m\left(\lambda_m e_{15}+\frac{\partial e_{14}}{\partial\theta}\right)$$

$$s_1(\theta)=\frac{1}{\eta_{22}}\left(2\lambda_m\eta_{12}+\frac{\partial\eta_{22}}{\partial\theta}\right),\quad s_2(\theta)=\frac{1}{\eta_{22}}\lambda_m\left(\lambda_m\eta_{11}+\frac{\partial\eta_{12}}{\partial\theta}\right),\quad s_3(\theta)=-\frac{e_{26}}{\eta_{22}},$$

$$s_4(\theta)=-\frac{1}{\eta_{22}}\left[\lambda_m(e_{16}+e_{21})+e_{22}+\frac{\partial e_{26}}{\partial\theta}\right],\quad s_5(\theta)=-\frac{1}{\eta_{22}}\left[\lambda_m\left(\lambda_m e_{11}+e_{12}+\frac{\partial e_{21}}{\partial\theta}\right)+\frac{\partial e_{22}}{\partial\theta}\right],$$

$$s_6(\theta)=-\frac{e_{22}}{\eta_{22}},\quad s_7(\theta)=-\frac{1}{\eta_{22}}\left[\lambda_m(e_{12}+e_{26})-e_{26}+\frac{\partial e_{22}}{\partial\theta}\right],\quad s_8(\theta)=-\frac{1}{\eta_{22}}(\lambda_m-1)\left(\lambda_m e_{16}+\frac{\partial e_{26}}{\partial\theta}\right),$$

$$s_9(\theta) = -\frac{e_{24}}{\eta_{22}},\quad s_{10}(\theta) = -\frac{1}{\eta_{22}}\left[\lambda_m(e_{14}+e_{25}) + \frac{\partial e_{24}}{\partial \theta}\right],\quad s_{11}(\theta) = -\frac{1}{\eta_{22}}\lambda_m\left(\lambda_m e_{15} + \frac{\partial e_{25}}{\partial \theta}\right)$$

V. References

Bogy, D. B., Wang, K. C., 1971. Stress singularities at interface corners in bonded dissimilar isotropic elastic material. *International Journal of Solids and Structures* 7, 993-1005.

Burton, W. S., Sinclair, G. B., 1986. On the singularities in Reissner's theory for the bending of elastic plates. *Journal of Applied Mechanics, ASME* 53, 220-222.

Chaudhuri, R.A., Xie, M., 2000. A novel eigenfunction expansion solution for three-dimensional crack problems. *Composite Science and Technology* 60, 2565-2580.

Chen, T. H., Chue, C. H., Lee, H.T., 2004. Stress singularities near the apex of a cylindrically polarized piezoelectric wedge. *Archieve of Applied Mechanics* 74, 248-261.

Chue, C. H., Chen, C. D., 2002. Decoupled formulation of piezoelectric elasticity under generalized plane deformation and its application to wedge problems. *International Journal of Solids and Structures* 39, 3131-3158.

Chue, C. H., Chen, C. D., 2003. Antiplane stress singularities in a bonded bimaterial piezoelectric wedge. *Archieve of Applied Mechanics* 72, 673-685.

Dempsey, J. P., Sinclair, G. B., 1981. On the stress singular behavior at the vertex of a bi-material wedge. *Journal of Elasticity* 11, 317-327.

Ding, H. J., Chen, B., Liang, J., 1996. General solutions for coupled equations for piezoelectric media. *International Journal of Solids and Structure,* 33(16), 2283-2298.

England, A. H., 1971. On stress singularities in linear elasticity. International *Journal of Engineering Science* 9, 571-585.

Hartranft, R.J., Sih, G.C., 1969. The use of eigenfunction expansions in the general solution of the three-dimensional crack problems. J*ournal of Mathematics and Mechanics* 19, 123-138.

Hein, V. L., Erdogan, F., 1971. Stress singularities in a two-material wedge. *International Journal for Fracture Mechanics* 7, 317-330.

Huang, C. S., 2002a. Corner singularities in bi-material Mindlin plates. *Composite Structures* 56, 315-327.

Huang, C. S., 2002b. On the singularity induced by boundary conditions in a third-order thick plate theory. *Journal of Applied Mechanics, ASME* 69, 800-810.

Huang, C. S., 2003. Stress singularities in angular corners in first-order shear deformation plate theory. *International Journal of Mechanical Science* 45, 1-20.

Huang, C. S., Leissa, A.W., 2007. Three-dimensional sharp corner displacement functions for bodies of revolution. *Journal of Applied Mechanics, ASME* 74, 41-46.

Huang, C. S., Leissa, A. W., 2008. Stress singularities in bimaterial bodies of revolution. *Composite Structures* 82(4), 488-498.

Hwu, C., Ikeda, T., 2008. Eletromechanical fracture analysis for corners and cracks in piezoelectric materials, *International Journal of Solids and Structures* 45, 5744-5764.

Li, Y. L., Hu, S. Y., Munz, D., Yang, Y. Y., 1998. Asymptotic description of the stress field around the bond edge of a cylindrical joint. *Archieve of Applied Mechanics* 68(7), 552-565.

Li, Y. L., Hu, S. Y., Yang, Y. Y., 2000. Stresses around the bond edges of axisymmetric deformation joints. *Fracture Mechanics* 66(2), 153-170.

Li, Y., Sato, Y., Watanabe, K., 2002. Stress singularity analysis of axisymmetric piezoelectric bonded structure. *JSME International Journal Series A* 45(3), 363-370.

Love A. E. H. *A*, 1927. *Treatise on the Mathematical Theory of Elasticity*, 4th ed., The Macmillan Co, New York.

Müller, D.E., 1956. A method for solving algebraic equations using an automatic computer. *Mathematical Tables and Aids to Computation* 10, 208-215.

McGee, O.G., Kim, J.W., 2005. Sharp corner functions for Mindlin plates. Journal of Applied Mechanics, ASME 72(1), 1-9.

Saidi, A.R., Hejripour, F., Jomehzadeh, E., 2010. On the stress singularities and boundary layer in moderately thick functionally graded sectorial plates. *Applied Mathematical Modeling* 34(11), 3478-3492.

Shang, F., Kitamura, T., 2005. On stress singularity at the interface edge between piezoelectric thin film and elastic substrate, *Microsystem Technology* 11, 1115-1120.

Shang, F., Kitamura, T., Hirakata, H., Kanno, I., Kotera, H. M., Terada, K., 2005. Experimental and theoretical investigations of delamination at free edge of interface between piezoelectric thin films on a substrate, *International Journal of Solids and Structures* 42, 1729-1741.

Sosa, H. A., Pak, Y. E., 1990. Three-dimensional eigenfunction analysis of a crack in a piezoelectric material. *International Journal of Solids and Structures* 26, 1-15.

Sze, K. Y., Wang, H. T., Fan, H., 2001. A finite element approach for computing edge singularities in piezoelectric materials, *International Journal of Solids and Structures* 38, 9233-9252.

Timoshenko, S. P., Goodier, J. N., 1970. Axisymmetric stress and deformation in a solid of revolution. In: *Theory of elasticity*, 3rd ed. Kogakusha: McGraw-Hill, 428-429.

Ting. T. C. T., Jin, Y., Chou, S. C., 1985. Eigenfunctions at a singular point in transversely isotropic materials under axisymmetric deformations. *ASME Journal of Applied Mechanics* 52(3), 565-569.

Wang, Z., Zheng, B., 1995. The general solution of three dimensional problems in piezoelectric media, *International Journal of Solids and Structures* 32, 105-115.

Williams, W. L., 1952a. Stress singularities resulting from various boundary conditions in angular corners of plates in extension. *Journal of Applied Mechanics, ASME* 19, 526-528.

Williams, W. L., 1952b. Stress singularities resulting from various boundary conditions in

angular corners of plates under bending. *Proceedings of 1st U. S. National Congress of Applied Mechanics*, ASME, New York, 325-329.

Williams, M.L., Owens, R.H., 1954. Stress singularities in angular corners of plates having linear flexural rigidities for various boundary conditions. *Proceeding of 2nd U.S. National Congress of Applied Mechanics*, 407-411.

Xu, J. Q., Mutoh, Y., 2001. Singularity at the interface edge of bonded transversely isotropic piezoelectric dissimilar materials. *JSME International Journal Series A* 44(4), 556-566.

Xu, X. L., Rajapakse, R. K. N. D., 2000. On singularities in composite piezoelectric wedges and junctions. I*nternational Journal of Solids and Structures* 37, 3235-3275.

Ying, X., Katz, I. N., 1987. A uniform formulation for the calculation of stress singularities in the plane elasticity of a wedge composed of multiple isotropic materials. *Computers and Mathematics with Applications* 14, 437-458.

Zak, A.R., 1964. Stresses in the vicinity of boundary discontinuities in bodies of revolution. *Journal of Applied Mechanics*, ASME 31, 150-152.

Table 2.1 Material properties

Material	**Stiffness [GPa]**					**Piezoelectric const. [C/m^2]**			**Dielectric const. ×10^{-10}[F/m]**	
	$\hat{c}_{11}$	$\hat{c}_{12}$	$\hat{c}_{13}$	$\hat{c}_{33}$	$\hat{c}_{44}$	$\hat{e}_{15}$	$\hat{e}_{31}$	$\hat{e}_{33}$	$\hat{\eta}_{11}$	$\hat{\eta}_{33}$
CdSe	74.1	45.2	39.3	83.6	13.2	-0.138	-0.159	0.347	0.844	0.903
PZT-4	139.0	77.8	74.3	115.0	25.6	12.7	-5.2	15.1	64.6	56.2
PZT-5H	126.0	55.0	53.0	117.0	35.3	17.0	-6.5	23.3	151.0	130.0
$BaTiO_3$	275.0	179.0	152.0	165.0	54.3	21.3	-2.69	3.65	175.0	9.88
PZT-6B(Im.)	168.0	60.0	60.0	163.0	27.1	43.0	-14.0	36.0	200.0	247.0
PZT-6B	168.0	60.0	60.0	163.0	27.1	4.6	-0.9	7.1	36.0	34.0
Si	166.2	64.6	64.6	166.2	50.8	-	-	-	-	-

Table 2.2 Convergence of minimum Re[λ_m] for PZT-4 wedges

γ	Boundary conditions	Number of Sub-domains	Terms									Published results
			5	6	7	8	9	10	12	14	15	
360°	FOFO	3	0.4985	0.4978	0.4916	0.4417	0.4980	0.4998	0.4750	0.5000	0.4999	0.5000#
		4	0.4996	0.4963	0.4993	0.4999	0.4999	0.4984	0.4999	0.4999	0.4999	
		6	0.5000	0.4993	0.4999	0.4999	0.5000	0.5000	0.4999	0.5000	0.5000	
		8	0.4999	0.4999	0.4999	0.4999	0.4999	0.5000	0.5000	0.4999	0.5000	
360°	FOCC	3	0.1769	0.1969	0.2052	0.1602	0.1718	0.1965	0.1724	0.1954	0.1895	0.1869*
		4	0.1855	0.1895	0.1847	0.1877	0.1879	0.1857	0.1877	0.1865	0.1869	
		6	0.1869	0.1869	0.1869	0.1869	0.1869	0.1869	0.1869	0.1869	0.1869	
		8	0.1869	0.1869	0.1869	0.1869	0.1869	0.1869	0.1869	0.1869	0.1869	
180°		2	0.3710	0.3751	0.3749	0.3740	0.3736	0.3735	0.3741	0.3737	0.3738	0.3739*
		3	0.3741	0.3737	0.3738	0.3739	0.3739	0.3739	0.3739	0.3739	0.3737	
		4	0.3738	0.3739	0.3739	0.3739	0.3739	0.3739	0.3739	0.3739	0.3739	
		6	0.3739	0.3739	0.3739	0.3739	0.3739	0.3739	0.3739	0.3739	0.3739	

Note: * denotes results from Hwu and Ikeda (2008)

# denotes results from Sosa and Pak (1990)

Table 2.3 Comparisons between the present and the published λ_m for PZT-4 wedges

γ	Boundary conditions	Direction of polarization	Roots of λ_m	Published results	Present results
360°	FOCC	Y	λ_0	0.1869*	0.1869
			λ_1	0.3131*	0.3131
			λ_2	0.6869*	0.6869
357°	FOFO	Y	λ_0	0.5000#	0.5000
			λ_1	0.5094#	0.5094
			λ_2	0.5046#	0.5046
		Z	λ_0	0.5000#	0.5000
			λ_1	0.5085#	0.5085
			λ_2	0.5042#	0.5042
330°	FOFO	Y	λ_0	0.5021#	0.5021
			λ_1	0.5499#	0.5498
			λ_2	0.6109#	0.6109
		Z	λ_0	0.5015#	0.5014
			λ_1	0.5455#	0.5455
			λ_2	0.5982#	0.5981
180°	FOCC	Y	λ_0	0.3739*	0.3739
			λ_1	0.5000*	0.5000
			λ_2	0.6261*	0.6261

Note: * denotes the results of Hwu and Ikeda (2008)

#: denotes the results of Sze et al. (2001)

Table 3.1: Convergence of minimum Re[λ_m] for bodies of revolution

Geometry	Material 1/ Material 2	Number of Sub-domains	Number of Polynomial terms							Published results
			5	6	7	9	11	13	15	
I	CdSe/ PZT-5H	2	0.9363	0.9348	0.9357	0.9377	0.9387	0.9383	0.9380	0.9381*
		4	0.9379	0.9381	0.9382	0.9381	0.9381	0.9381	0.9381	
		6	0.9381	0.9381	0.9381	0.9381	0.9381	0.9381	0.9381	
		8	0.9381	0.9381	0.9381	0.9381	0.9381	0.9381	0.9381	
	CdSe/ PZT-6B	2	0.9268	0.9242	0.9308	0.9302	0.9280	0.9272	0.9278	0.9281*
		4	0.9286	0.9289	0.9279	0.9281	0.9281	0.9281	0.9281	
		6	0.9281	0.9281	0.9281	0.9281	0.9281	0.9281	0.9281	
		8	0.9281	0.9281	0.9281	0.9281	0.9281	0.9281	0.9281	
	CdSe/ $BaTiO_3$	2	0.8949	0.9588	0.9429	0.9172	0.9394	0.9256	0.9284	0.9429*
		4	0.9436	0.9430	0.9430	0.9430	0.9429	0.9429	0.9429	
		6	0.9429	0.9428	0.9428	0.9429	0.9429	0.9429	0.9429	
		8	0.9429	0.9428	0.9429	0.9429	0.9429	0.9429	0.9429	
	PZT-6B/ PZT-6B(Im.)	2	0.98792	0.98475	0.98641	0.98793	0.98713	0.98828	0.98792	0.98724^{+}
		4	0.98742	0.98732	0.98731	0.98720	0.98613	0.98725	0.98724	
		6	0.98802	0.98764	0.98764	0.98733	0.98724	0.98724	0.98724	
		8	0.98730	0.98724	0.98723	0.98724	0.98724	0.98724	0.98724	
II	PZT-6B/ PZT-6B(Im.)	3	0.54766	0.53669	0.52792	0.52053	0.52716	0.52670	0.53197	0.52819^{+}
		6	0.52694	0.52758	0.52801	0.52836	0.52819	0.52818	0.52820	
		9	0.52803	0.52809	0.52823	0.52820	0.52820	0.52820	0.52820	

Note: * denotes the results of Sato and Watanabe (2002)

+: denotes the results of Xu and Mutoh (2001)

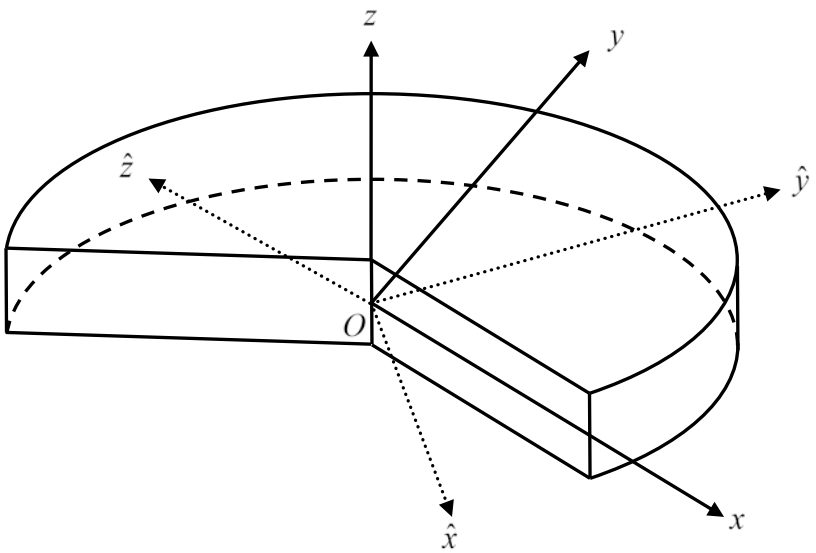

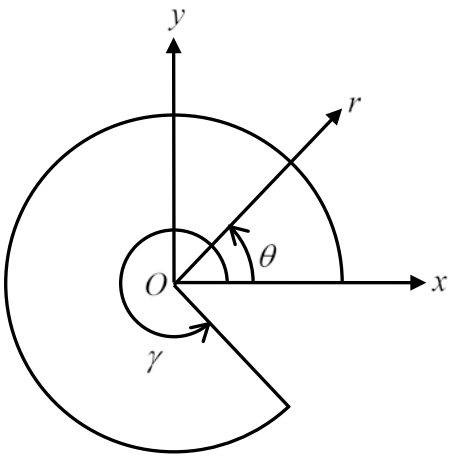

Fig. 2.1 Coordinate systems for a wedge

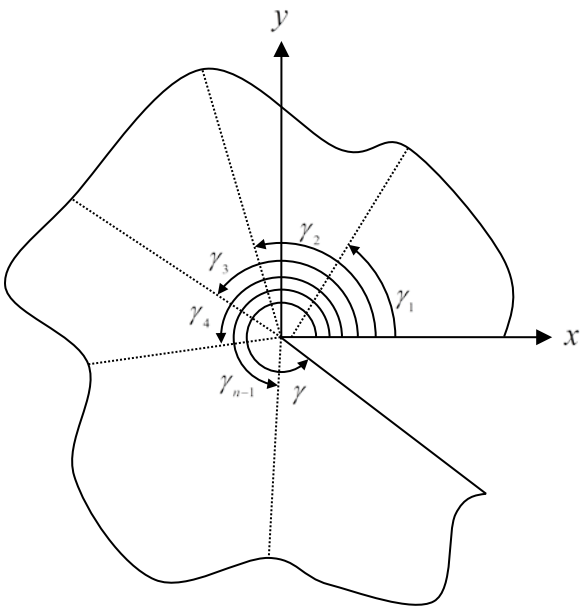

Fig. 2.2 Sub-domains for $\theta \in [0, \gamma]$

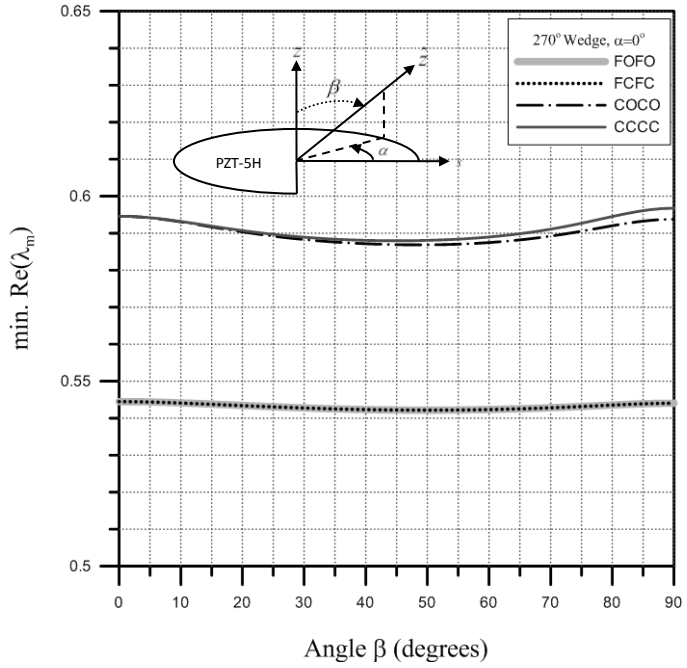

(a)

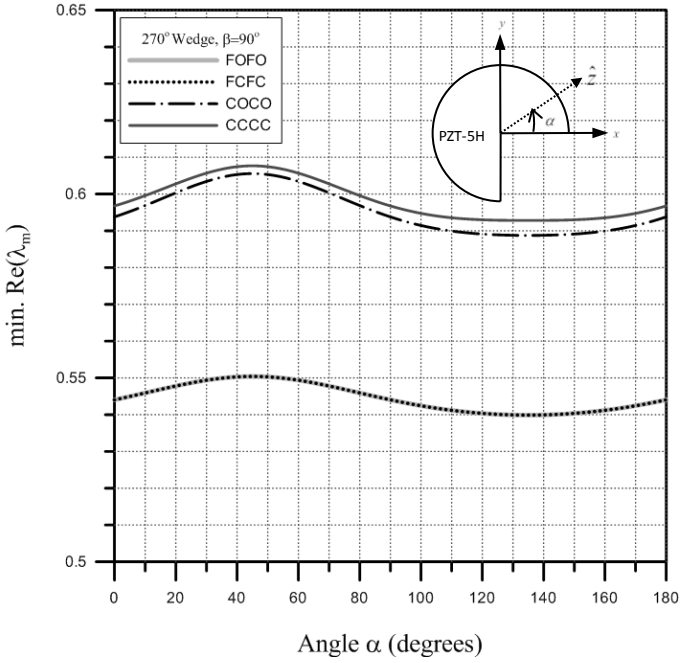

(b)

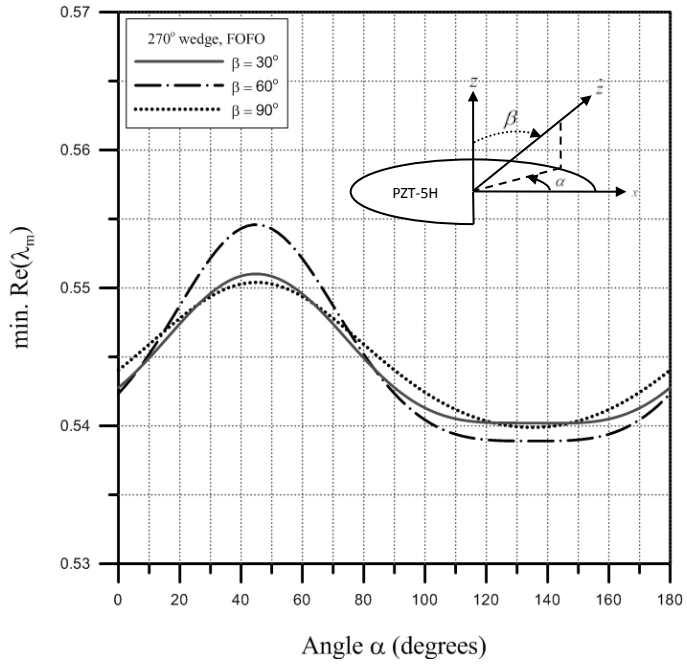

(c)

Fig. 2.3 Variation of minimum Re[λ_m] with direction of polarization for a 270^o PZT-5H wedge (a) $\alpha = 0^o$ (on *x*-*z* plane), (b) $\beta = 90^o$ (on *x*-*y* plane), (c) $\beta = 30^o,\ 60^o$ and 90^o

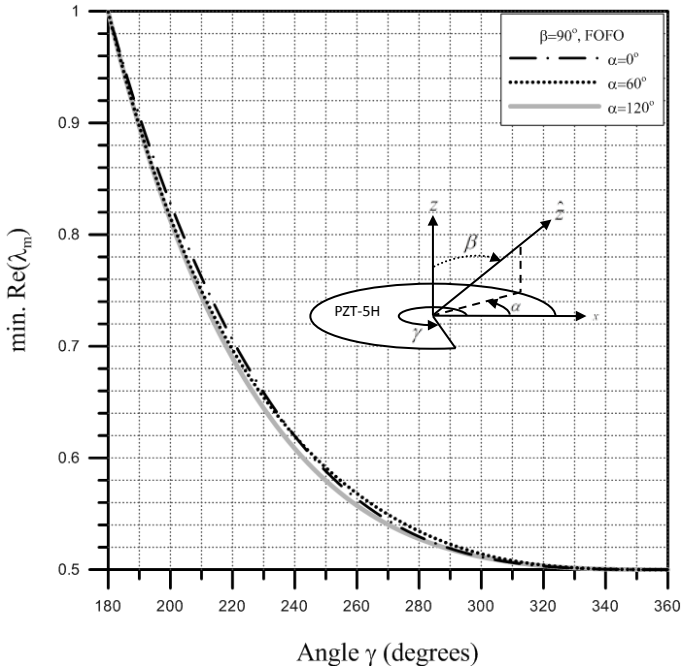

(a)

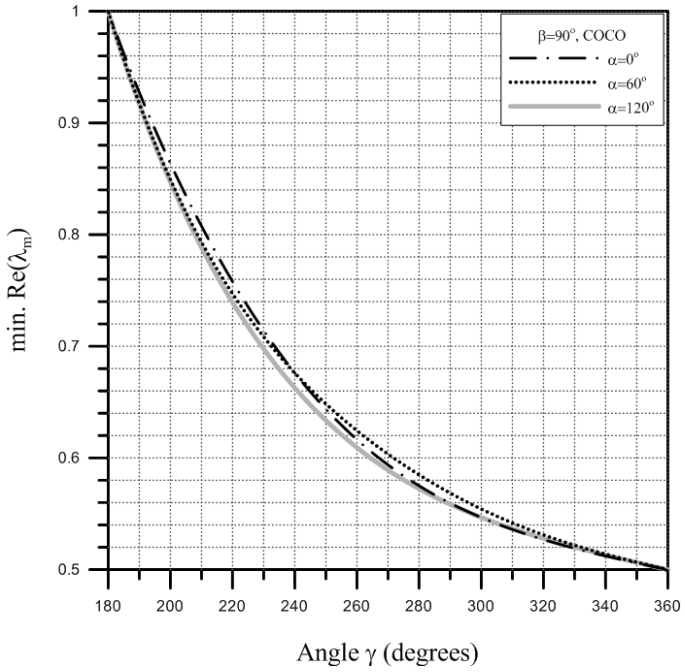

(b)

Fig. 2.4 Variation of minimum Re[λ_m] with wedge angle for PZT-5H wedges
(a) FOFO boundary conditions,
(b) COCO boundary conditions

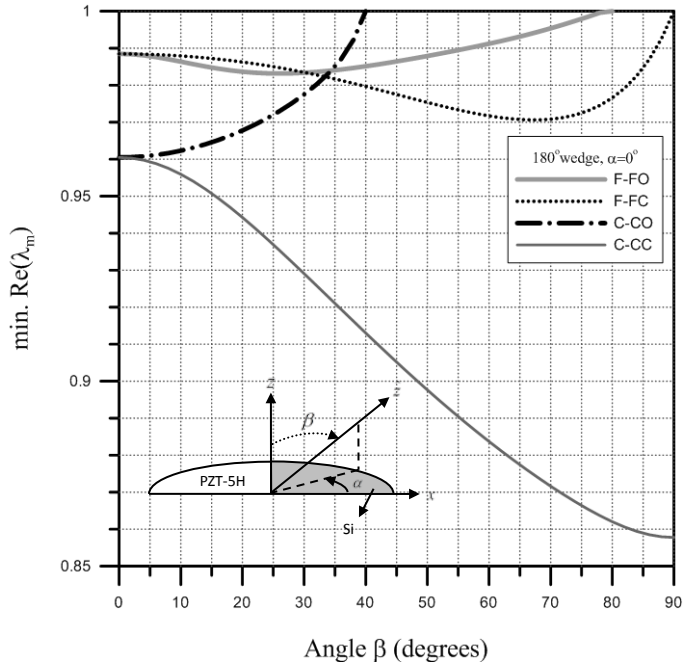

(a)

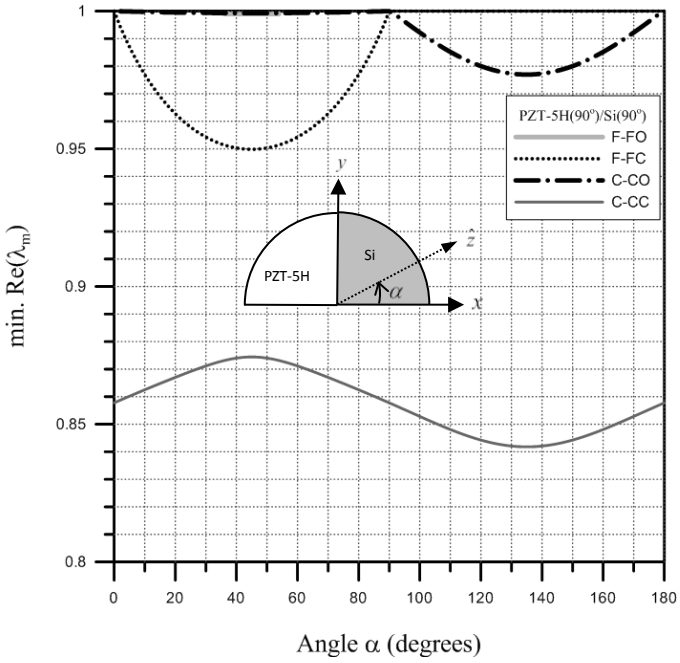

(b)

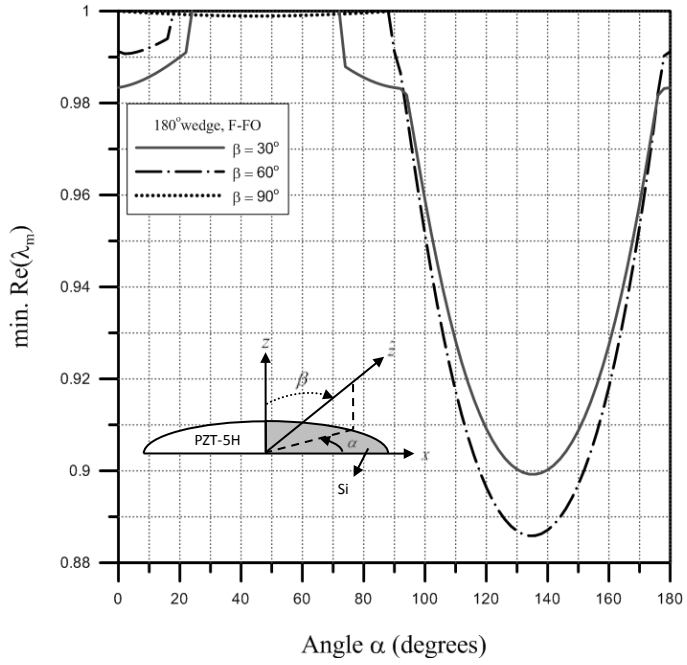

(c)

Fig. 2.5 Variation of minimum Re[λ_m] with direction of polarization for a 180^o PZT-5H/ Si bi-material wedge

(a) $\alpha = 0^o$ (on *x*-*z* plane), (b) $\beta = 90^o$ (on *x*-*y* plane), (c) $\beta = 30^o,\ 60^o$ and 90^o

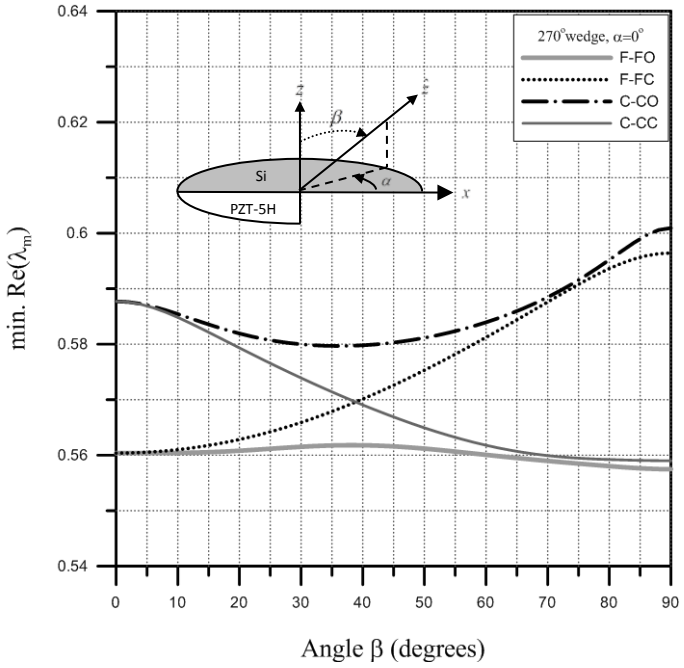

(a)

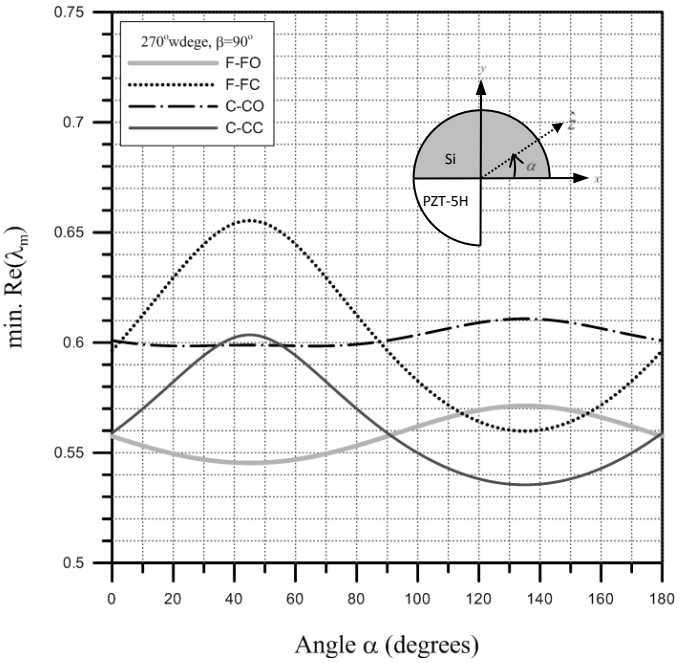

(b)

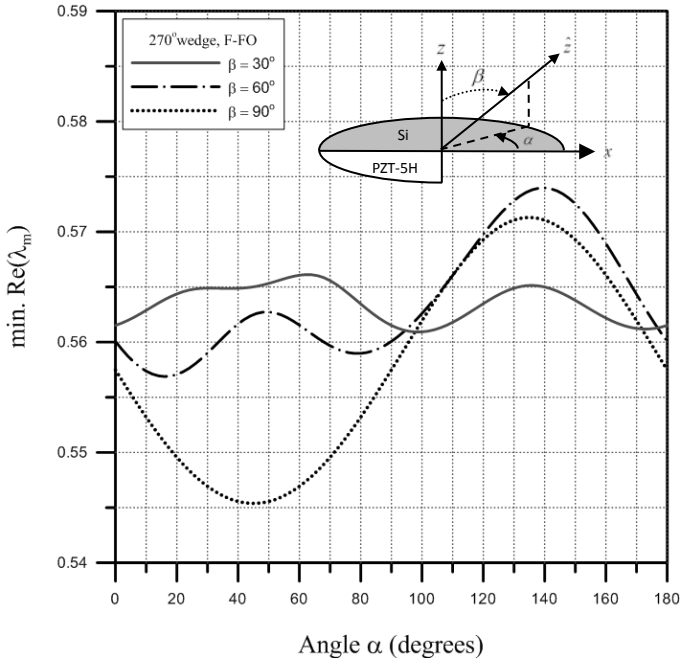

(c)

Fig. 2.6 Variation of minimum Re[λ_m] with direction of polarization for a 270^o PZT-5H/ Si bi-material wedge (a) $\alpha = 0^o$ (on *x*-*z* plane), (b) $\beta = 90^o$ (on *x*-*y* plane), (c) $\beta = 30^o,\ 60^o$ and 90^o

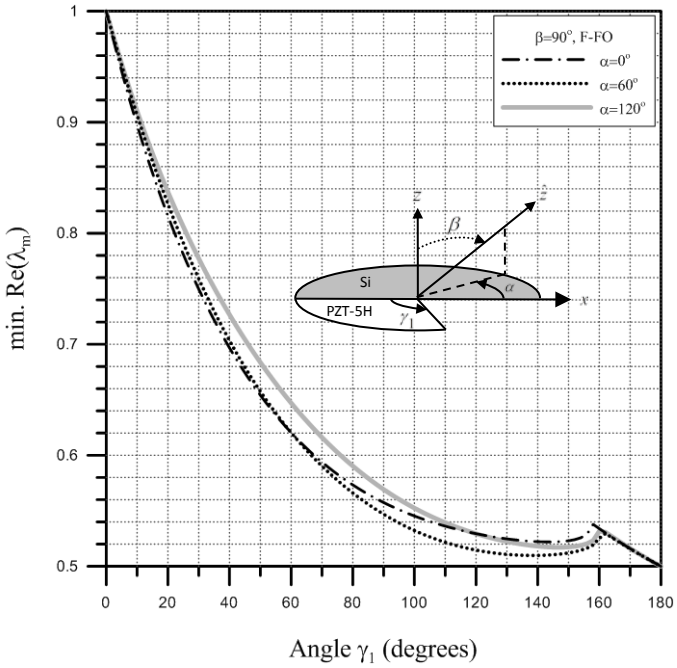

(a)

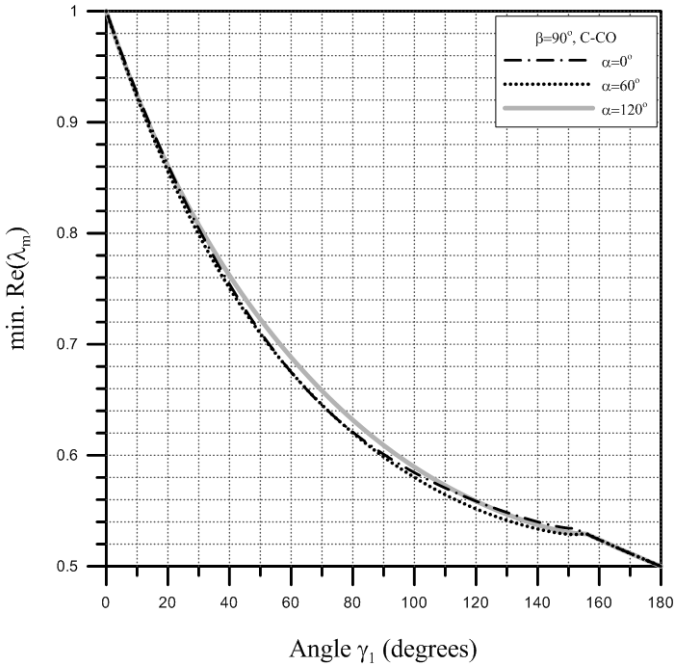

(b)

Fig. 2.7 Variation of minimum Re[λ_m] with wedge angle for PZT-5H/Si wedges
(a) F-FO boundary conditions,
(b) C-CO boundary conditions

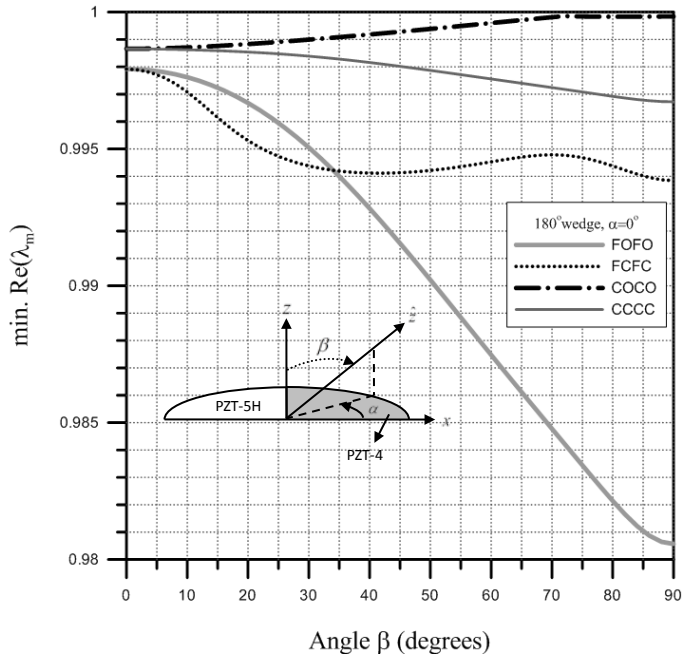

(a)

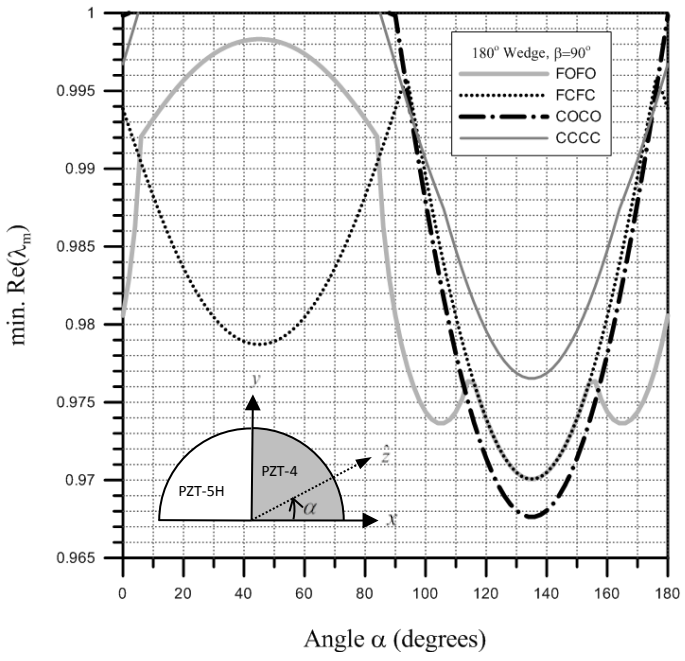

(b)

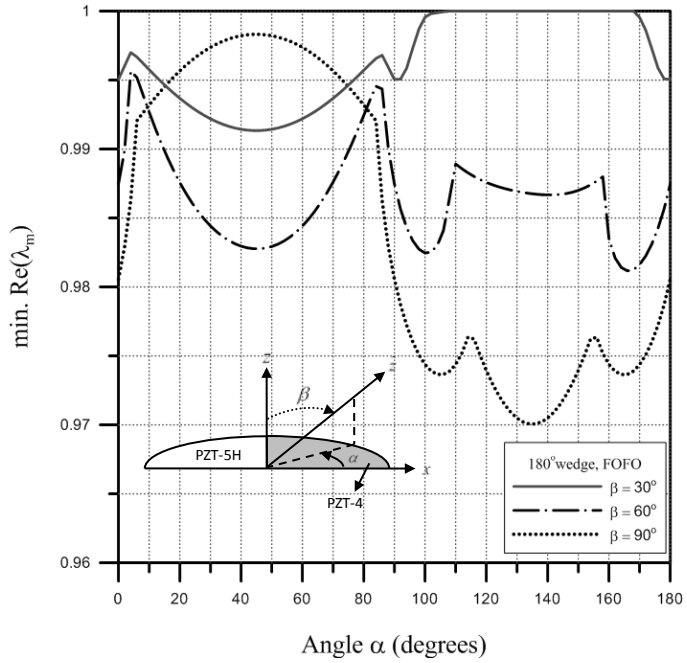

(c)

Fig. 2.8 Variation of minimum Re[λ_m] with direction of polarization for a 180^o PZT-5H/ PZT-4 bi-material wedge

(a) $\alpha = 0^o$ (on *x*-*z* plane), (b) $\beta = 90^o$ (on *x*-*y* plane), (c) $\beta = 30^o$, 60^o and 90^o

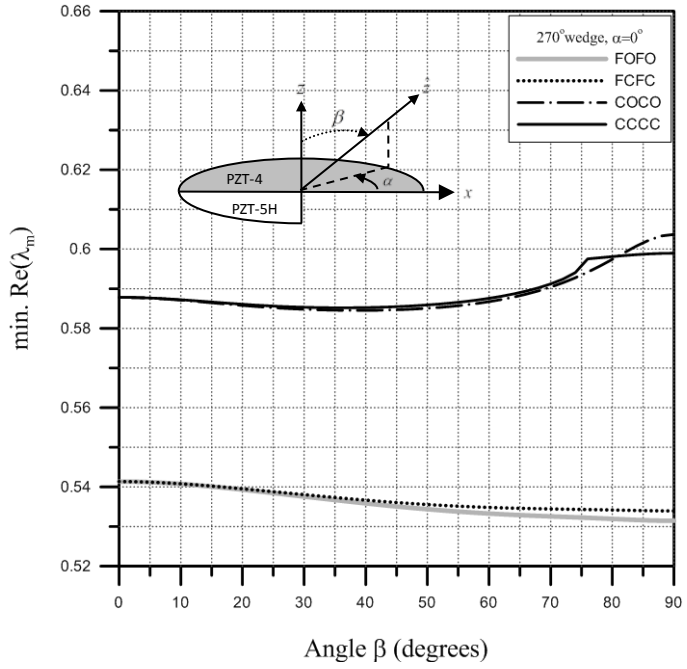

(a)

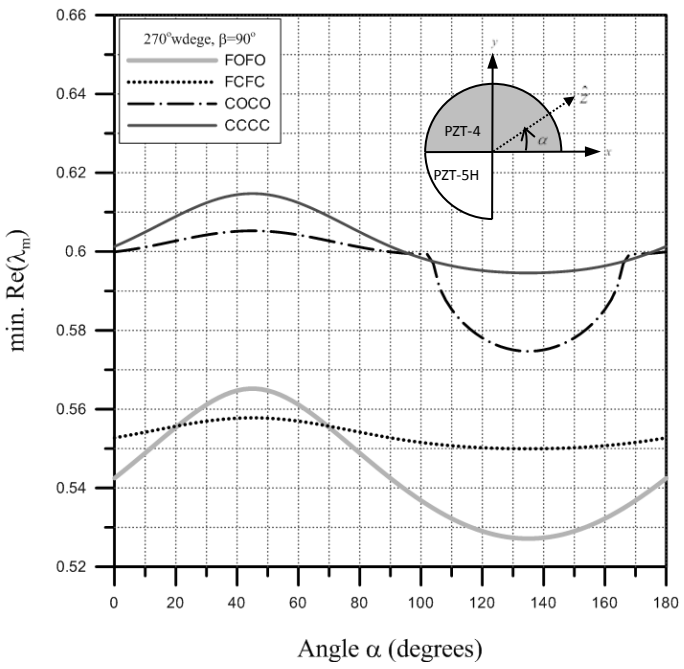

(b)

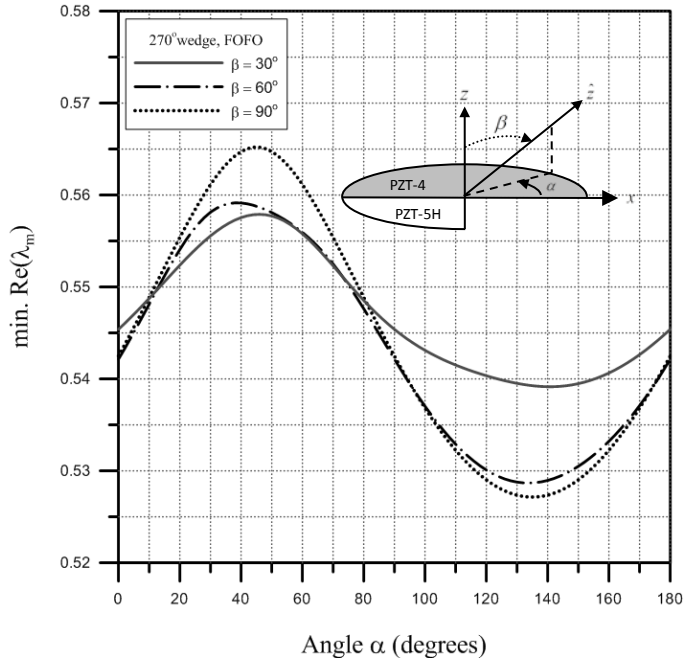

(c)

Fig. 2.9 Variation of minimum Re[λ_m] with direction of polarization for a 270^o PZT-5H/ PZT-4 bi-material wedge

(a) $\alpha = 0^o$ (on *x*-*z* plane), (b) $\beta = 90^o$ (on *x*-*y* plane), (c) $\beta = 30^o,\ 60^o$ and 90^o

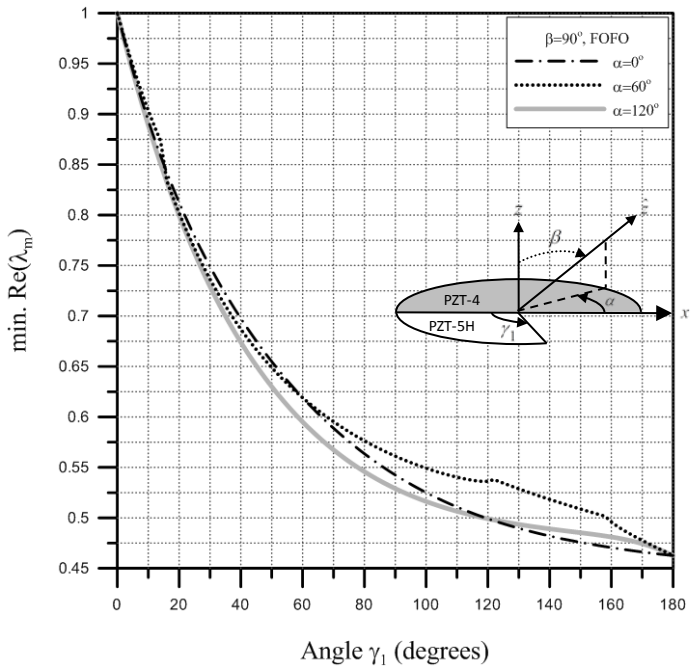

(a)

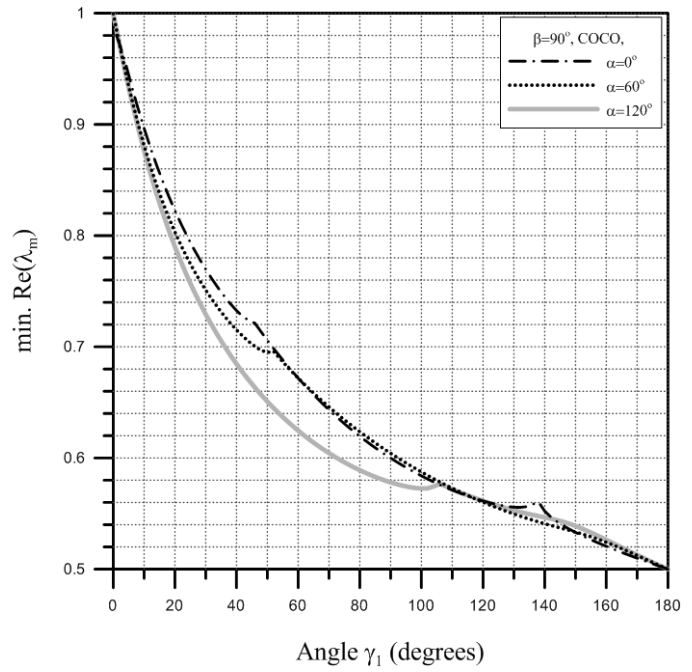

(b)

Fig. 2.10 Variation of minimum Re[λ_m] with wedge angle for PZT-5H/PZT-4 wedges
(a) FOFO boundary conditions,
(b) COCO boundary conditions

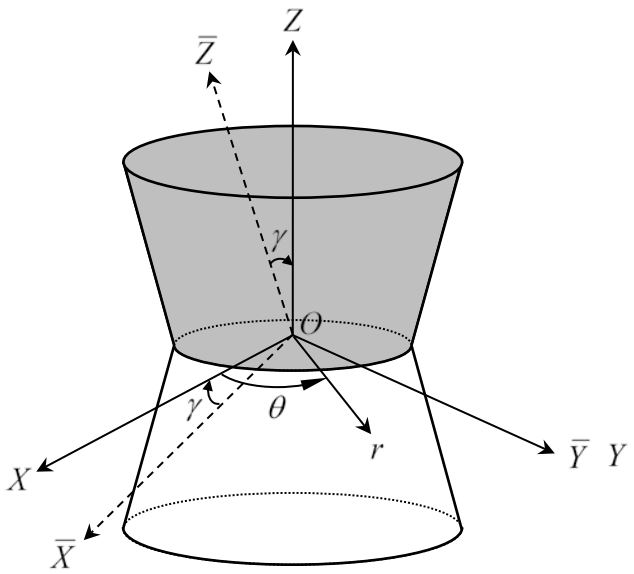

Fig. 3.1 Bi-material body of revolution with a sharp corner

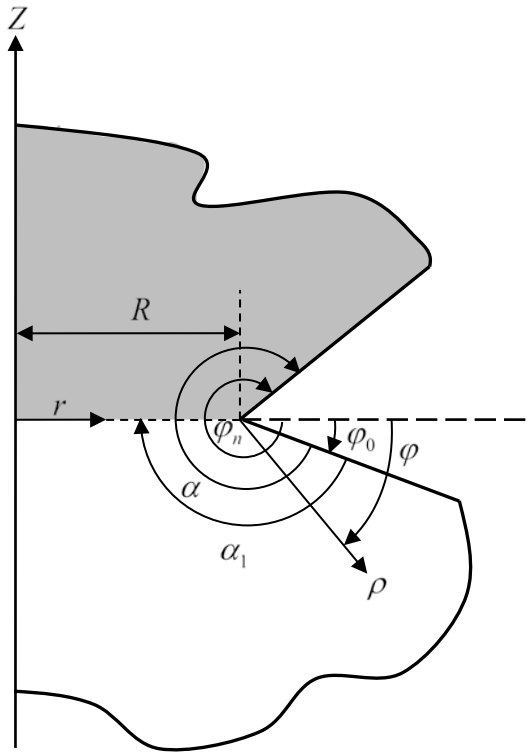

Fig. 3.2 Cylindrical (r, Z) and sharp corner (ρ,φ) coordinates

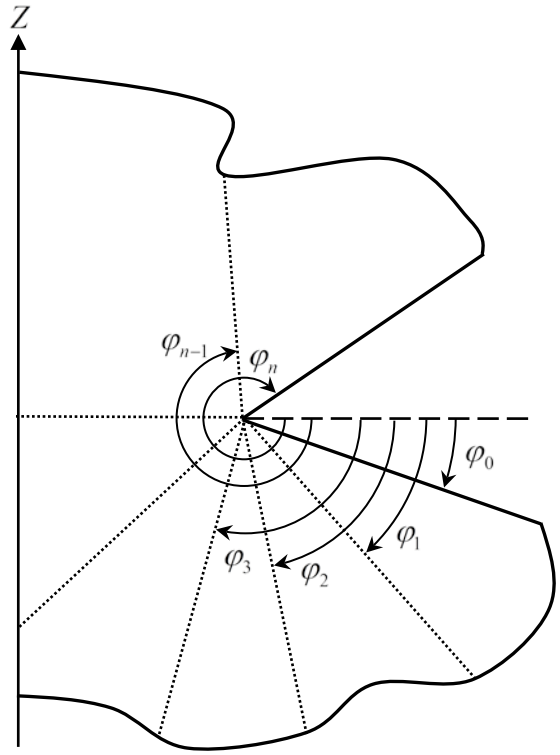

Fig. 3.3 Sub-domains for $\varphi \in [\varphi_0, \varphi_n]$

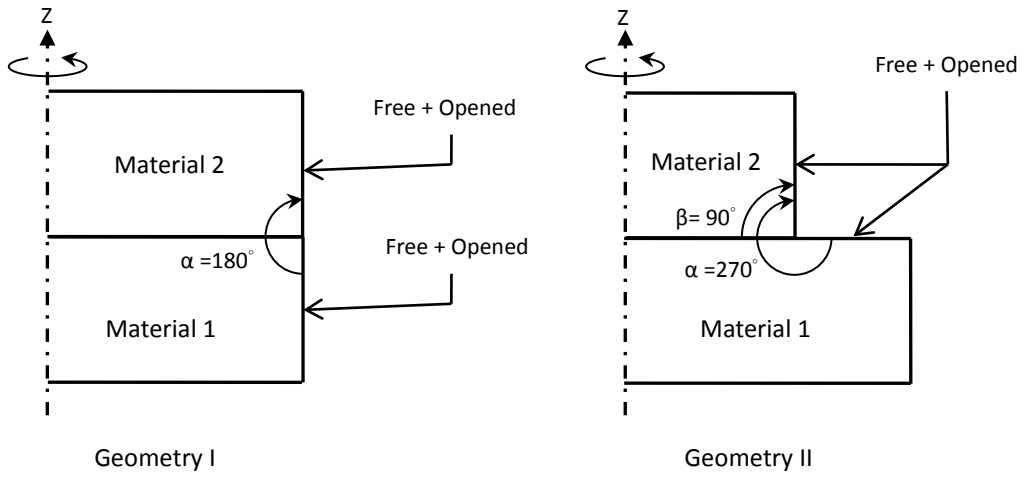

Fig.3.4 Geometry and boundary conditions for bodies of revolution considered in convergence studies

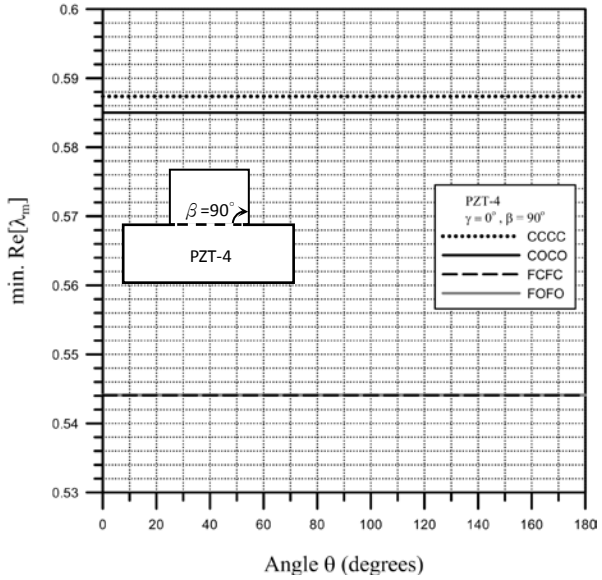

(a)

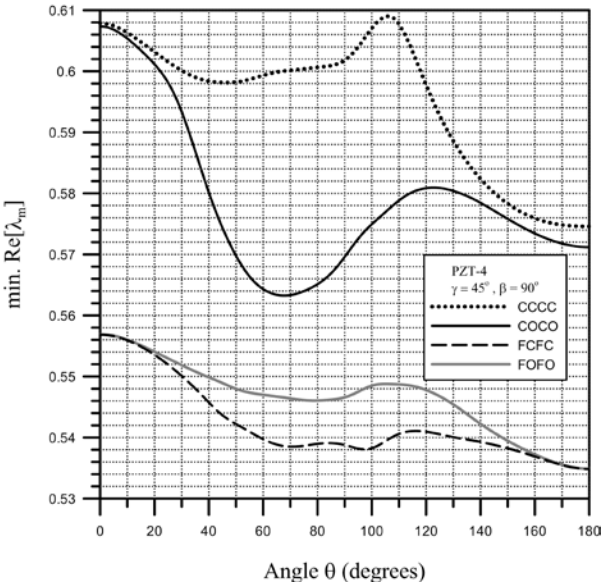

(b)

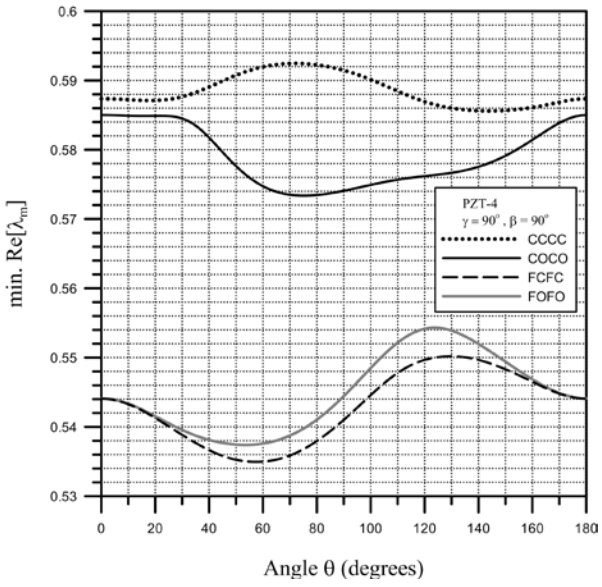

(c)

Fig. 3.5 Variation of minimun Re[λ_m] with θ for PZT-4 of bodis of revolution with β = 90°: (a) γ = 0°, (b) γ = 45°, (c) γ = 90°

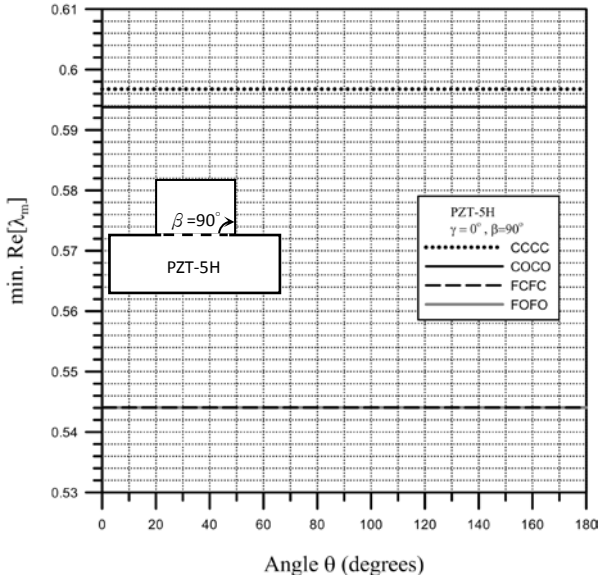

(a)

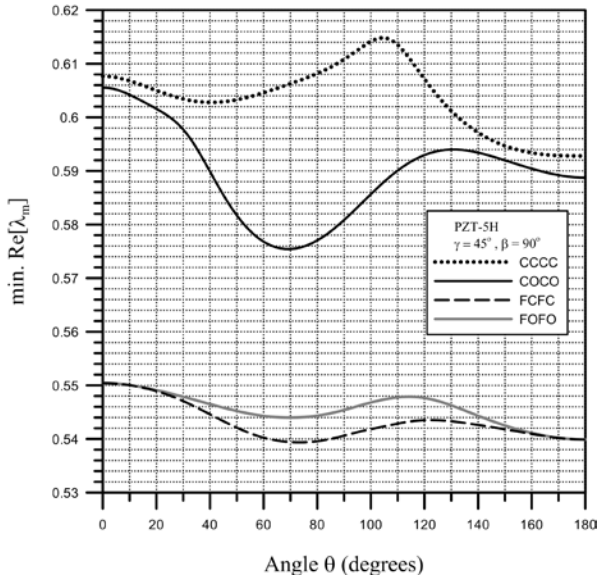

(b)

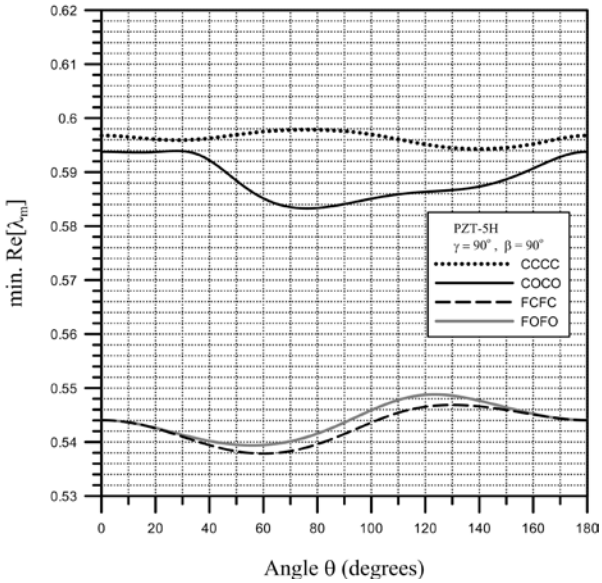

(c)

Fig. 3.6 Variation of minimun Re[λ_m] with θ for PZT-5H of bodis of revolution with β = 90°: (a) γ = 0°, (b) γ = 45°, (c) γ = 90°

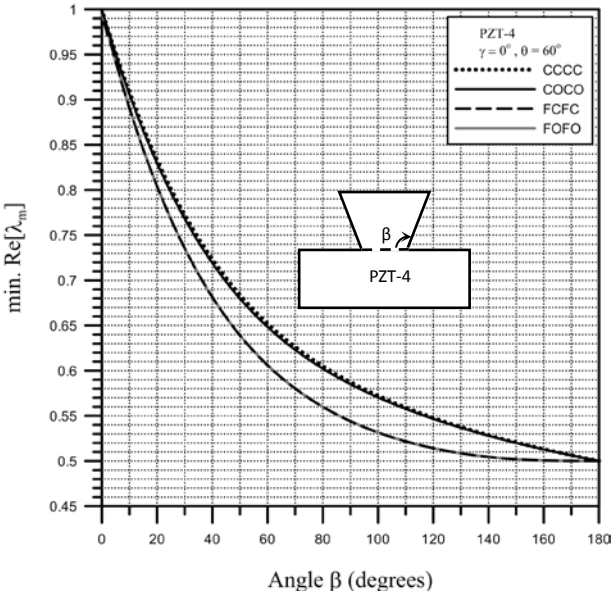

(a)

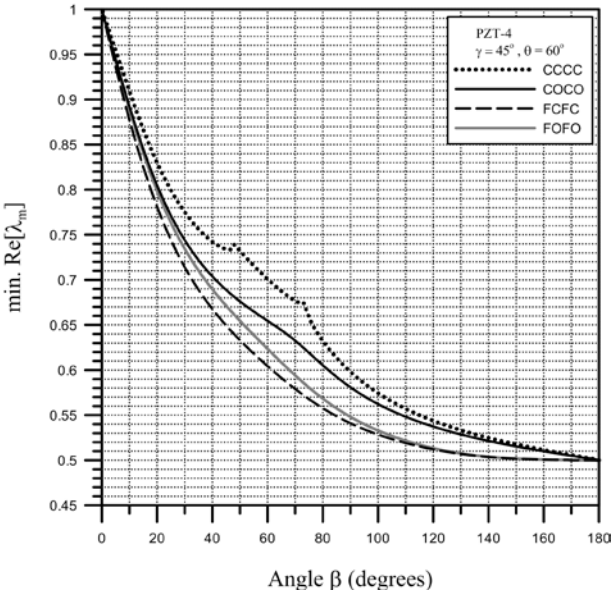

(b)

Fig. 3.7 Variation of minimun Re[λ_m] at $\theta = 60°$ with β for PZT-4 bodies of revolution: (a) $\gamma = 0°$, (b) $\gamma = 45°$

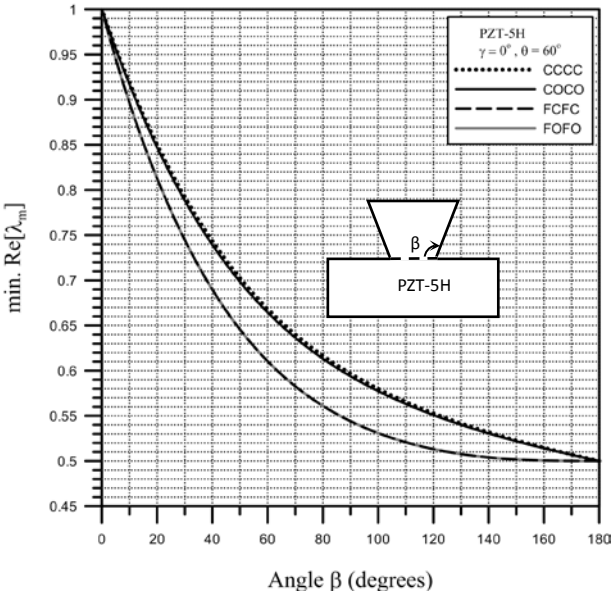

(a)

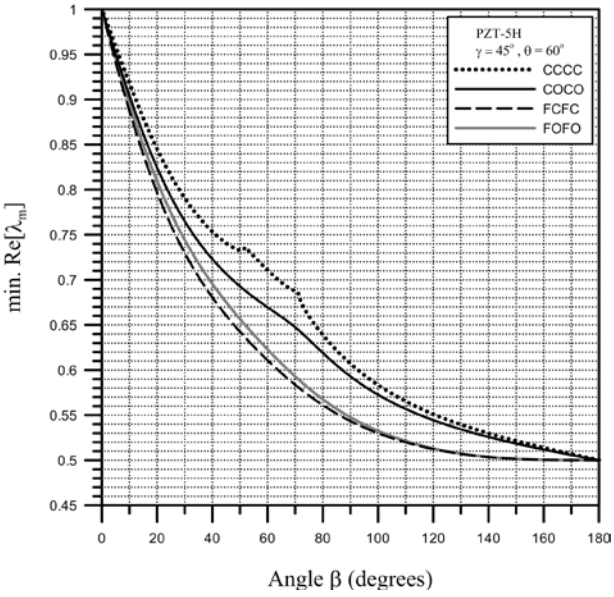

(b)

Fig. 3.8 Variation of minimun Re[λ_m] at θ = 60° with β for PZT-5H bodies of revolution: (b) γ = 0°, (b) γ = 45°

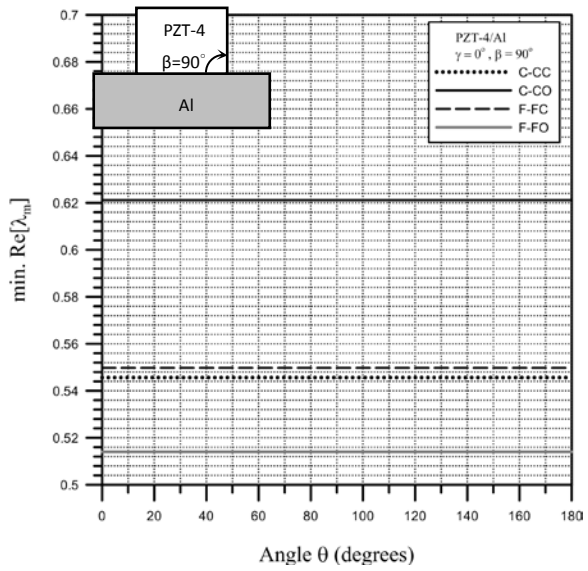

(a)

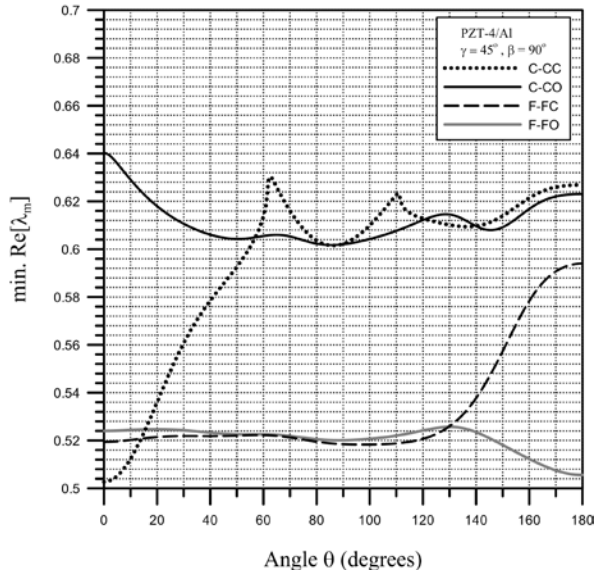

(b)

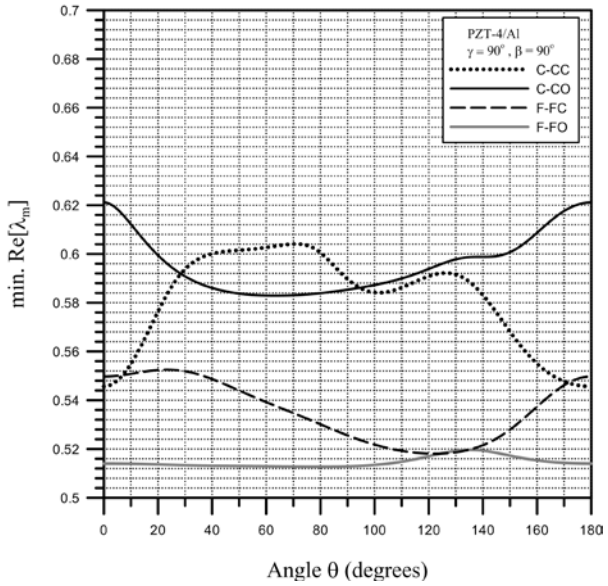

(c)

Fig. 3.9 Variation of minimun Re[λ_m] with θ for PZT-4/Al of bodis of revolution with β = 90°: (a) γ = 0°, (b) γ = 45°, (c) γ = 90°

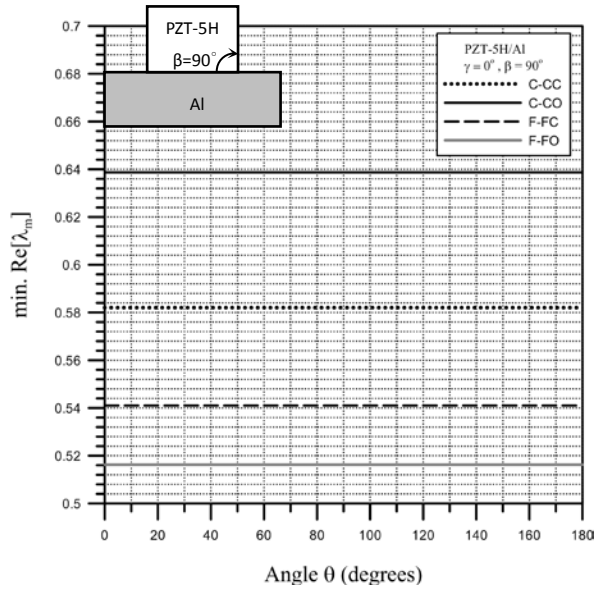

(a)

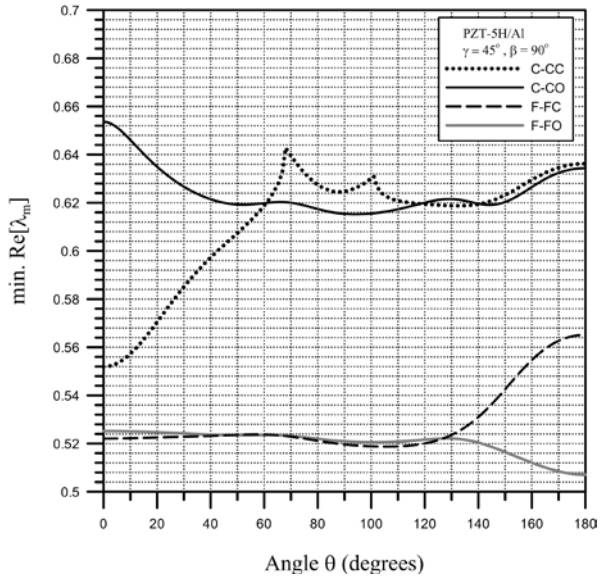

(b)

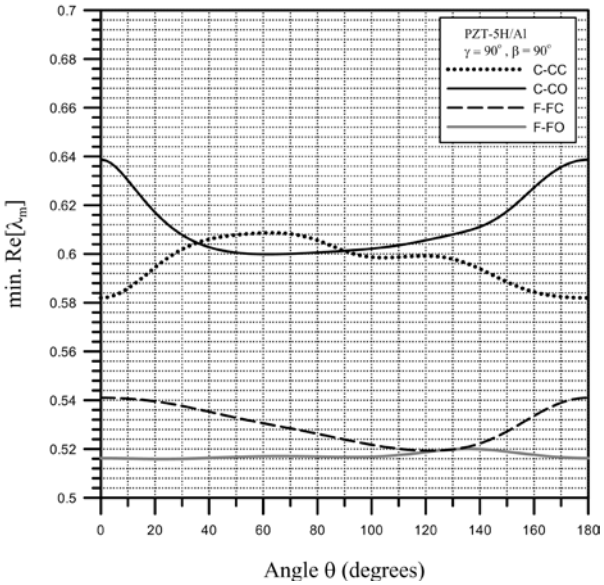

(c)

Fig. 3.10 Variation of minimun Re[λ_m] with θ for PZT-5H/Al of bodis of revolution with β= 90°: (a) γ = 0°, (b) γ = 45°, (c) γ = 90°

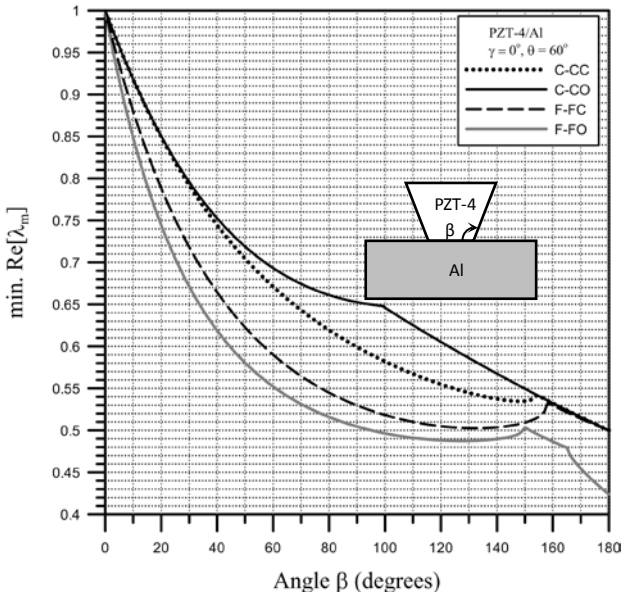

(a)

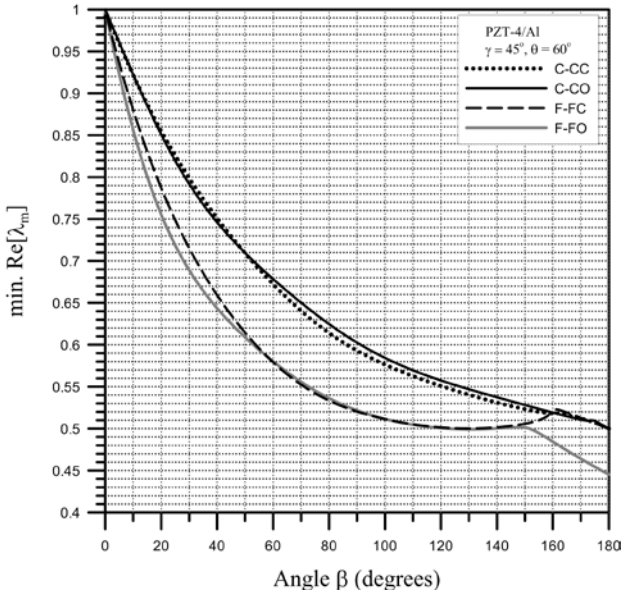

(b)

Fig. 3.11 Variation of minimun Re[λ_m] at θ = 60° with β for PZT-4/Al bodies of revolution: (a) γ = 0°, (b) γ = 45°

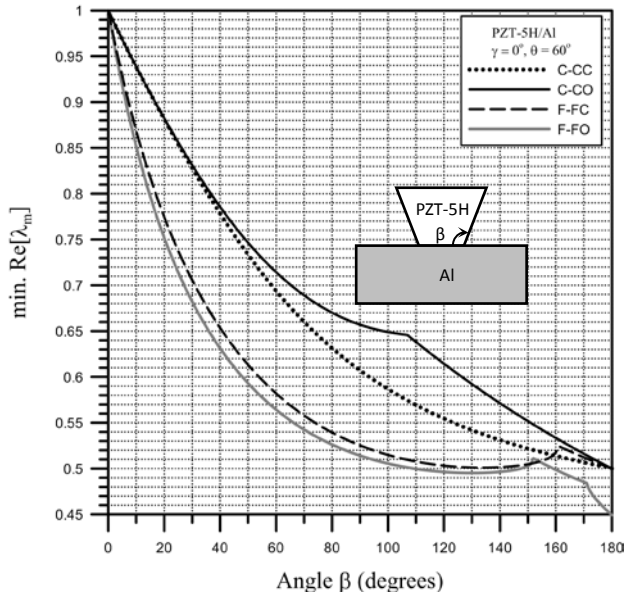

(a)

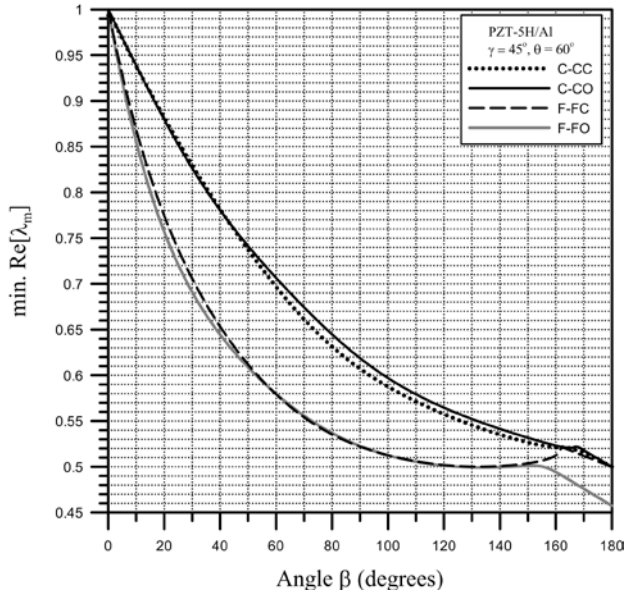

(b)

Fig. 3.12 Variation of minimun Re[λ_m] at θ=60° with β for PZT-5H/Al bodies of revolution: (a) γ = 0°, (b) γ = 45°

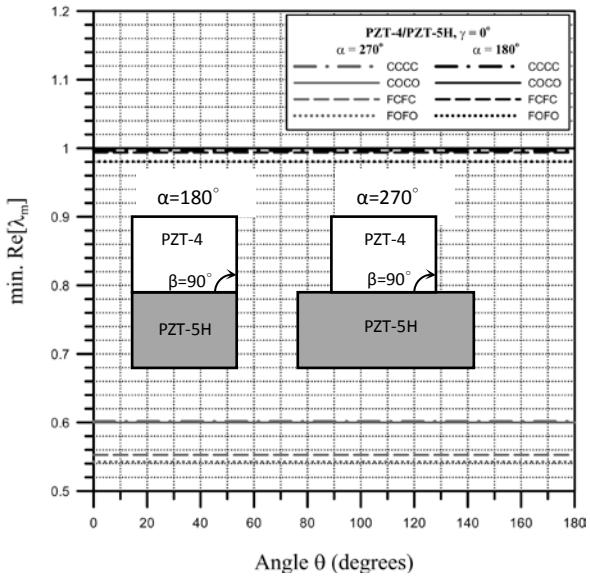

(a)

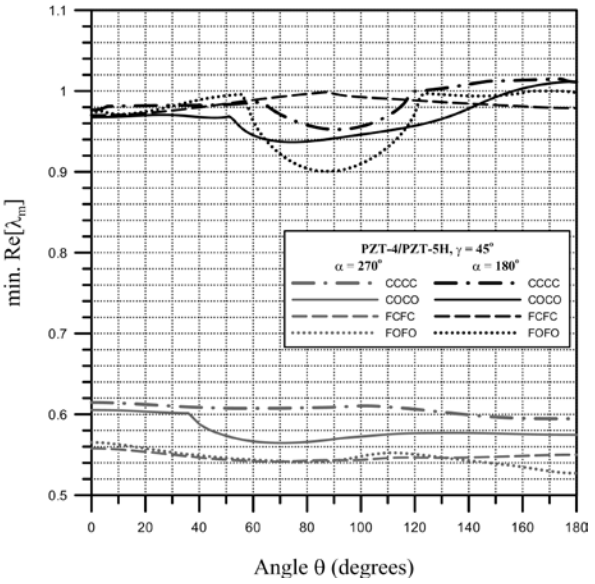

(b)

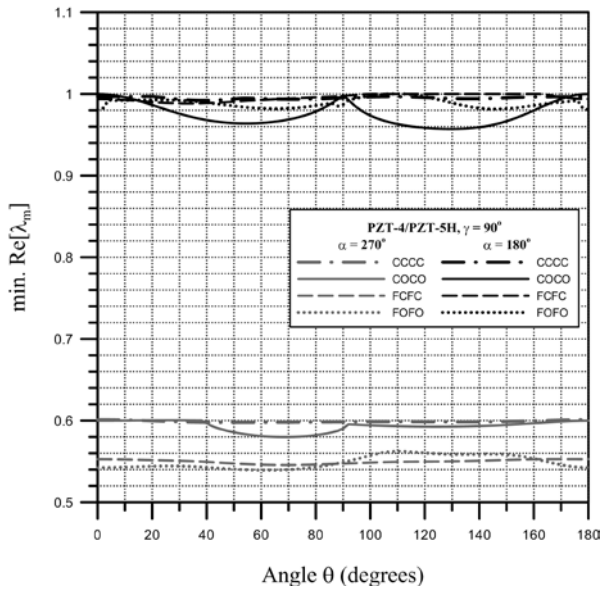

(c)

Fig. 3.13 Variation of minimun Re[λ_m] with θ for PZT-4/ PZT-5H of bodis of revolution with β = 90°: (a) γ = 0°, (b) γ = 45°, (c) γ = 90°

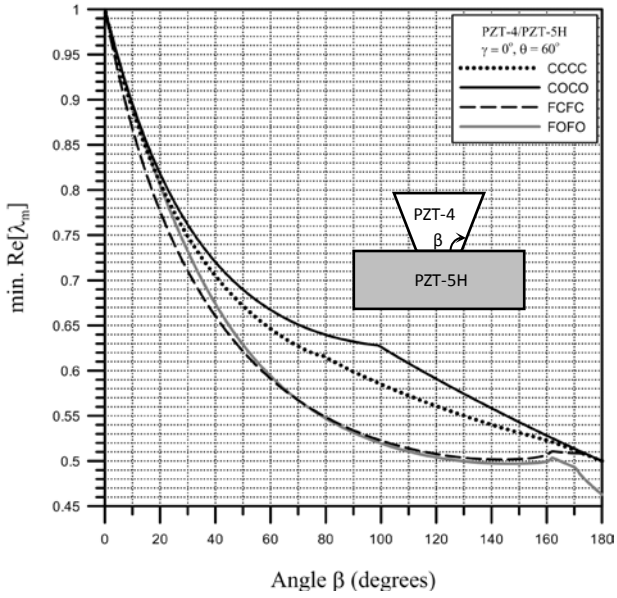

(a)

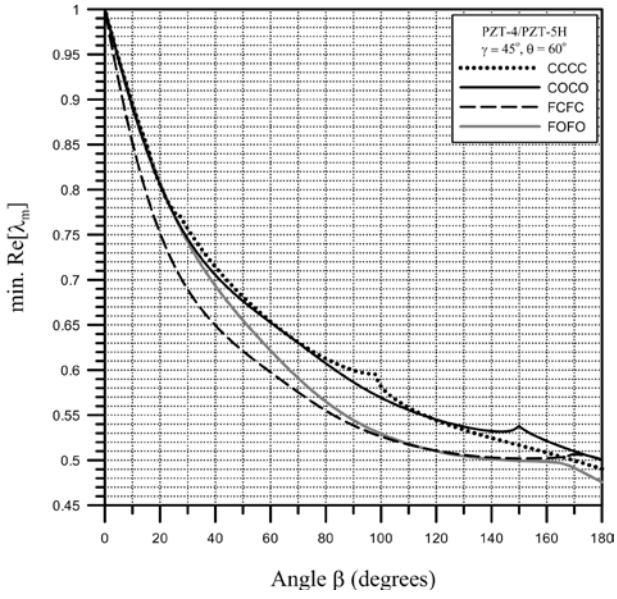

(b)

Fig. 3.14 Variation of minimun Re[λ_m] at θ=60° with β for PZT-4/ PZT-5H bodies of revolution: (a) γ = 0°, (b) γ = 45°.